# Transition of cell-cell signaling dynamics in collective cell migration during the development of *Dictyostelium* cells

Hidenori Hashimura

Department of Biological Science, Graduate School of Science,

Osaka University

Doctor thesis

2019, February

# Contents

**Results**

**Discussion**

## Abbreviations

| | |
|---|---|
| ACA: | Adenylyl cyclase A |
| ACB: | Adenylyl cyclase B |
| ACG: | Adenylyl cyclase G |
| cAMP: | cyclic adenosine 3',5'-monophosphate |
| CAR: | cAMP receptor |
| cGMP: | cyclic guanosine 3',5'-monophosphate |
| CRAC: | cytosolic regulator of adenylyl cyclase |
| GBF: | G-box binding factor |
| PH domain: | Pleckstin Homolog domain |
| PIP3: | phosphatidylinositol 3,4,5-trisphosphate |
| PKA: | Protein kinase A |

**Abstract**

Collective cell migration is organized movements of multiple cell and involved in various biological activities such as morphogenesis, wound healing and cancer invasion. Understanding how the collective cell migration is organized sptaio-temporally is the crucial issues in biology. Social amoebae *Dictyostelium discoideum* is a model organism for study of collective cell migration because of its unique morphogenesis and simple cell-cell interaction via diffusible chemical guidance, cyclic adenosine 3',5'-monophosphate (cAMP). *Dictyostelium* cells usually behave as unicellular organisms but they show aggregate to form multicellular bodies. It has been though that cell-cell communication via cAMP called cAMP relay plays key roles in organizing collective cell migration during the multicellular morphogenesis of *Dictyostelium* cells. However, the dynamics of cAMP signaling at the multicellular phase remain unclear. In this work, how the cells interact via cAMP signals during collective cell migration was investigated by live imaging technique through the development of *Dictyostelium* cells. Direct monitoring of intracellular cAMP levels revealed that the cAMP signals oscillate and propagate between cells during aggregation and the intermediate stage of multicellular formation, but such oscillations caused by cAMP relay gradually disappeared when the multicellular bodies were formed. A similar transition of signaling dynamics occurred with phosphatidylinositol 3,4,5-trisphosphate signaling, which is upstream of the cAMP signal pathway. These suggest that cAMP relay is not always needed for collective cell migration after multicellular body formation. This hypothesis is supported by the result that the mutant which lacks the ability of cAMP relay could aggregate and migrate as multicellular bodies without any cAMP oscillations under the certain condition. This transition was programmed with concomitant developmental progression and relative to the internalization of cAMP receptors from plasma membrane. Therefore, this study propose a new model in which cAMP oscillation and propagation between cells, which are important at the unicellular stage, shows dramatic transition in dynamics and becomes unessential for collective cell migration at the multicellular stage. The mechanisms for transition of cAMP signaling and organization of collective cell migration in multicellular bodies are still unclear and thus further investigation is needed in future.

## Introduction

### 1. Collective motion of organisms is a ubiquitous phenomenon in nature.

In nature, mobile organisms and their components (individual member of school, cells, proteins, etc) show various modes of motion in their life style. One mode is migration of a single biological element, such as migration of an animal individual or single cell movement, and this simple mode of biological motion is widely described in detail (Dingle & Drake, 2007; Gruler & Bültmann, 1984; Kareiva & Shigesada, 1983; Takagi, Sato, Yanagida, & Ueda, 2008). On the other hand, when the self-propelled biological elements gather, their motion are aligned with each other and finally they show cooperative migration rather than collection of random movements in some cases. This is called collective motion, which is the other mode of biological motion in nature. Collective motion is a ubiquitous phenomenon and exists across wide scales from molecules to individuals (Vicsek & Zafeiris, 2012). At the molecule scale, biological motile molecules such as actin, tubulin filaments and motor molecules show collective motion (Butt et al., 2010; Sumino et al., 2012). At the individual scale, bird flocks and fish schools show collective motion, which is the famous examples of animal cooperative behavior (Bajec & Heppner, 2009; Parrish & Hamner, 1997; Parrish, Viscido, & Grünbaum, 2002). The collective motion occurs spontaneously, but it sometimes play important roles in various biological activities. For example, fish schools gain hydrodynamics advantages and defense ability against predators (Magurran, 1990; Partridge & Pitcher, 1979). In the case of actin, the network composed of actin (F-actin) and actin-related proteins which are interacted each other show collective motion of molecules and organized actin elongation in a cell, resulting in more dynamics behavior such as formation of pseudopods and cell movement (Bailly et al., 2001; Pollard, 2007). These biological functions work properly when the collective motion is organized spatio-temporally. Therefore, exploring the principle of the collective motion leads an understanding the complex behavior of biological phenomenon.

## 2. Collective cell migration contributes to various biological activities.

There are many kinds of collective motion in nature, but one of the most studied collective motion in biology is cooperative behavior of multiple cells, namely collective cell migration. Single cell movement itself is involved in many events and has been studied extensively (e. g., immune cells and germ cells: Doitsidou et al., 2002; Kunwar, Siekhaus, & Lehmann, 2006; Redd et al., 2006), but collective cell migration shows more complex behavior and contributes to various biological activities (Friedl & Gilmour, 2009; Rørth, 2009). For examples, collective cell migration of fibroblast or epithelial cells occurs during the wound healing of scratched monolayer (Matsubayashi, Razzell, & Martin, 2011; Nobes & Hall, 1999), and collective cell migration in embryos of multicellular organisms is particularly prevalent during morphogenesis and causes the formation of complex tissue and organ (McMahon, Supatto, Fraser, & Stathopoulos, 2008; Migeotte, Omelchenko, Hall, & Anderson, 2010). Furthermore, it has been recently revealed that collective cell migration of tumor cells is involved in cancer invasion (Friedl, Hegerfeldt, & Tusch, 2004; Gaggioli et al., 2007; Sahai, 2005). These event show that collective cell migration is organized activities of cell populations worked as a whole rather than just a collection of independent cell movements. Because of these crucial roles of collective cell migration in multicellular organisms, understanding the mechanisms for organization of collective cell migration is an important issue in biology.

It has been thought that collective cell migration is organized by cell-cell interactions or cell-environment interactions via physical and chemical guidance cues, such as cell-cell adhesion and diffusible factor-mediated signaling (Haeger, Wolf, Zegers, & Friedl, 2015). Cell-cell contacts plays important roles in maintaining the polarity of cell population which drives collective cell migration (Scarpa & Mayor, 2016). It has been reported that E-cadherin-mediated cell-cell contact maintains the polarity of mesendoderm cells in Zebrafish, which drives collective cell migration (Dumortier et al., 2012). In embryos of *Drosophila*, adhesion via E-cadherin between border cells and their substrate, the nurse cells introduce the stable forward protrusion and directed cell movements, resulting in cluster polarization and collective cell migration (Cai et al., 2014).

As an example of chemical guidance for collective cell migration, primodium of the lateral line in zebrafish migrate as a population of approximately 100 cells and its directed migration is guided by self-generate gradients of chemokine CXCL12/SDF-1 through the ligand-receptor internalization (Donà et al., 2013). During the migration of *Drosophila* border cells in egg chamber, PVF1 and EGF function as chemical guidance cue (Duchek & Rørth, 2001; Duchek et al., 2001). These various cues (physical and chemical guidance) are integrated and act in parallel in organism (Haeger et al., 2015). For example, neural crest cells show collective chemotaxis toward SDF-1 in N-cadherin-mediated cell-cell contact-dependent manner (Theveneau et al., 2010). Therefore, the mechanisms for guidance of multiple cells lead supracellular polarization of cell populations and thus concerted position changes of cell populations relative to the substrate (Friedl & Gilmour, 2009; Venhuizen & Zegers, 2018). As described above, researchers have investigated the collective cell migration in the various biological activities and revealed the mechanisms for organization of such cooperative behavior. However, most studies of collective cell migration have focused on particular biological scene, although actual collective behavior of cell populations is diverse at the time and place in organisms. Thus, how the transition of collective cell migration is organized is not fully understood.

**3. Model organism for collective cell migration: *Dictyostelium discoideum*.**

In the studies of collective cell migration, researchers use various organisms such as primodium of the lateral line in zebrafish, border cells in oocyte of fruit fly, epithelial cells in mammals and so on (Friedl & Gilmour, 2009). One of the model organism for collective cell migration is social amoebae, *Dictyostelium discoideum.* This organism usually behaves as unicellular organism, but they show unique morphological changes in their life cycle. *Dictyostelium* cells feed bacteria or take in nutrient by pinocytosis from liquid media and proliferate at the vegetative stage. However, when the cells are starved, they undergo transition from a unicellular to multicellular state (**Fig. 1**). Starved cells start to aggregate and are aligned to form streams after the obvious aggregation centers appear. Streams flow into the aggregation center to form hemispherical cell masses, called loose mounds. Cells in loose mounds show rotational collective migration. Loose mounds become tightly packed mounds called tight mounds by both secretion of the extracellular

matrix and the strengthening of cell-cell contacts.

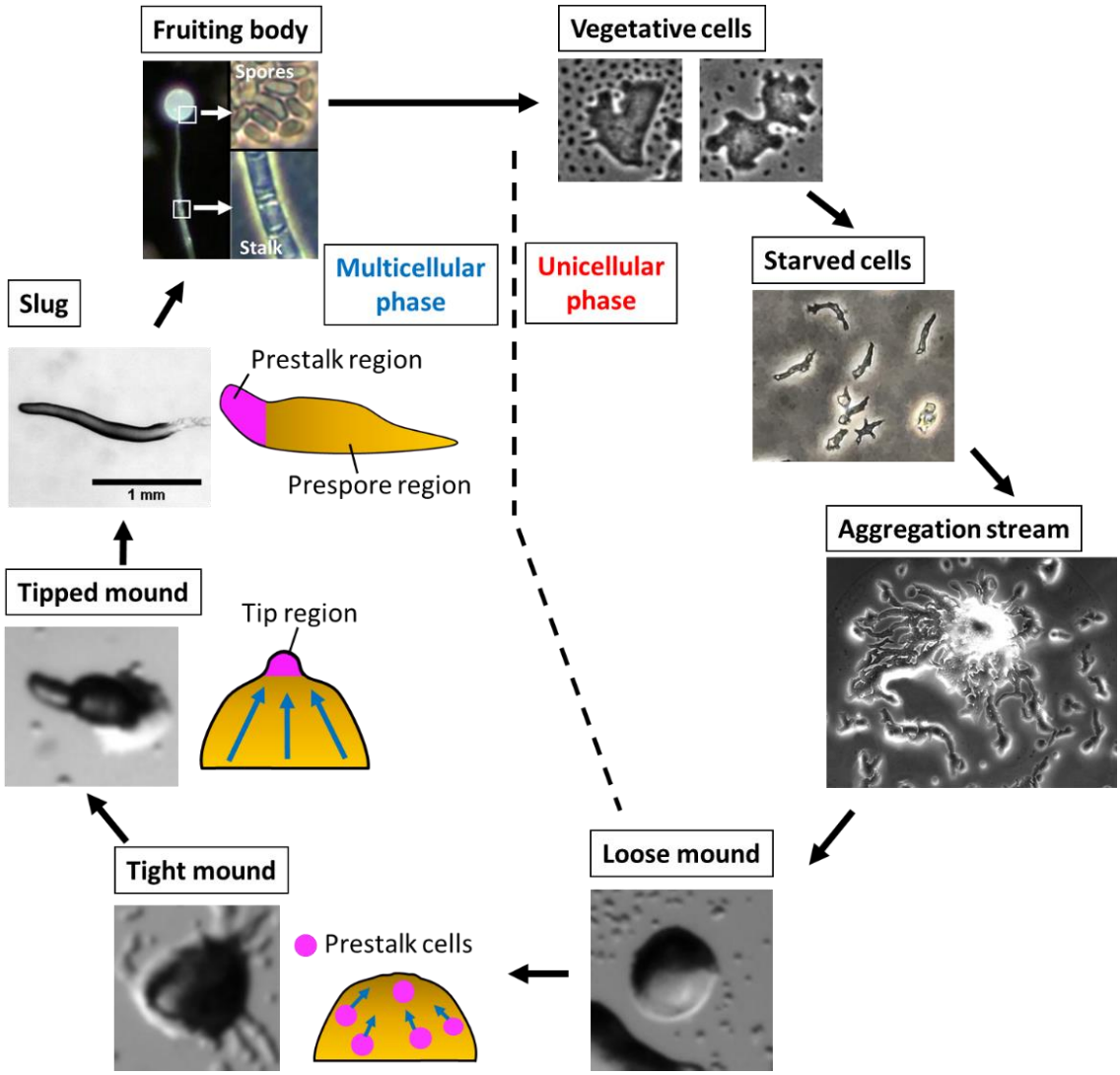


**Figure 1. Life cycle of *Dityostelium discoideum.***

(Unicellular phase): Vegetative cells eat bacteria (left panel) or absorb nutrient from surrounding liquid media, and proliferate by cytokinesis (right panel). Starved cells with clear cell polarity move actively and gain the chemotactic ability. These cells aggregates and are finally aligned to form streams. Streams flow into the aggregation center resulting in formation of loose mounds. (Multicellular phase): In tightly packed mounds, cells start to differentiate into either minor prestalk or major prespore cells, and prestalk cells are sorted into top of the mound to form tip. Tipped mounds then elongate and start to migrate as slugs. Slugs consist of anterior prestalk region and posterior prespore region and show organized multicellular movement. After slug migration, slugs start to culminate and form fruiting bodies. Fruiting bodies consist of stalk cells and spores, which are differentiated from prestalk and prespore cells, respectively. After dormancy, spores germinates and amoebae start to proliferate again as unicellular organisms.

In tight mounds, cells start to differentiate into two cell types, prestalk and prespore cells. Prestalk cells are sorted at the top of the mound to form the tip, which elongates and forms the front of a multicellular body, called a slug. Cells in a slug adhere to each other and move cooperatively, which makes a slug to migrate as an animal individual. Slugs show obvious anterior-posterior polarity: prestalk cells made up about 20% region on the anterior side of slugs, while prespore cells made up about remaining 80% region of slugs (Bonner, 1952; Sternfeld & David, 1982). Slugs migrate straightforward and change moving direction in response to external stimuli such as light (e. g., phototaxis and thermotaxis). After the migration, slugs stop their migration and start to form fruiting bodies which consists of spore masses and the stalk. During the fruiting body formation, prespore and prestalk cells differentiate into spores and stalk cells, respectively. This transition from unicellular to multicellular phases completes within about 24 hours. Through the development, *Dictyostelium* cells show various collective cell migration such as aggregation, rotational movements, cell sorting and multicellular movements. Thus, diverse collective behavior can be observed easily at the experimental condition using *Dictyostelium* cells, compared with other multicellular model organisms. This makes *D. discoideum* a model organism for the study of collective cell migration.

**4. Mechanism for organizing collective cell migration in *Dictyostelium* : cAMP relay.**

*D. discoideum* cells show chemotactic response to various compounds such as folic acid and pteridine (Pan, Hall, & Bonner, 1972; Tillinghast & Newell, 1987), but especially cyclic adenosine 3',5'-monophosphate (cAMP) works as the self-produced diffusible chemoattractant (Bonner et al., 1969; Konijn, Chang, & Bonner, 1969; Konijn et al., 1969) and plays key roles in organizing collective cell migration through the development. Starved cells autonomously start to synthesize and secret cAMP, which triggers the subsequent signal transduction in cells (**Fig. 2a**). When *Dictyostelium* cells sense extracellular cAMP signals through G protein-coupled cAMP receptors (cARs), PI3-kinases are activated through G proteins to produce phosphatidylinositol 3,4,5-trisphosphate (PIP3) transiently on the plasma membrane of the cell front, leading to the transient localization of CRAC (cytosolic regulator of adenylyl cyclase) to the membrane via the Pleckstin Homolog (PH) domain that binds to PIP3 which activates adenylyl cyclase (Insall et al., 1994; Parent et al., 1998).

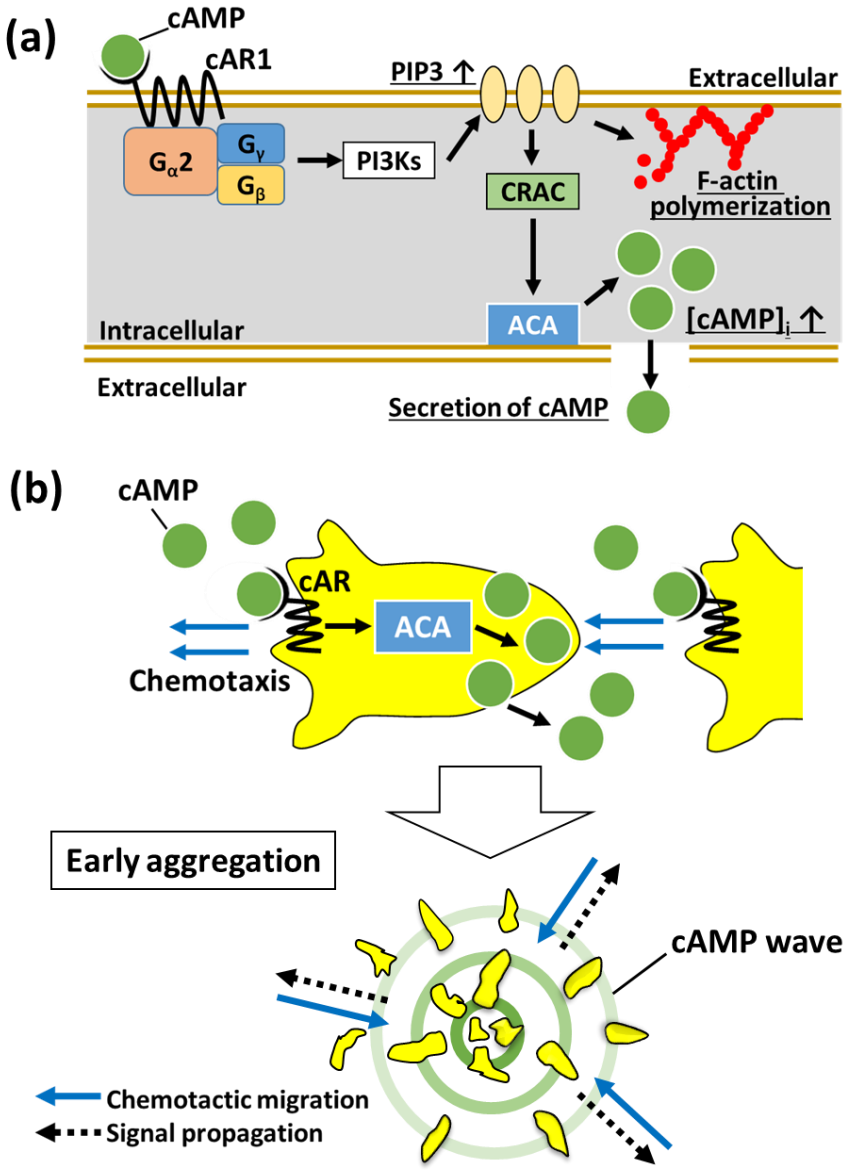


**Figure 2. Intracellular and intercellular cAMP signal system in *Dictyostelium* cells.**

(a) Intracellular signal transduction in response to external cAMP signals (Parent & Devreotes, 1996; Swaney, Huang, & Devreotes, 2010). (b) Intercellular cAMP signal propagation (cAMP relay). Extracellular cAMP signals causes intracellular cAMP production, cAMP secretion to neighbor cells and chemotactic migration toward cAMP gradients subsequently. This leads cAMP signal propagation as signal waves and cooperative migration of multiple cells toward signal center, resulting in cAMP relay and cell aggregation.

cAMP is synthesized in cells by adenylyl cyclase in response to external cAMP signals and secreted, resulting in inducing neighboring cells to similarly reatcion (Devreotes, Derstine, & Steck, 1979; Dinauer, MacKay, & Devreotes, 1980). Simultaneously, the transient accumulation of PIP3 at the cell front in response to external cAMP also induces actin polymerization and pseudopod formation, resulting in chemotactic migration (Comer & Parent, 2002). These reactions finally cause the propagation of cAMP signals as travelling waves called cAMP relay and chemotactic migration toward the aggregation center (**Fig. 2b**). Isotope dilution assay revealed that cAMP relay gives the spatial pattern of cell-cell communication (spiral signal propagation) and organizes collective cell migration during aggregation stage after the starvation (Tomchik & Devreotes, 1981). Thus, cAMP relay organize collective cell migration during aggregation spatio-temporally.

The *D. discoideum* genome encodes four subtypes of cARs (CAR1−4) and the time course of their expression pattern is different. CAR1 is expressed immediately after the starvation and onset of CAR3 expression is at the later aggregation stage (Johnson et al., 1993a; Klein, Vaughan, Borleis, & Devreotes, 1987). CAR2 and CAR4 are expressed after multicellular bodies are formed (Louis, Ginsburg, & Kimmel, 1994; Yu & Saxe III, 1996). Especially, CAR1 mainly mediates chemotactic response to cAMP during the development because the cells lacking CAR1 cannot aggregate after starvation (Sun, Van Haastert, & Devreotes, 1990). In *D. discoideum*, only one Gβ and Gγ subunit has found (Lilly, Wu, Welker, & Devreotes, 1993; Zhang, Long, & Devreotes, 2001), while the genome contain at least twelve Gα subunits (Hadwiger, 2007). In particular, Gα2 subunits coupled with cAR1 plays important roles on chemotaxis and toward cAMP and cAMP relay (Kumagai, Hadwiger, Pupillo, & Firtel, 1991; Swaney et al., 2010). *D. discoideum* has three subtypes of adenylyl cyclase (ACA, ACB and ACG), but only ACA is activated by external cAMP signals (Meima & Schaap, 1999), meaning that ACA is an essential adenylyl cyclase for generating cAMP relay and aggregation. In fact, mutant cells lacking ACA cannot aggregate after starvation (Pitt et al., 1992). The orchestrated reaction of these molecules finally causes cAMP relay.

It has been argued that cAMP relay is also essential for the organization of collective cell migration during developmental events following the aggregation (Weijer, 1999) (**Fig. 3**). Traditionally, microscopic observation is a powerful tool for investigation of role of cAMP relay in collective cell migration of *Dictyosytelium* cells. Under the dark-filed observation, optical densities of cell populations during aggregation describe synchronous changes in cell shapes by chemotaxis and act as an index of cAMP relay (Siegert & Weijer, 1989). Propagation of these optical density waves have been observed in aggregation field, streams and mounds in the opposite direction of cell movements, giving evidence that cAMP relay controlled collective cell migration at these stages (Dormann & Weijer, 2001; Rietdorf, Siegert, & Weijer, 1996). Sorting of prestalk cells to the tip of the tight mound during mound elongation also can be explained by cAMP relay. There is a difference in the response of chemotaxis toward cAMP between prespore and prestalk cells in mounds, resulting in cAMP relay from the top of the tight mound guiding the sorting of prestalk cells to the tip of the mound (Sternfeld & David, 1981; Traynor, Kessin, & Williams, 1992). At the slug stage, propagation of optical density waves from the tip of slugs to the posterior side has been detected (Dormann & Weijer, 2001). Cells dissociated from slugs produce cAMP upon extracellular cAMP stimulation (Otte et al., 1986) and show chemotactic movement toward cAMP (Early, Abe, & Williams, 1995), indicating that slug cells have the ability of cAMP relay and chemotaxis toward cAMP. Furthermore, cAMP microinjection in slugs causes chemotactic attraction of some cells in the population and perturbation of the optical density wave propagation (Dormann & Weijer, 2001; Rietdorf, Siegert, & Weijer, 1998). These observations suggest that cAMP signals control cell movement in slugs. Thus, cAMP relay is regarded as an essential mechanism for organized collective cell migration, such as cell sorting and multicellular movement, in *Dictyostelium* cells.

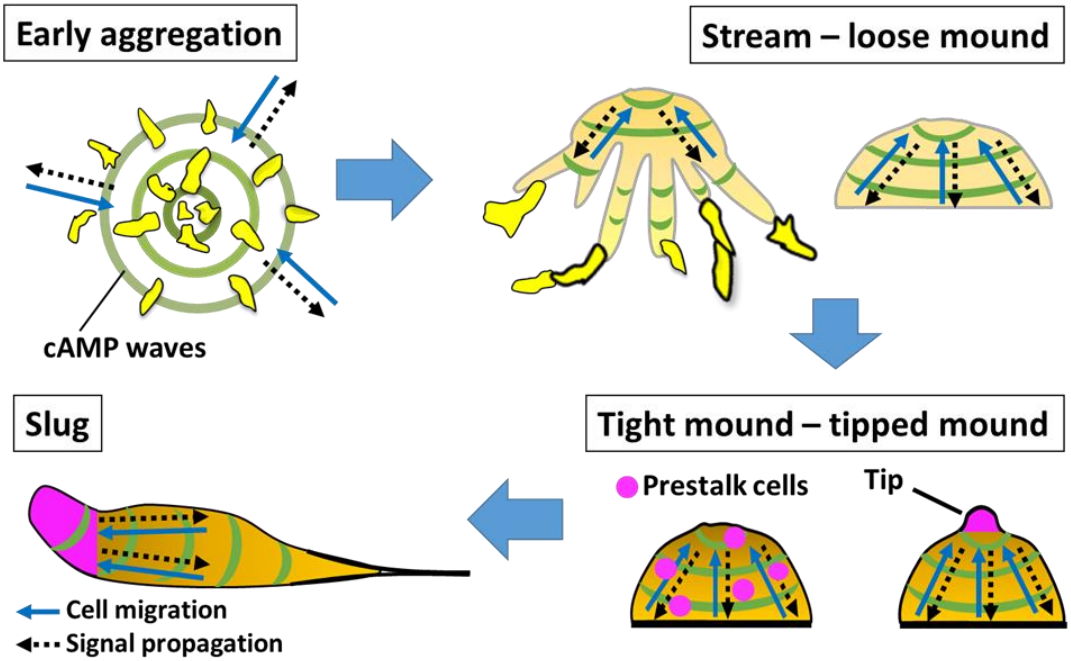


**Figure 3. Assumption that cAMP relay plays key roles in collective cell migration through the development of *Dictyostelium* cells.**

## 5. cAMP signals also play important roles in *Dictyostelium* development

In addition to organizing collective cell migration, cAMP signals also contribute to development progression. Periodic cAMP pulses induce the expression of postaggregative genes some of which are involved in development and cell differentiation (Iranfar, Fuller, & Loomis, 2003; Schaap et al., 1986). In fact, exogenous cAMP pulses can restore the development of mutants which show developmental arrest phenotype (Pitt et al., 1993; Soede, Insall, Devreotes, & Schaap, 1994). One of the pulse induced genes is *tgrC1*, which mediates cell-cell contact and plays important roles in development. Gene disruption of *tgrC1* causes development arrest at loose mound stage (Dynes et al., 1994). Intracellular cAMP signal which arises in response to external cAMP stimuli activates Protein kinase A (PKA). PKA is a heterodimer of regulatory and catalytic subunits. When intracellular cAMP binds to the regulatory subunit of PKA, the catalytic subunit are dissociated from the regulatory subunit and becomes active. Genetically-manipulated inactivation of PKA results in inhibition of development and cell differentiation (Harwood et al., 1992; Mann & Firtel, 1991; Mann, Yonemoto, Taylor, & Firtel, 1992). Furthermore, intracellular cAMP signals plays important roles in stalk and spore cell differentiation (Chen et al., 2017; Kay, 1989; Kwong, Sobolewski, & Weeks, 1988; Loomis, 2014). These suggest that intracellular cAMP and PKA signal pathway is important for controlling development and cell differentiation. PKA activates the transcription factor GtaC which induces the expression of cAMP-pulse induced genes (Cai et al., 2014; Loomis, 2014). Recently it has been reported GtaC shows oscillatory nucleocytoplasmic shuttling in response to cAMP relay and its shuttling is important for proper expression of early development genes and development progression (Cai et al., 2014). Continuous cAMP relay during aggregation finally causes accumulation of cAMP at high concentration, which induces the expression of the other transcription factor GBF. GBF regulates the expression of postaggregative and cell-type specific genes and lacking of GBF causes the developmental arrest at loose mound stage, indicating that GBF is required for the transition to multicellularity (Firtel, 1995; Schnitzler, Fischer, & Firtel, 1994). Thus, cAMP signals including cAMP relay is required for multicellular development of *Dictyostelium* cells.

## 6. Question: how is the collective cell migration at the multicellular phase in *Dictyostelium* controlled?

In spite of these traditional views of cAMP relay for the organization of collective cell migration in *Dictyostelium*, some observations suggest that the role of cAMP relay in multicellular slugs is controversial. *acaA*-null cells, which lack the ability of cAMP relay, normally cannot aggregate and form multicellular bodies (Pitt et al., 1992). However, the phenotypes of the mutant are rescued by constitutive activation of PKA, which is downstream of the cAMP signaling pathway, implying that *Dictyostelium* cells have developmental ability without cAMP oscillation (Wang & Kuspa, 1997). Previous research has shown that optical density waves which can be seen in streams and mounds disappear at the slug stage (Rietdorf et al., 1996) and that the frequency of the optical density wave observations depends on the cell strain (Dormann & Weijer, 2001). However, the disappearance of optical density waves in slugs does not necessarily indicate the disappearance of cAMP relay, because there is a possibility that factors unrelated to the cAMP signals make it impossible to detect optical density waves in the slugs. The secretion of extracellular matrix and tight packing of cells by the strengthening of cell-cell contacts at the slug stage affect the detection of small changes in cell shape under dark field observation (Rietdorf et al., 1996). These points indicate that the optical density measurement is not an appropriate method for assessing the cAMP relay in slugs and that previous studies based on observation of optical density waves cannot conclude the presence or absence of cAMP relay in slugs. Furthermore, cAMP signals in mounds and slugs have not been directly investigated, whereas the cAMP relay during cell aggregation has been verified by live imaging of cAMP signals using sophisticated cAMP-sensitive fluorescent probes, which has revealed that intracellular and extracellular cAMP levels show synchronous oscillations in cell populations and propagation of the oscillations between cells (Gregor, Fujimoto, Masaki, & Sawai, 2010; Ohta, Furuta, Nagai, & Horikawa, 2018; Ohta et al., 2016). Therefore, no clear evidence exists for cAMP relay in slugs, and thus the mechanisms for organizing collective cell migration at the multicellular stage remain unclear.

## 7. Aim of this study: toward understanding the relationship between cAMP signal dynamics and collective cell migration through *Dictyostelium* development.

In this study, the dynamics of cAMP signals through the development of *Dictyostelium* cells is investigated to reveal the relationship between cAMP signaling dynamics (cAMP relay) and collective cell migration in *Dictyostelium* cells. Because the direct measurement of extracellular cAMP changes can be performed only under the submerged culture condition which inhibits the normal development after aggregation (Ohta et al., 2016), I used the method for visualizing the changes in cytosolic cAMP levels ($[cAMP]_i$) with genetically-encoded fluorescence cAMP indicator Flamindo2 (Odaka, Arai, Inoue, & Kitaguchi, 2014). This approach enables us to investigate the $[cAMP]_i$ dynamics through the natural development of *Dictyostelium* which arises on solid substrate. $[cAMP]_i$ show oscillation in response to periodic propagation of extracellular cAMP signals (Gregor et al., 2010; Ohta et al., 2018), thus monitoring of $[cAMP]_i$ is a reliable index of cAMP relay. Through the live-imaging approaches, I aimed to demonstrate the roles of cAMP relay on various collective cell migration including aggregation, cell sorting and multicellular movement through the development of *Dictyosteliu*, which leads the further understanding of the mechanism for organizing diverse collective cell migration.

## Materials & Methods

### 1. Cell strains and culture conditions.

The *Dictyostelium discoideum* cell strains used in this study are shown in **Table 1**. Cells except for NC4 and XP55 strain were grown axenically in HL5 medium (Formedium, UK) in culture dishes or shaking flasks at 21ºC. NC4 and XP55 cells were cultivated with gram-negative bacteria *Klebisiella aerogens* suspended in KK2 phosphate buffer (20 mM $KH_2PO_4/K_2HPO_4$, pH 6.0) in culture dishes or shaking flasks at 21ºC. Transformants were maintained at 20 μg/ml G418, 10 μg/ml BlastcidinS, or 100μg/ml Hyglomycin B.

| Strain name | Parental strain | Source |
|---|---|---|
| NC4 | Natural isolates | Dr. Kei Inouye laboratory (Kyoto University) (Raper, 1935) |
| AX2 (wild type) * | NC4 | Dr. Guenther Gerisch laboratory (Max Planck Institute of Biochemistry) |
| XP55 | NC4 | NBRP-nenkin stock center (Ratner & Newell, 1978) |
| *acaA*$^-$ | AX2 | Laboratory stock (Matsuoka et al., 2006) |
| *gc*$^-$ (*gca*$^-$ / *sgcA*$^-$) | AX3 * | Laboratory stock (Sato et al., 2009) |
| *gbfA*$^-$ | AX2 | NBRP-nenkin stock center. |
| RI9 (*carA*$^-$ / *carC*$^-$) | JB4 (AX3) | Laboratory stock (Kim et al., 1997) |

**Table 1. List of cell strain used in this study.**

*: AX2 strain is selected from NC4 based on the ability of axenically growth by subculture under the liquid medium (Watts & Ashworth, 1970). AX3 is the axenic strain isolated from NC4 strain independently of AX2 strain (W.F. Loomis, 1971). NC4 and its derivate XP55 cells grow only under the two-membered culture with food source bacteria, but AX2 cells can be cultivated with only liquid medium. Because of ease of handling, AX2 cells are widely used as wild type cells among the researchers of *D. discoideum.*

**2. Plasmid construction and genetic manipulation.**

The plasmids used in this study are shown in **Table 2.** pHK12neo_Citrine was constructed by the insertion of PCR amplified Citrine fragments into the *Bgl*II and *Spe*I sites of pHK12neo by the In-Fusion technique (Clontech laboratories Inc.). pHK12neo_Flamindo2 was constructed by the insertion of synthesized Flamindo2 sequences (GenScript) into the *Bgl*II and *Spe*I sites of pHK12neo. The codon usages of the Flamindo2 sequence were optimized to those of *D. discoideum* for efficient protein expression in *Dictyostelium* cells. pDM324_CAR1-RFP was constructed by the insertion of PCR amplified *carA* sequence into the *Bgl*II and *Spe*I sites of pDM324 by the In-Fusion technique. pDM358_CAR1-RFP was constructed as follows: Hyglomycin resistant cassette was cut out from the *BamH*I and *Xho*I sites of pDM358 and the fragment was inserted into the *BamH*I and *Xho*I sites of pDM324_CAR1-RFP. pDMV18neo was constructed by replacing the act6 promoter of pDM304 with PCR amplified V18 (*rpl11*) promoter sequence. pDMV18neo_Flamindo2 was constructed by the insertion of Flamindo2 fragment into the the *Bgl*II and *Spe*I sites of pDMV18neo. Vectors except for pEcmAO-RFPmars allow constitutive expression of the target proteins in all cells through the development under the control of *act15* promoter which is widely-used constitutive active promoter in *Dictyostelium* cells. The wild-type strain and mutant cells were transformed with about 1.5 μg plasmid by electroporation (Kuwayama, Yanagida, & Ueda, 2008), and transformants were selected with G418, Blastcidin S and Hyglomycin B at a final concentration of 20 μg/ml, 10 μg/ml and 100μg/ml, respectively.

| Plasmid name | Source |
|---|---|
| pEcmAO-mRFPmars | Dictybase stock center |
| pHistone2B-RFP | Dr. Tetsuya Muramoto laboratory (Toho University) |
| pBIG_$PH_{Akt/PKB}$-GFP | Laboratory stock (Asano, Nagasaki, & Uyeda, 2008) |
| pHK12neo | Laboratory stock (Morio et al., 2001) |
| pDM304 | Laboratory stock (Veltman, Akar, Bosgraaf, & Van Haastert, 2009) |
| pDM324 | NBRP stock center (Veltman, Akar, Bosgraaf & Van Haastert, 2009) |
| pDM358 | Laboratory stock (Veltman, Akar, Bosgraaf & Van Haastert, 2009) |
| pDMV18neo | Constructed in this study |
| pHK12neo_Citrine | Constructed in this study |
| pHK12neo_Flamindo2 | Constructed in this study |
| pDMV18neo_Flamindo2 | Constructed in this study |
| pDM324_CAR1-RFP | Constructed in this study |
| pDM358_CAR1-RFP | Constructed in this study |

**Table. 2 List of plasmids used in this study.**

**3. Instruments for image acquisition.**

In all experiments of this study, cells were observed at room temperature (approximately 21ºC). Confocal images including a series of Z-stacks were taken by a confocal laser microscope (A1 confocal laser microscope system, Nikon) with an objective (Plan Apo VC 20×/0.75 NA, Nikon) and oil immersion lenses (Plan Fluor 40×/1.30 NA and Apo TIRF 60×/1.49 NA, Nikon) or an inverted microscope (Eclipse Ti, Nikon) equipped with a CSU-W1 confocal scanner unit (Yokogawa), two sCMOS cameras (ORCA-Flash4.0v3, Hamamatsu Photonics) and objective lenses (Plan Fluor 4×/0.13 NA, Plan Apo 10×/0.45 NA and Plan Apo 20×/0.75 NA, CFI APO λS 60×/1.4 NA, Nikon). Z-stack images were acquired at high-speed with the piezo z-stage (Nano-Drive, Mad City Labs). Flamindo2, GFP and Citrine were excited by a 488 nm solid-state CW laser, and RFP and tetramemethylrhodamine-maleimide (TMR, Invitrogen) was observed using a 561 nm solid-state laser. Epifluorescence imaging was taken by using an inverted epifluorescence microscope (IX83, Olympus) equipped with a 130 W mercury lamp system (U-HGLGPS, Olympus), sCMOS cameras (Zyla4.2, Andor Technology or Prime 95B, Photometrics) and objective lenses (UPLSAPO 4×/0.16 NA and UPLSAPO 20×/0.75 NA, Olympus). Flamindo2 and TMR were observed using fluorescence mirror units U-FGFP (Excitation BP 460–480, Emission BP 495–540, Olympus) and U-FMCHE (Excitation BP 565–585, Emission BP 600–690, Olympus), respectively.

**4. Image analysis.**

All images were processed and analyzed by Fiji (https://fiji.sc/) and R software (https://www.r-project.org/). For cell tracking, laboratory-made software (Yasui, Matsuoka, & Ueda, 2014) of which function was expanded for 3D cell tracking was used. In the sequential time-lapse images, the positions of each cells at the first frame were set manually from the fluorescence signal of Histone2B-RFP. Positions of cells at each frame were determined based on Gaussian fitting and then cells were tracked automatically. Flamindo2 signals at the individual cell level were estimated by measuring the mean intensities of Flamindo2 in the about 3–5 $\mu m^2$ regions positioned on the cytosol which was determined by automatic cell tracking at each frame.

Cell velocity was calculated by dividing the displacement between two sequential frames by the interval time, and the unit of velocity was converted to μm/min. The period of an oscillating signals was calculated by averaging the intervals between the peaks of the oscillation (Flamindo2 signals and cell velocity data) or defined as the first largest peak at $t > 0$ of the autocorrelation function of the $PH_{Akt/PKB}$-GFP translocation data. Data with at least three peaks in the oscillation were used for the analysis. In general, the fluorescence intensities of Flamindo2 were normalized with intensities at $t = 0$ as 1.

**5. Inducing development of *Dictyostelium* cells and image acquisition of the development.**

To induce starvation and development, cells were harvested during the exponential phase ($1.5 – 3\times10^6$ cells/ml) and collected by centrifugation at × 500 g for 1–2 min at 4 ºC. After removal of liquid medium or bacteria-suspended buffer, cells were washed three times (bacterially growth cells, four times) by resuspendeing KK2 phosphate buffer and centrifugation. In this study, two methods were used to observe development of *Dictyostelium* cells (aggregation and multicellular formation). To observe aggregation phase, 1 ml of cells suspension at a density of $5– 7\times10^6$ cells/ml were plated on 2% water agar plates (1 ml of melting 2% w/v Difco Bacto-agar in ultrapure water was poured in a 35-mm plastic dish) and settled for 10 min. After cell attachment to agar, excess buffer was removed. In this condition, cells covered the entire surface of agar plate uniformly at a density of $5– 7\times10^5$ cells/$cm^2$. Plates was then incubated at 21ºC for 3–10 h to induce aggregation. To observe the mound and slug stages, 5 μl of cell suspension at a density of $2–4\times10^7$ cells/ml was deposited on 2% water agar and settled for 10 min to allow cells attaching to agar. For efficient cell tracking in slugs, 0.5–2% of Histone-labelled cells (Histone2B-RFP expressing cells) were mixed in non-Histone labelled cells and deposited on agar, because a slug consists of ~$10^5$ cells and it is difficult to trace large number of cells simultaneously. After removal of excess buffer, plates were incubated at 21ºC for 6–15 h to induce mound or slug formation. To take images of development, a method described previously was used (**Fig. 4**: Dormann & Weijer, 2006).

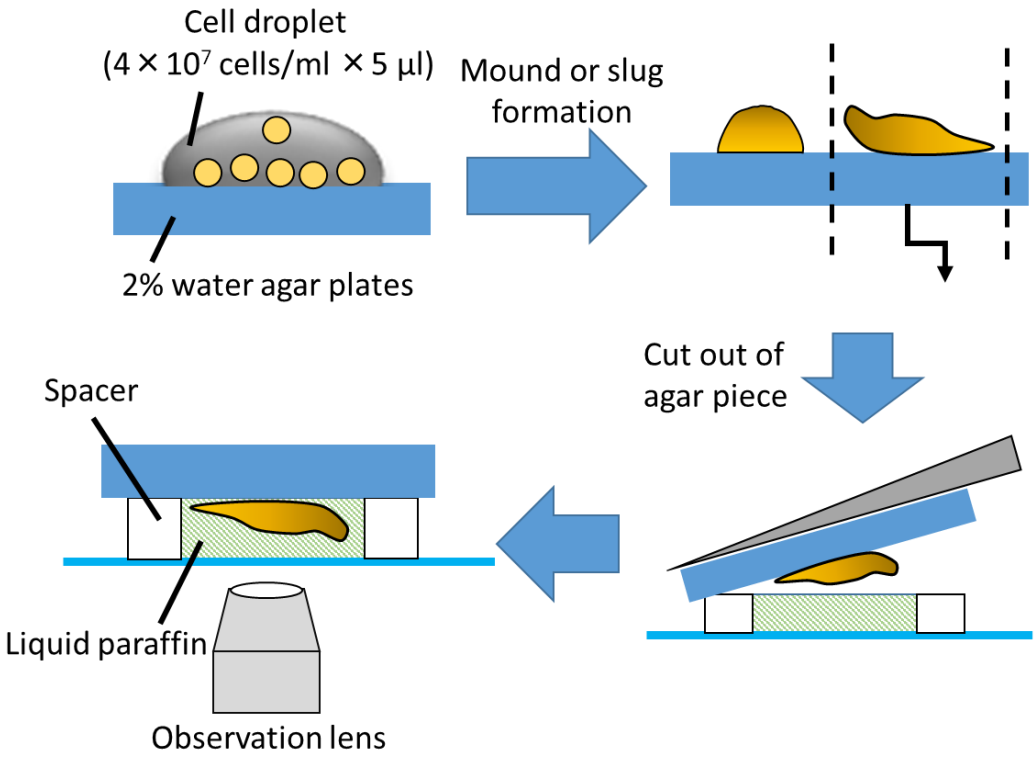


**Figure 4. Experimental scheme of observing multicellular stages.**

Here, a piece of agar was cut out and placed upside down on a 35-mm glass bottom dish (12 mm diameter glass, Iwaki) directly or on a spacer (thickness: 50, 100 or 150 μm) attached to the dish. The spacer was filled with liquid paraffin (Nacalai Tesque) which has the approximately same refraction index as slugs and can avoid scattering of observation light. To prevent desiccation during the observation, piece of wet paper was placed in the dish and the agar piece was covered with liquid paraffin and the dish was sealed with parafilm. In this condition, movements of cells and multicellular bodies were not restricted and their development proceeded normally for more than 12 h under the microscope. The Z series of fluorescence images was taken by the confocal microscope at 10–30 s intervals.

In addition to the methods for observation of slugs described above, I also applied the "mini slug" technique for efficient cell tracking in slugs (Bonner, 1998; Rieu et al., 2004), because three-dimensional (3D) scroll movement of the slug, thickness of the tissue and large number of cells in slugs (~$10^5$) make it difficult to follow individual cell movements in normal slugs. 1 μl of cell suspension at a density of $4\times10^7$ cells/ml was deposited on 2% water agar plates together with 2 μl liquid paraffin. A coverslip was placed over the suspension and the chamber was incubated at 22ºC for more than 15 h to allow mini slug formation (**Fig. 5a**). The Z series of the fluorescent images was acquired at 15-s intervals for 20–30 min by the confocal microscope. Because the mini slug has only few (~ 4) cell layers (**Fig. 5b**) and 3D scroll movement of slugs was restricted by enclosing glass and agar, efficient tracking of cell movements in slugs was possible compared with normal slugs. The mini slugs showed similar properties with normal slugs with respect to cell movement and proportion of cell types (**Fig. 5c**: Bonner, 1998; Rieu et al., 2004).

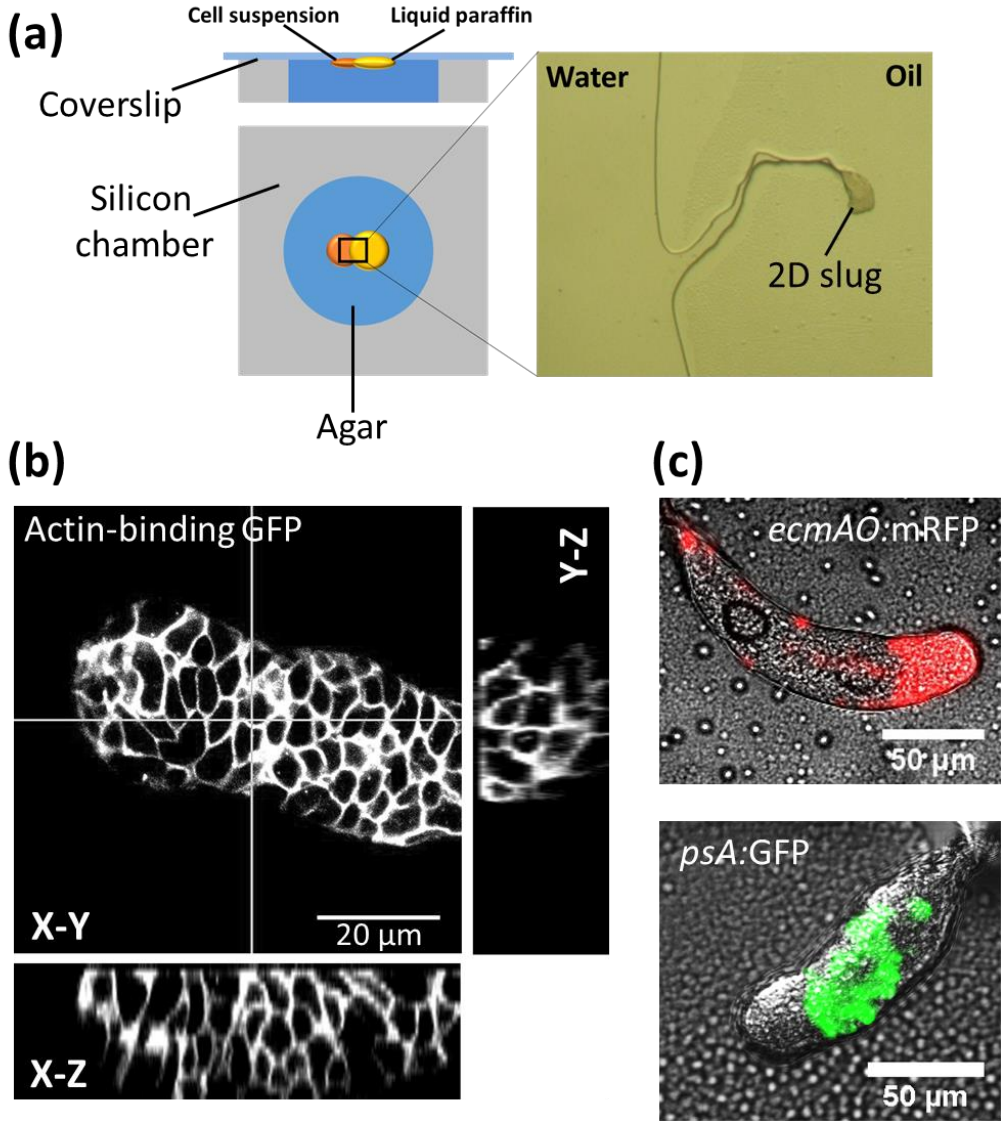


**Figure 5. Properties of the "mini slug".**

(a) Experimental scheme of mini slug formation. Mini slugs were formed at the boundary of water and liquid paraffin under the two-dimensionally confined condition. (b) Three-dimensional structure of mini slug taken by a confocal microscope. Cell contour is visualized by fluorescence labeling of cell cortex with GFP fused with actin-binding domain. (c) Proportion of cell type in mini slugs. *ecmAO*:mRFP and *psA*:GFP are prestalk and prespore cell marker, respectively. In mini slugs, prestalk cells accounts for anterior 1/3 region of the slugs, while the posterior 2/3 region consists of prespore cells, like normal slugs (see **Fig. 1**).

**6. Verification of Flamindo2 as an indicator of $[cAMP]_i$ changes in *Dictyotelium* cells at the unicellular stage.**

To examine the response to cAMP stimulation of starved cells which have an ability of cAMP relay, chemotactic-competent cells were prepared as follows: cells expressing Flamindo2 or Citrine were harvested and washed as described in **Section 5**. Cells were resuspended in 1 ml of developmental buffer (DB: 5 mM $Na/KPO_4$, 2 mM $MgSO_4$, 0.2 mM $CaCl_2$, pH 6.5) at a density of $5\times10^5$ cells/ml and settled on 35-mm dish for 1 h, and incubated for a subsequent 5 h in the presence of 100 nM cAMP pulses given at 6-min intervals. Cells were then washed three times with 1 ml DB and resuspended in DB at a density of $10^6$ cells/ml. 40 μl of the cell suspension was deposited onto a glass bottom dish. cAMP stimulation assay to chemotactic-competent cells were performed under a microscope as follows: cells were stimulated by adding 160 μl cAMP solution (the target concentration of cAMP) to 40 μl of the cell droplet under microscopic observation. In caffeine treatment experiments, cells were exposed to 4 mM caffeine in DB for 30 min on a glass bottom dish and then stimulated by cAMP solution with 4mM caffeine. Fluorescent images were acquired by the confocal microscope at 5-s intervals during stimulation. Averaged fluorescence intensities of Flamindo2 or Citrine in 4–5 $\mu m^2$ regions positioned within the cytosol were measured at each time point.

To confirm that Flamindo2 which has an $EC_{50}$ of 3.2 μM to cAMP and Hill coefficient of 0.95 (Odaka et al., 2014), can cover the range of cytosolic cAMP levels in *Dictyostelium* cells through the development, I estimated intracellular cAMP concentrations based on three parameters reported in literatures: cAMP concentration (about 2–75 pmol/mg protein: Brenner, 1978; Meima & Schaap, 1999; Otte et al., 1986), protein amount per cell ($7\times10^{-8}$ mg/cell: calculated based on the notation that $10^9$ cells equals about 1 g wet cells, which equals about 70 mg protein (Aubry & Klein, 2006)) and cell volume (0.43 pl/cell: Waddell, 1988).

**7. Verification of proper function of Flamindo2 as the intracellular cAMP indicator at the slug stage.**

Cells expressing Flamindo2 and *ecmAO*::mRFPmars were harvested and washed as described in **Section 5**. 1 ml of cell suspension in KK2 buffer at density of $10^7$ cells/ml was deposited on entire surface of a 47-mm cellulose membrane filter (Advantec) and incubated at 21ºC for 12 h to allow slug formation. The slugs were harvested in KK2 buffer and dissociated into single cells by repeated passages through a 25 or 26G needle (Terumo) with a 1 ml syringe on ice (Inouye & Gross, 1993). Slug-dissociated cells were resuspended in DB at a density of $10^6$ cells/ml, and 40 μl of the suspension was deposited onto a 12-mm glass bottom dish. cAMP stimulation and caffeine treatment to slug-dissociated cells were performed as described in **Section 6**. Fluorescent images were acquired by the confocal microscope at 5-s intervals during stimulation. Averaged fluorescence intensities of Flamindo2 in 4–5 $\mu m^2$ regions positioned within the cytosol were measured at each time point. Cell types of slug-disaggregated cells were distinguished by the intensity of *ecmAO*::mRFPmars (cells show strong fluorescence signals of mRFPmars are prestalk cells).

I also performed the cAMP stimulation assay on intact slugs by microinjection of cAMP solution into water agar (**Fig. 6a**). Cells were developed on 2% water agar plates until slug formation as described in **Section 5**, and a piece of agar was cut out and placed directly on a glass bottom dish. To avoid light scattering and desiccation, the agar piece was covered with liquid paraffin. A Femtotip microcapillary (1 μm tip diameter, Eppendorf) filled with 10 mM cAMP diluted in ultrapure water was mounted onto a Femtojet pump and micromanipulator (Eppendorf). To visualize the diffusion of cAMP solution in the water agar after injection from the capillary, 10 μM TMR was added to the cAMP solution. The injection pressure and injection time were set to 1500 hPa and 0.1 s, respectively. In this condition, 20 pl of solution was emitted from the microcapillary. The volume of injected solution was estimated from the diameter of spherical droplets of the cAMP solution injected in a drop of liquid paraffin.

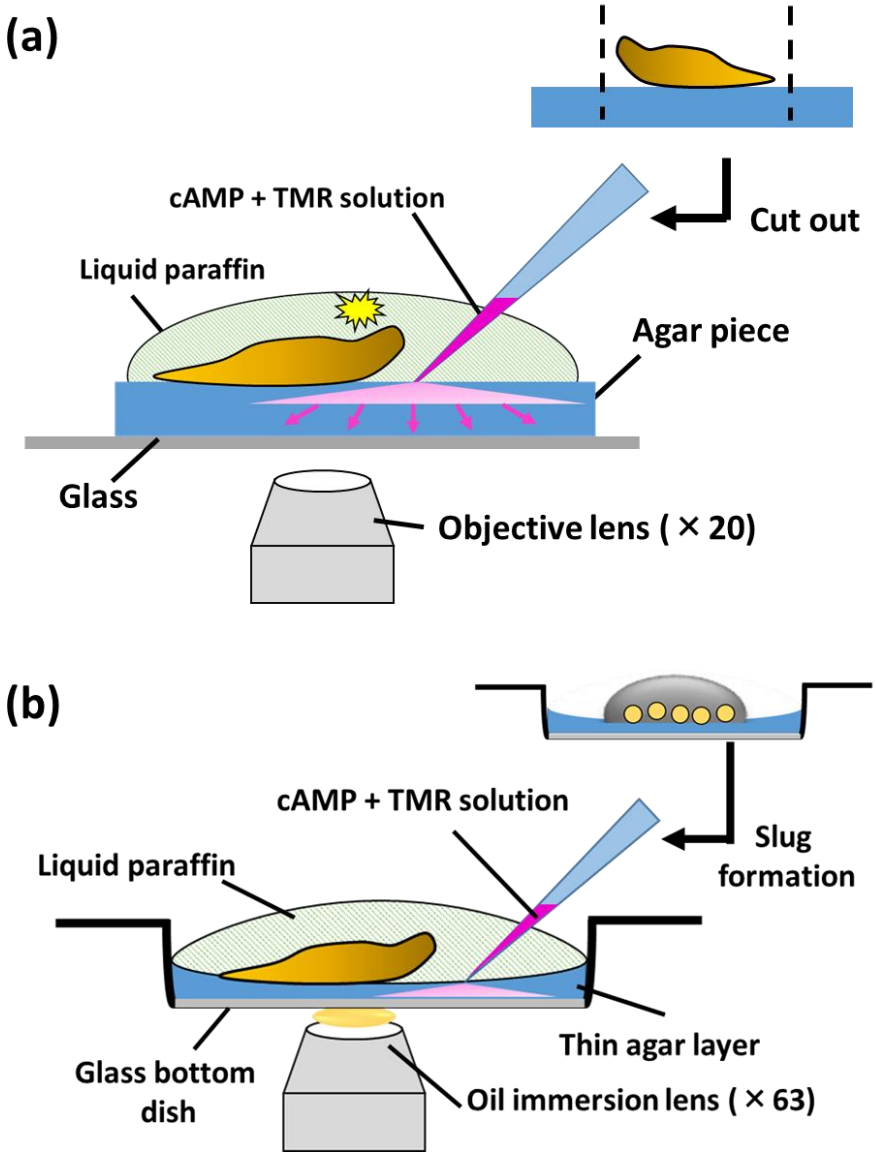


**Figure 6. Experimental scheme of cAMP microinjection assay to intact slugs.**

(a) cAMP microinjection assay under the condition of observing entire intact slugs. Slugs were developed on agar and agar piece mounting slugs was cut out to put on the glass. Slugs were stimulated by injection of cAMP solution from a microcapillary. (b) cAMP microinjection assay with high magnification. Slugs were developed on thin agar layer covered directly on a glass bottom dish. Response of slugs to cAMP stimulation was observed by ×60 oil immersion lens.

A tip of the capillary was touched to the agar surface near a slug, and cAMP solution was injected into the agar at a given time. The stimulation was applied at 6-min intervals as performed in a previous study (Dormann & Weijer, 2001). Fluorescent images of Flamindo2, TMR and DIC images were acquired at 15-s intervals by the epifluorescence microscope.

**8. Investigation of $PH_{AKT/PKB}$-GFP translocation to cAMP-stimulated cells dissociated from multicellular bodies or intact slugs.**

Cells expressing $PH_{AKT/PKB}$-GFP were harvested and washed as described in **Section 5**. Cell suspension was deposited on a cellulose membrane filter at a density of $5\times10^5$ cells/$cm^2$ as described in **Section 7** and incubated at 21ºC for 12 h to allow slug formation, or 5 μl of cell suspension at a density of $4\times10^7$ cells/ml was deposited on 2% water agar and incubated at 21ºC for 6 h to allow loose mound formation. Mechanical dissociation of cells from loose mounds or slugs was performed as described in **Section 7**. 40 μl of the cell suspension in DB (loose mound cells, $5\times10^5$ cells/ml; slug cells, $2\times10^6$ cells/ml) was deposited onto a 12-mm glass bottom dish and settled for 5 min (loose mound cells) or 20 min (slug cells) to allow cell attachment. Cells were stimulated by 10 μM cAMP under microscopic observation as described in **Section 6.** Fluorescent images were acquired by the confocal microscope at 5-s intervals during stimulation. Averaged fluorescence intensities of $PH_{AKT/PKB}$-GFP in 4 $\mu m^2$ regions positioned within the cytosol were measured at each time point.

In addition, we also performed the cAMP microinjection assay on intact slugs expressing $PH_{AKT/PKB}$-GFP as **Section 7** to investigate the response of $PH_{AKT/PKB}$-GFP in intact slugs to cAMP stimulation. To acquire fluorescent images of $PH_{AKT/PKB}$-GFP localization in slug cells with high magnification, slugs were formed on thin agar covered directly on the glass bottom dish. This observation condition was prepared as follows: 100 μl of melting agar was poured into a well of 12-mm glass bottom dish and then 65 μl of agar was sucked up, resulting in the formation of a uniform thin agar layer on the glass. 5 μl of cell suspension at a density of $4\times10^7$ cells/ml was dropped at the center of the thin agar layer and incubated at 21ºC for 12 h to allow for slug formation (**Fig. 6b**).

The manipulation of cAMP microinjection was performed as described in **Section 7**.

**9. Induction of *acaA*-null cell aggregation and slug formation by exogenous cAMP pulses.**

To induce the development of *acaA*-null cells which do not aggregate at normal experimental condition described in **Section 5**, the method by Pitt et al. (1993) was applied with some modification. *acaA*-null cells expressing Flamindo2 were harvested and washed as described in **Section 5.** 1 ml of cell suspension in DB at a density of $6\times10^6$ cells/ml was settled on a 35-mm plastic dish (Iwaki) and incubated for 4 h in the presence of 30 nM cAMP pulses given at 6-min intervals. Cells were then washed and suspended in 1 ml DB again and subsequently incubated on a 35-mm plastic dish or a 35-mm glass bottom dish (with 27-mm diameter glass, Iwaki) for more than 12 h with 30 μM cAMP pulses given at 60-min intervals. This treatment induced cell aggregation and clump formation of *acaA*-null cells in DB. After terminating the exogenous cAMP pulse treatment, *acaA*-null cells were washed and resuspended in DB at a density of about $4\times10^7$ cells/ml. Because a submerged culture as described above inhibits the multicellular development of even wild-type cells, 5 μl of cell suspension was dropped on 2% water agar plates and incubated at 21ºC for more than 5 h to allow the multicellular development. Fluorescence and DIC images during the development were acquired at 30-s intervals by the confocal microscope. I confirmed that the clumps of *acaA*-null cells formed after cAMP pulse treatment could not synthesize cAMP in response to external cAMP signals by monitoring Flamindo2 signals. After the cAMP pulse treatment, the cell clumps were washed by DB three times and then resuspended in 450 μl DB on a glass bottom dish. 50 μl of 1 mM cAMP (final concentration: 100 μM) was applied to the dish under the microscopic observation. Fluorescent images were acquired by the confocal microscope at 5-s intervals during the stimulation. Average intensities of Flamindo2 in a 25 $\mu m^2$ region positioned on the cell clumps were measured at each time point.

**10. Monitoring the effect of caffeine treatment on slug migration.**

Cells expressing Citrine were harvested and washed as described in **Section 5**. 5 μl of cell suspension in KK2 buffer at a density of $4\times10^7$ cells/ml was deposited on a cellulose membrane filter and incubated at 21ºC for 12 h to allow for slug formation. A piece of filter was cut out and placed upside down on a spacer (thickness, 100 μm) which was attached to a glass bottom dish and filled with liquid paraffin. A piece of 2% water agar with or without 4 mM caffeine was then put on the filter. For caffeine treatment to slugs, the dishes were settled for 5 min before observation to allow the caffeine to permeate through the filter. Fluorescence images were acquired at 30-s intervals for 30 min by the confocal microscope. Slug migration distance was quantified by measuring the displacement between the positions of the slug tip at 0 and 30 min. Because the speed of slug migration is proportional to the slug size (Inouye & Takeuchi, 1979), the migration distance for 30 min divided by each slug length was regarded as the migration rate which is an index of migration independent of slug size.

**11. Immunoblot analysis.**

Cells were harvested, washed and developed on a cellulose membrane filter as described in **Section 5 and 7**. Developed cells were harvested at 5 and 12 h after starvation. Vegetative and developed cells were lysed by 4 × SDS sample buffer (Wako Pure Chemical Industries, Ltd.) and boiled at 95 ºC for 5 min. Proteins from $4\times10^5$ cells were loaded on polyacrylamide gel (SuperSep™ Ace, 5-20% ,Wako) and SDS-PAGE were performed. Proteins on the gel were blotted onto a polyvinylidene difluoride membrane (PDM) and PDM was blocked with blocking solution (1% skim milk in TBS-T) for 1h. After washing, PDM was then reacted with polyclonal anti-GFP antibody (Anti-GFP pAb-HRP-DirecT, Medical & Biological Laboratories) diluted 1:1000 in blocking solution. Signals were visualized by the chemiluminescence of reactions with HRP substrate (Luminata™ Forte Western HRP Substrate, Millipore), and images were acquired with ChemiDoc™ XRS (BioRad).

**12. Gene expression analysis through the *Dictyostelium* development.**

To examine gene expression pattern in wild type and *gbfA*-null cells at each developmental stages, qRT-PCR analysis was performed. Cells were collected and developed on the filter as described in **Section 5 and 7.** Then the developed cells were harvested at 5, 7, 10 and 12 hours after starvation. Total RNA was extracted by the RNeasy mini kit (QIAGEN) and the contaminating genomic DNA was removed using DNase I (RNase-Free DNase Set, QIAGEN). cDNA was synthesized by reverse transcription of 1 μg total RNA using random hexamers and PrimeScript RT$^{TM}$ Reagent Kit (Takara Bio). qPCR amplifications were performed using PowerUp$^{TM}$ SYBR Green Master Mix (Applied Biosystems) and primer pairs listed in **Table 3** on Step One Real Time PCR System (Applied Biosystems). The results were analyzed using the relative standard curve method with the amplification of *rnlA* and *DDB_G280765* as controls (Chen et al., 2017; Parikh et al., 2010).

| Primer name | Sequence (5'- 3') |
|---|---|
| *acaA* qPCR Forward | AATGTCTGATTTCGCTTTGGAT |
| *acaA* qPCR Reverse | CTGATACCGATACAACCAGCAA |
| *carA* qPCR Forward | TTGCATGTTTTTGTGCTACCTC |
| *carA* qPCR Reverse | ATAACAAGGGAAACCACCATTG |
| *dagA* qPCR Forward | GCAGGTGGAAATGGTAAAGGA |
| *dagA* qPCR Reverse | TGTGGTTCTTGTTTATCGTCTGG |
| *DDB_G280765* qPCR Forward | TGGAGGTTGTGCTTCTGGTG |
| *DDB_G280765* qPCR Forward | TGGTTGGAGTTGAAATTGGTG |
| *gpaB* qPCR Forward | TGCATCATCAATGGAAGGAGA |
| *gpaB* qPCR Reverse | CCAGATTCACCAGCACCAAG |
| *Ig7* (*rnlA)* qPCR Forward | AATTTAAAGGAGGCGCTGGT |
| *Ig7* (*rnlA)* qPCR Reverse | TACCGCCCCAGTCAAACTAC |

**Table. 3 List of primers using qRT-PCR in this study.**

## Results

**1. Verification function of the genetically-encoded fluorescence indicator in *Dictyostelium* cells for monitoring $[cAMP]_i$ changes in response to external cAMP.**

To investigate cAMP relay in collective cell migration during the development of *Dictyostelium* cells, I monitored $[cAMP]_i$ changes, which is caused by external cAMP signals and thus an index of cAMP relay, by using a genetically-encoded fluorescence cAMP indicator, Flamindo2 (Odaka et al., 2014). The Flamindo2 sequence encodes a YFP variant, Citrine, whose sequence is separated by inserting the cAMP binding domain of mouse Epac1 inside it. The increase in concentration of cAMP binding to Epac domain in the probe causes a decrease in the fluorescence intensity of the probe (**Fig. 7a**). Thus, it can be expected that the dynamics of cAMP signaling (cAMP relay) in cell populations are visualized by the changes in fluorescence intensity of the probe in cytosol (**Fig. 7b**). Flamindo2 could be expressed uniformly in cytosol under constitutive active promoter at both unicellular and multicellular stages (**Fig. 8a**). Immunoblot analysis also confirmed that Flamindo2 was stably expressed in *Dictyostelium* cells at both unicellular and multicellular stages (**Fig. 8b**). Expression of the probe causes no obvious toxic effects in the developmental progression (**Fig. 8c**). The purified Flamindo2 has an $EC_{50}$ of 3.2 μM to cAMP and Hill coefficient of 0.95 (Odaka et al., 2014), which covers the range of cytosolic cAMP levels measured biochemically in unstimulated and cAMP-stimulated *Dictyostelium* cells at all development stages (0.3–12 μM, **Table 4**) (Brenner, 1978; Meima & Schaap, 1999; Otte et al., 1986). Therefore, Flamindo2 can be expected as the optimal tool for monitoring $[cAMP]_i$ dynamics through the *Dictyostelium* development.

To assess the function of Flamindo2 as the cytosolic cAMP indicator in *Dictyostelium* cells, I investigated whether the probe can detect $[cAMP]_i$ changes in chemotactic-competent cells induced by external cAMP stimulation (see **Fig. 2a)**. Due to the fluorescence property of the probe, the inverse of the fluorescence intensity of the probe increases when the $[cAMP]_i$ in cells is elevated. Throughout this study, $[cAMP]_i$ changes in cells monitored by Flamindo2 was shown by the inverse of the fluorescence intensity of the probe.

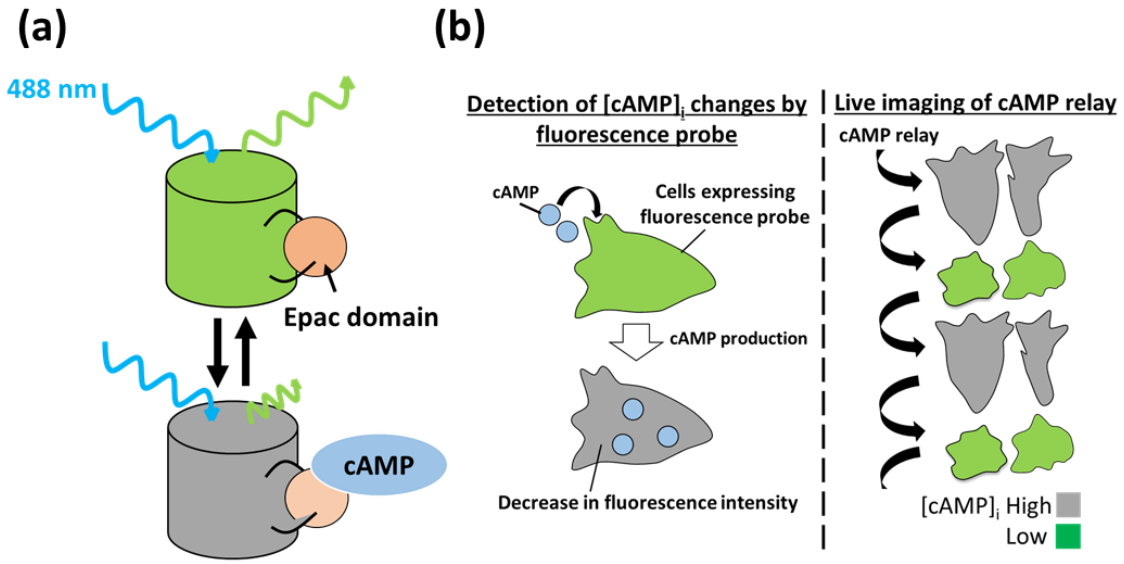


**Figure 7. Principle of live imaging of cAMP signaling dynamics in *Dictyostelium* cells using Flamindo2.**

(a) Fluorescence characteristics of Flamindo2. Flamindo2 was excited with 488-nm laser. The fluorescence intensity of the probe decreases when cAMP binds to Epac domain inserted into Flamindo2. (b) Visualization of $[cAMP]_i$ dynamics in *Dictyostelium* cells. When the $[cAMP]_i$ of cells expressing Flamindo2 increases in response to external cAMP signals, the changes in $[cAMP]_i$ can be detected by the decrease of fluorescence intensity of the probe in cytosol (right). If periodic external cAMP signals are propagated in the cell population which causes cooperative oscillation of $[cAMP]_i$, such cell-cell communication can be visualized by the oscillation and propagation of fluorescence signals of the probe (left).

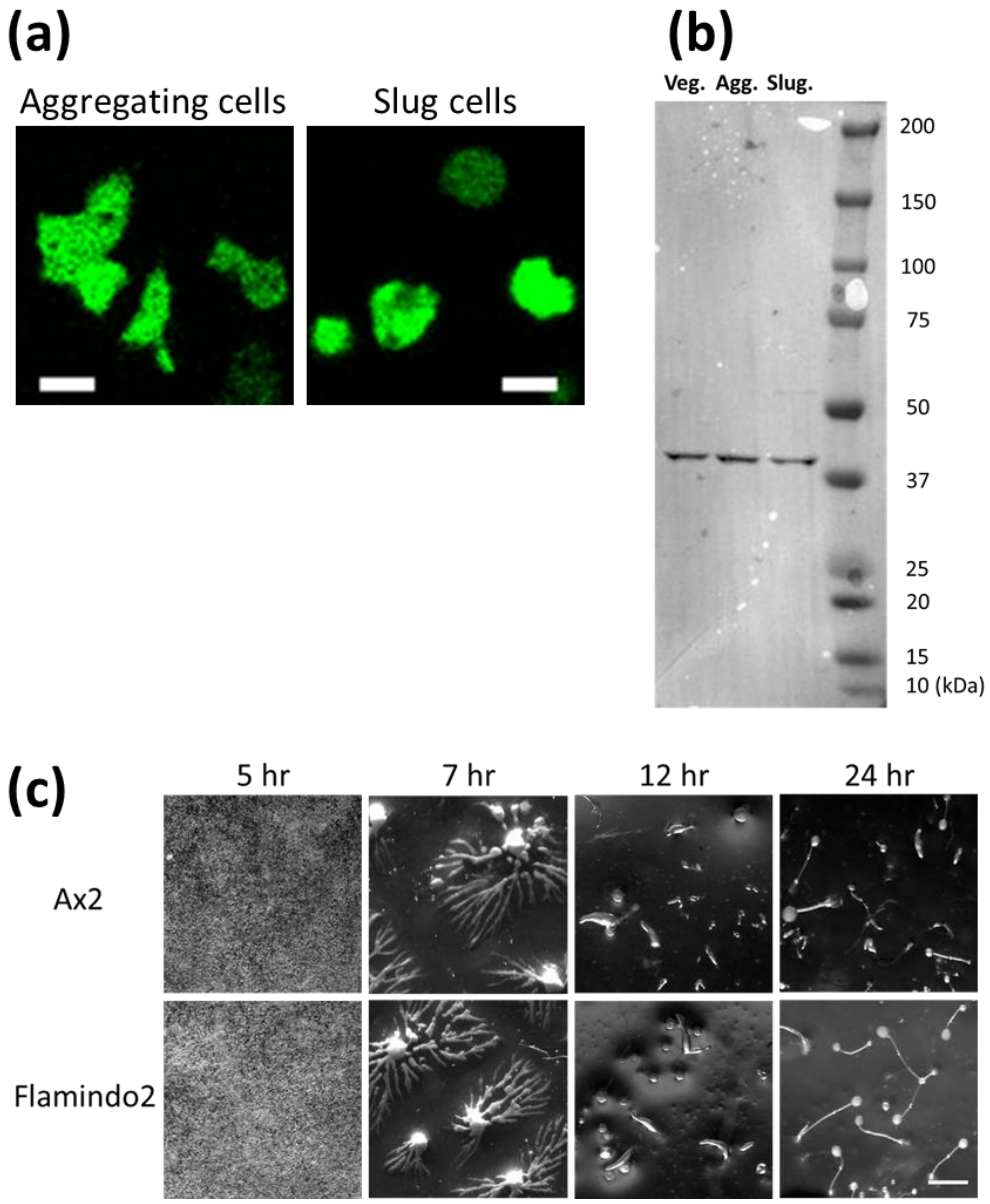


**Figure 8. Stable expression of Flamindo2 in *Dictyostelium* cells through development without obvious defect in the development process.**

(a) Fluorescence images of cells expressing Flamindo2 under the control of constitutive active promoter *act15*. Left, aggregating cells (unicellular phase). Right, cells dissociated from slugs (multicellular phase). Scale bar, 10 μm. (b) Immunoblot analysis of lysates of cells expressing Flamindo2 at each developmental stage using a polyclonal anti-GFP antibody. Cells were developed and harvested 5 hr (early aggregation stage) and 12 hr (slug stage) after starvation. Veg, vegetative stage (development, 0 hr). Agg, early aggregation stage. Slug, slug stage. M, molecular weight marker. (c) Developmental time course of cells expressing Flamindo2. Panels show developmental stages of Ax2 cells (upper panels) and cells expressing Flamindo2 (lower panels) on agar. Aggregation (5 h), aggregating stream (7 h), tipped mounds and slugs (12 h), and fruiting bodies (24 h). Scale bar, 1 mm.

| | cAMP (pmol/mg protein) | cAMP (μM) | Reference |
|---|---|---|---|
| Vegetative cells (0h starvation) | 6 | 0.976 | Meima and Schaap, 1999 |
| Cells starved for 15h starvation on agar | 25 | 4.07 | Meima and Schaap, 1999 |
| Cells starved for 6h (peak value after stimulation by 5 μM 2'H-cAMP) | 75 | 12.2 | Meima and Schaap, 1999 |
| Prestalk or prespore cells dissociated from slugs (steady state) | 2-5 | 0.326-0.814 | Otte, et al., 1986 |
| Prestalk or prespore cells dissociated from slugs (Peak value after stimulation by 5 μM 2'deoxy-cAMP) | 17.5-20 | 2.85-3.26 | Otte, et al., 1986 |
| Cells starved for 5 h on Millipore filter | - | 3 | Brenner, 1978 |
| Cells starved for 5 h on Millipore filter | - | 1 | Brenner, 1978 |

**Table 4. Estimation of $[cAMP]_i$ of *Dictyostelium* cells based on the biochemical measurement.**

The values listed above were calculated as described in **Materials & Methods Section 6**.

The signals of the probe in the cytosol of wild-type cells showed transient changes with two peaks after external cAMP stimulation; the first peak occurred 15 s after the stimulation, and the second peak gradually appeared 90–120 s after (**Fig. 9a**, first panel). In cells lacking *acaA* which encodes ACA, the first peak of the response was weaker than in wild-type cells, and the second peak had completely disappeared (**Fig. 9a**, second panel). When wild-type cells were treated with 4 mM caffeine, which is the inhibitor of adenylyl cyclases (Alvarez-Curto, Weening, & Schaap, 2007), the second peak of the fluorescence intensity after the cAMP stimulation had again disappeared (**Fig. 9a**, third panel). It has been reported that cytosolic cAMP and cGMP levels show different response times to cAMP stimulation and that the first response of cytosolic cGMP levels ($[cGMP]_i$) elevation occurs within 10 s of the stimulation, but the $[cAMP]_i$ elevation occurs later (Gerisch et al., 1977). Biochemical assays and FRET-based imaging analyses has shown that the peak of cAMP production by ACA occurs 60–120 s after external cAMP stimulation (Sgro et al., 2015; van Es et al., 2001). Considering the fact that Flamindo2 shows affinity not only to cAMP but also to cGMP with lower affinity than cAMP (Odaka et al., 2014), these results suggest that the first peak is an effect of $[cGMP]_i$ elevation and that the second peak was due to only the increase in $[cAMP]_i$. This conclusion is also proved by the results of *gc*- cells, which lack all guanylyl cyclases encoded in *D. discoideum* genome (*gca* and *sgcA*) and have no cGMP production ability (Veltman & van Haastert, 2008). *gc*- cells show Flamindo2 signal responses with only one peak at 90 s after the stimulation (**Fig. 9a**, fourth panel). When wild-type cells expressing only Citrine instead of Flamindo2 in the cytosol were stimulated with cAMP, the fluorescence intensity showed no response (**Fig. 9b**), indicating that changes in the Flamindo2 signal were not caused by cell deformation or other signals. The response of probe signals was dose-dependent to the concentration of the applied extracellular cAMP ($EC_{50}$, 0.72 nM; **Fig. 9c**), which agree well with a previous report (Gregor et al., 2010). Thus, these results demonstrate that Flamindo2 can detect the $[cAMP]_i$ changes of chemotactic-competent cells in response to external cAMP signals.

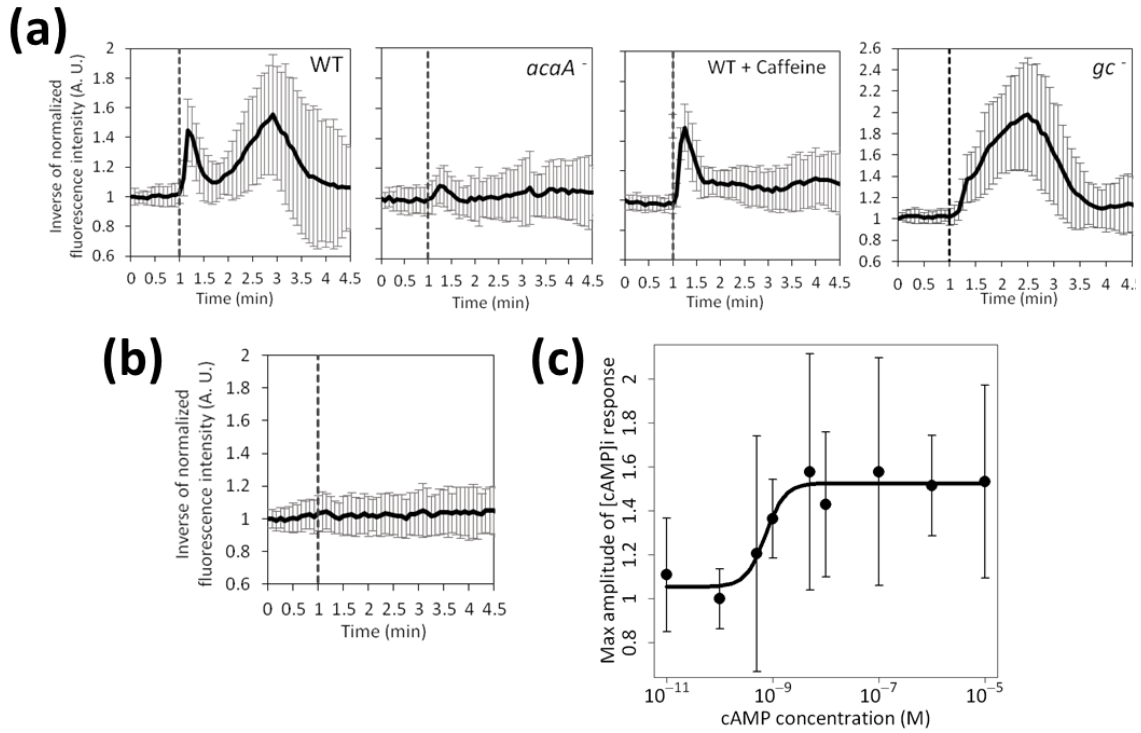


**Figure 9. Detection of $[cAMP]_i$ changes in response to external cAMP stimulation in chemotactic-competent cells by Flamindo2.**

(a) Time-course plots of Flamindo2 signals in chemotactic-competent cells after 10 μM cAMP stimulation. The inverse of the fluorescence intensity of Flamindo2 is plotted on the y-axis (mean ± SD: n = 30 cells in all panels). First panel, wild-type (Ax2) cells; second panel, *acaA*-null cells; third panel, wild-type cells treated with 4 mM caffeine; fourth panel, *gc*$^-$ cells. Dashed lines indicate the time point of the cAMP stimulation. (b) Time-course plot of the fluorescence intensity of Citrine in wild-type cells (expressing only Citrine and not Flamindo2) after 10 μM cAMP stimulation (n = 30 cells). (c) The dose-dependent curve of the $[cAMP]_i$ response to various cAMP stimulations (0.01 nM to 10 μM). The maximum amplitudes of the response were plotted against the cAMP concentration (mean ± SD). Sample number: 10 μM, n =30 cells; 10 nM, n = 19 cells; other data points, n = 20 cells.

The *act15* promoter used for expression of Flamindo2 throughout this study is the widely-used promoter as the constitutive active one among the researchers of *D. discoideum*, but its activity become somewhat lower after multicellular formation (Rosengarten et al., 2015) and the protein levels of Flamindo2 in slugs were actually less than those in aggregating cells (ca. 62%; **Fig. 10a**). Therefore, I assessed whether the protein expression levels affect the sensitivity of Flamindo2 in *Dictyostelium* cells. Fluorescence intensities of Flamindo2 show variation among the cell populations which reflects the heterogenous expression levels of the probe (**Fig. 8a**, **Fig. 10b**). Based on the fluorescence intensities in cells, cells were classified into three levels: low, moderate and high expression groups. The expression levels in the low group was about 30% that in the moderate group. In spite of the difference of expression levels, all groups showed similar responses to external cAMP stimulation at both high and low concentration (**Fig. 10c–f**). Therefore, the sensitivity of Flamindo2 was independent of the expression level variation throughout the development.

**2. Monitoring of $[cAMP]_i$ propagation and oscillations in cell populations during aggregation phase by Flamindo2.**

To see whether Flamindo2 is applicable to the monitoring of $[cAMP]_i$ during the development of *Dictyostelium* cells, I examined cell populations in the aggregation stage, which is the well-documented event as the collective cell migration organized by cAMP relay (Gregor et al., 2010; Tomchik & Devreotes, 1981). Fluorescence time-lapse imaging showed that aggregating cells expressing Flamindo2 on agar show oscillations of the probe signals and its propagation during aggregation and stream formation (**Fig. 11a–c)**. The spiral pattern of signal propagation is similar with the previous reports (Tomchik & Devreotes, 1981). The synchronous oscillations of Flamindo2 signals during aggregation were abolished by the pharmacological inhibition of ACA by caffeine treatment (**Fig. 11d**). Synchronous oscillations of Flamindo2 signals also could be seen in aggregating *gc*- cells (**Fig. 11e**). As expected, *acaA*-null cells did not aggregate (**Fig. 11f**) and showed no obvious oscillations of Flamindo2 signals after starvation (**Fig. 11g**). These demonstrate successful monitoring of ACA-dependent cAMP relay at the aggregation stage by using Flamindo2 similarly with a previous reports (Ohta et al., 2018).

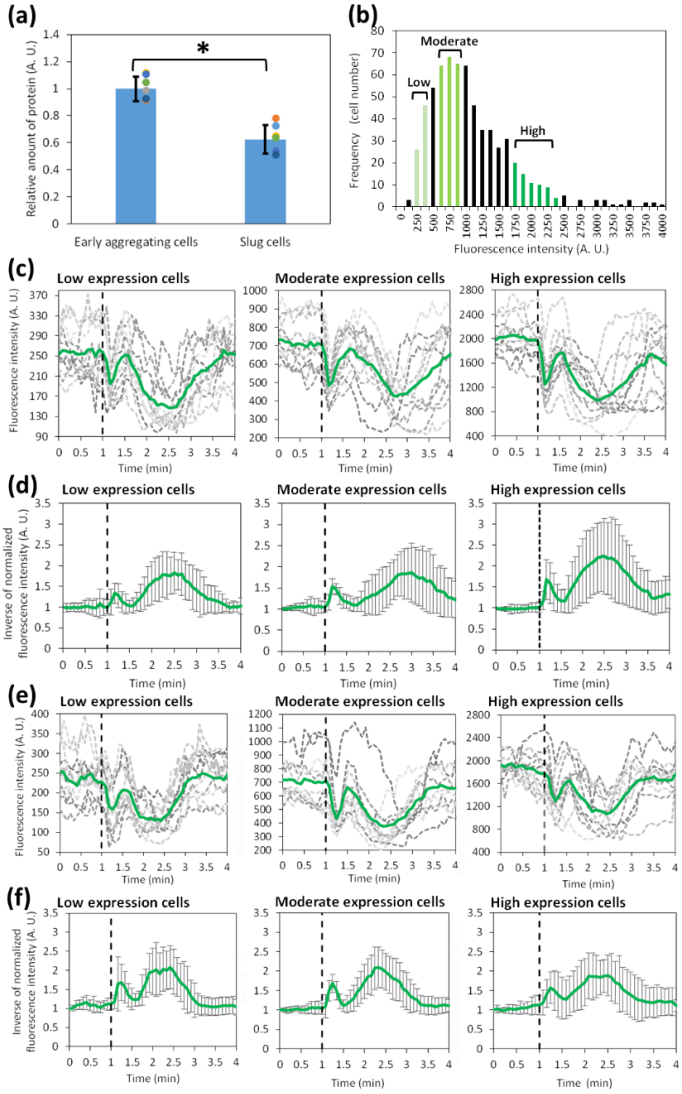


**Figure. 10 Sensitivity of Flamindo2 signal response to external cAMP stimulation was independent of Flamindo2 expression level.**

(a) Comparison of expression levels of Flamindo2 between aggregating cells (5 hr starvation) and slug cells. Chemiluminescent signals of Flamindo2 from immunoblot analyses were quantified and normalized (n = 7 samples). Dots plotted on the graph are original data point. *: $P < 10^{-7}$, Student's *t*-test. (b) Histogram of the fluorescence intensities of Flamindo2 in chemotactic-competent cells (n = 657 cells). Mean intensity of Flamindo2 in 5 $\mu m^2$ regions positioned in the cytosol of cells starved for 5 hr was measured. Based on the intensities, cells were classified into three representative groups: cells expressing Flamindo2 at low levels (125–375 A.U., light green), moderate levels (500–1000 A.U., green), and high levels (1625–2375 A.U., dark green). The expression levels in the low group (mean fluorescence intensity is about 250 A. U.) was estimated about 30% that in the moderate group (mean fluorescence intensity is about 750 A. U.). (c), (e) Time-course plots of Flamindo2 signals in cells of the three clades after (c) 10 μM or (e) 10 nM cAMP stimulation. The fluorescence intensity of Flamindo2 in 5 $\mu m^2$ regions positioned in the cytosol of cells was measured and plotted on the y-axis. In each graph, gray dashed lines show the data of 11 cells, and green lines show the average across those cells. (d), (f) Time-course plots of normalized Flamindo2 signals in cells of the three clades shown in (c) and (e), respectively. The fluorescence intensity of each cell shown in (c) and (e) was normalized at t = 0, and the inverse was averaged across the cells (mean ± SD). In (c) – (f), dashed black lines indicate the time points of the stimulation.

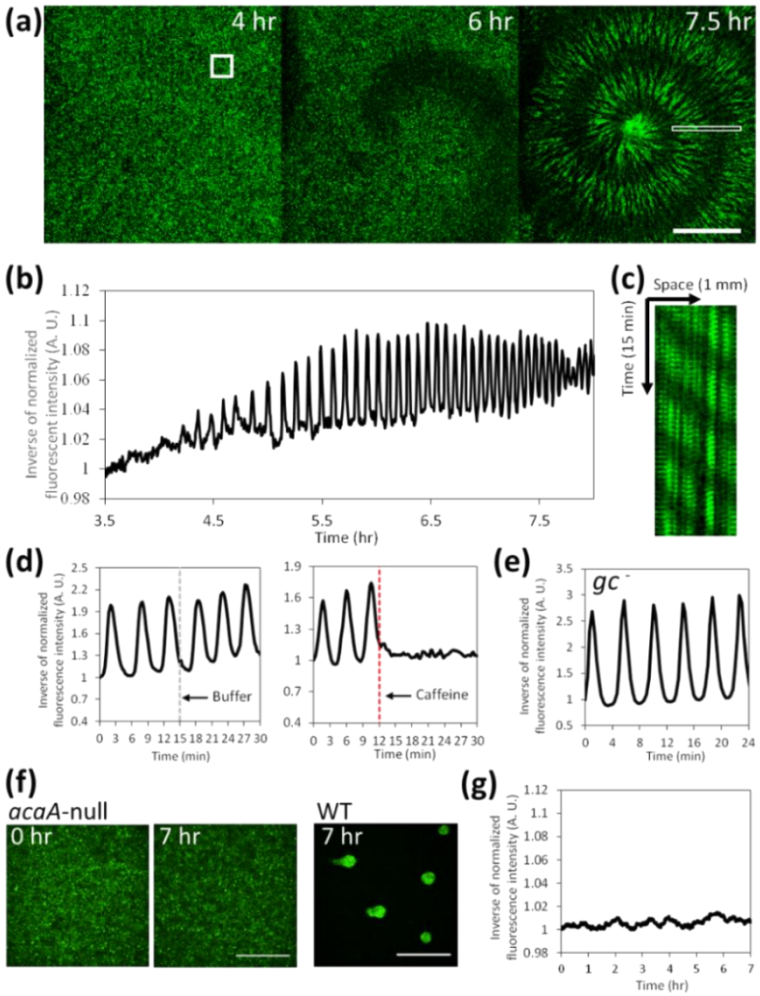


**Figure 11. Visualization of $[cAMP]_i$ oscillations and propagation in aggregating cell populations by Flamindo2.**

(a) Spiral pattern of $[cAMP]_i$ waves in cell populations at early aggregation. Fluorescence images of Flamindo2 in aggregating cell populations are shown. Scale bar, 1mm. Times after onset of starvation (hr) are indicated at the top lest of the images. Dark zones in the images represents the population of cells with high $[cAMP]_i$. (b) Time course plot of inverse Flamindo2 signals during aggregation. Data were obtained 3.5–8 hours after starvation. The mean intensity of Flamindo2 in a 300 $\mu m^2$ region in the cell population indicated by a white box in (a) was measured. (c) Kymograph of $[cAMP]_i$ wave propagation in the region indicated by a white rectangle (1000 × 50 μm) for 15 min duration in left panel of (a) (7.5hr). (d) Caffeine treatment inhibited the synchronous oscillations in the Flamindo2 signal. Cells were starved in developmental buffer (DB) on a glass bottom dish. DB with or without 4 mM caffeine (final concentration) was added to aggregating cell populations at the time points indicated by the dashed lines. The mean fluorescence intensity of Flamindo2 was measured in cell populations (318 $\mu m^2$ region). (e) *gc*- cell populations starved in buffer showed synchronous oscillations in the Flamindo2 signal during aggregation. The mean fluorescence intensity of Flamindo2 was measured in aggregating cell populations (250 $\mu m^2$ region). (f) Defect of aggregation and development in mutant cells lacking *acaA*. Fluorescent images of *acaA*-null and wild-type cells expressing Flamindo2 after starvation are shown. Wild-type cells formed mounds, while *acaA*-null cells did not aggregate after 7 hours of starvation. Scale bars, 500 μm. (g) Time course plot of Flamindo2 signals in *acaA*-null cells after starvation. The fluorescence intensity of Flamindo2 in a 100 $\mu m^2$ region in the left panels of (f) was measured.

### 3. Transition of cAMP signaling dynamics from oscillations to steady state during *Dictyostelium* development.

Using Flamindo2, I monitored the dynamics of cAMP relay at the each development stages of *Dictyostelium* cells. As shown in **Fig. 11a** and **Fig. 12a**, the propagation of $[cAMP]_i$ waves could be seen during aggregation and streams. At the loose mound stage, $[cAMP]_i$ waves showed rotational propagation (**Fig. 12b**). At the tight mound stage, $[cAMP]_i$ waves propagated from the top to the bottom of the mound with geometrical changes from loose mound stages (**Fig. 12c**). In both loose and tight mound stages, multiple cells migrate cooperatively toward the opposite direction of $[cAMP]_i$ wave propagation (e. g. direction of collective cell migration is the bottom to the top of tight mounds). In contrast, subsequent mound elongation and slug migration occurred without obvious $[cAMP]_i$ oscillations, but a stream flowing into the rear of the elongating slug showed wave propagation (**Fig. 12d**). These findings indicate the dynamics of cAMP signaling changes from propagating waves in aggregation, streams and mounds stages to steady state with no oscillations in the multicellular slug stage during *Dictyostelium* development. To characterize the transition of the cAMP signaling dynamics, I quantified Flamindo2 signals in cell populations from the onset of aggregation to the multicellular slug stage. Because the development of *Dictyostelium* cells which is transition from the unicellular to multicellular phase is three-dimensional morphogenetic process, Z-stack images of the entire cell populations were acquired by a confocal microscope at given time-internals (4D-imaging) and maximum z projection of images were used for analysis (**Fig. 13a**). During early aggregation, synchronized oscillations of $[cAMP]_i$ started with periods of about 6 min (**Fig. 13b, c (1)**). Such oscillations continued until mound formation (**Fig. 13b**). At the loose mound stage, the oscillations showed shorter periods of about 3 min (**Fig. 13c (2)**). However, the periods showed partial recovery and the similar value with the one at aggregation stage when the tight mound are formed. (**Fig. 13c (1), (3)**). In contrast to these development stages, when slugs were formed through mound elongation and tip formation, $[cAMP]_i$ oscillations became weaker and finally disappeared (**Fig. 13b and c (4)**). I further observed Flamindo2 signals of 24 migrating slugs for 20 minutes, but no slugs showed $[cAMP]_i$ oscillations.

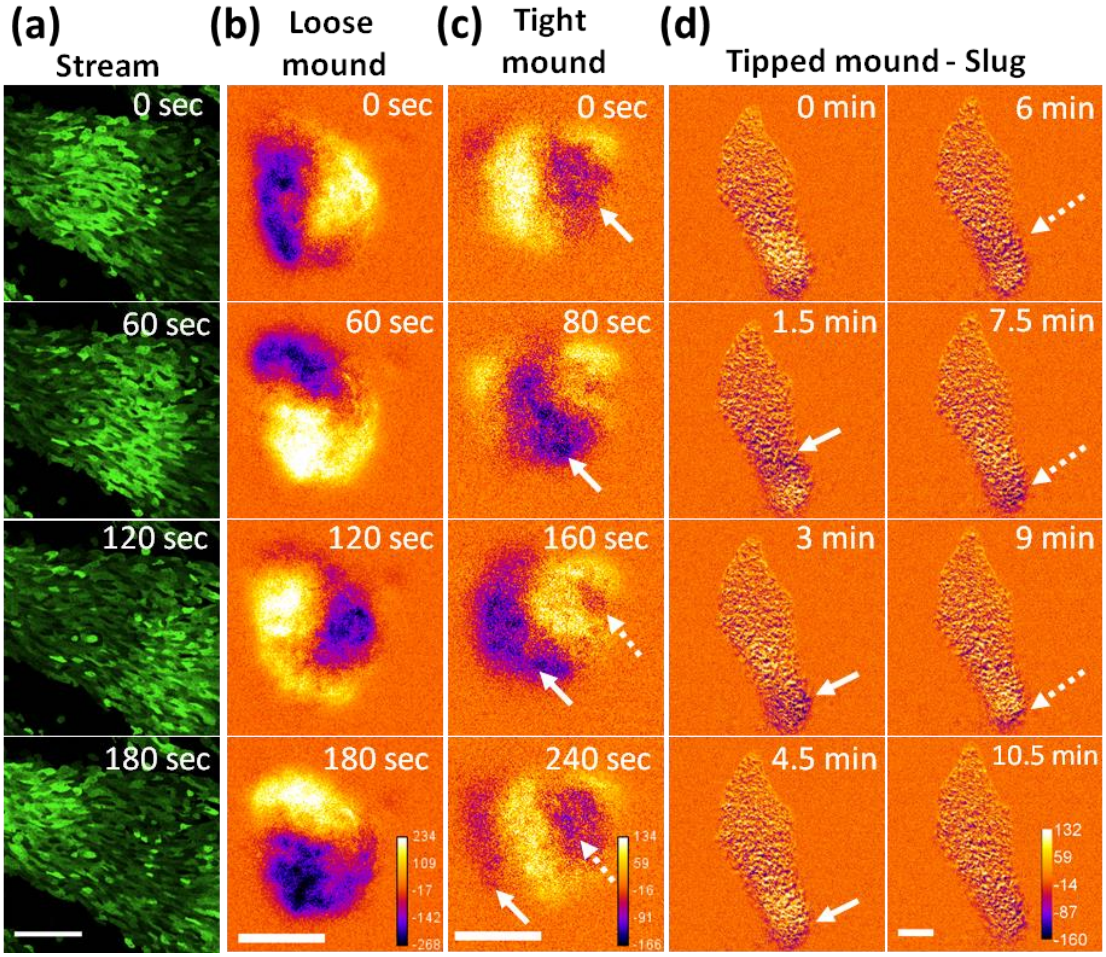


**Figure 12. Typical cAMP signaling dynamics at each developmental stage of *Dictyostelium* cells visualized by Flamindo2.**

(a) Wave propagation in an aggregating stream. (b) Rotational propagation in a loose mound. (c) Wave propagation from the top of a tight mound (right side of images) to the bottom. (d) A slug with a stream elongating toward the top of the images. Anterior part (top) of the slug faces the top side of the image. In (b)–(d), images were subtracted at 3–6 frame intervals to emphasize changes in fluorescence intensity. Solid and broken arrows show the positions of the first and second waves in each sequential image, respectively. Scale bars, (a) and (d) 100 μm, (b) and (c) 50 μm.

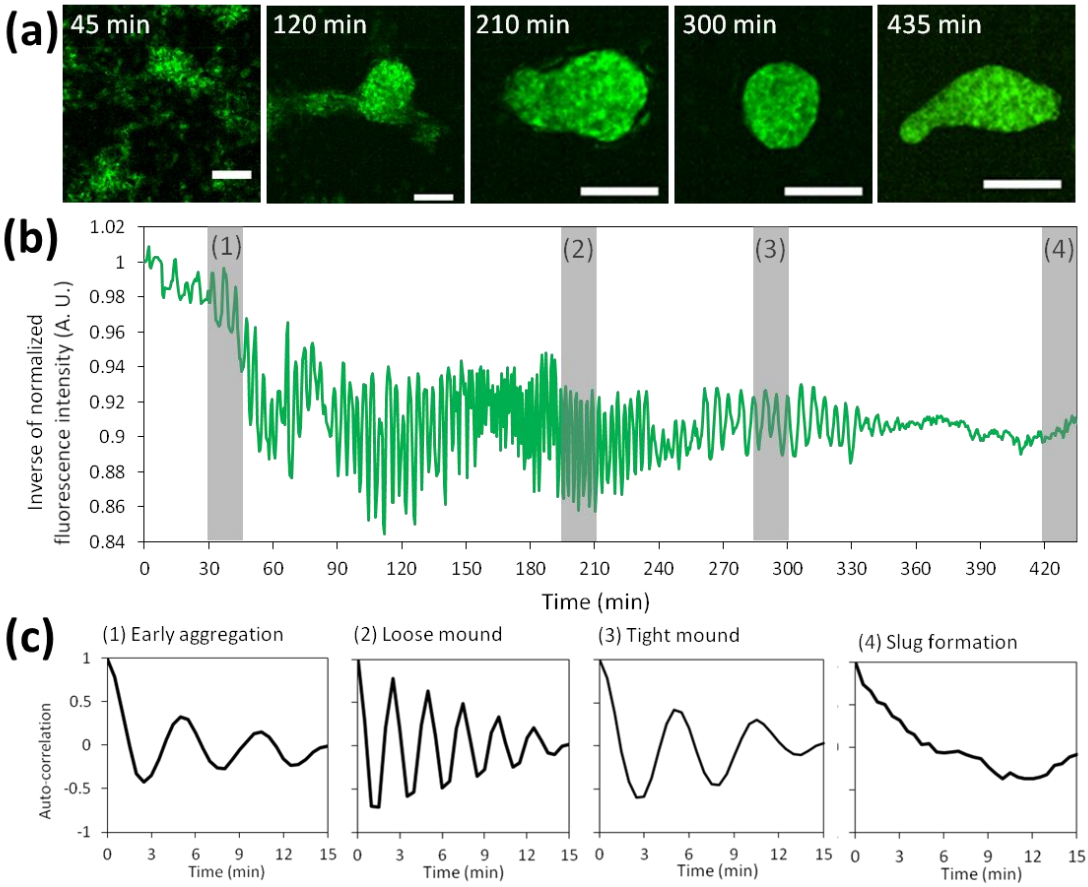


**Figure 13. Monitoring of $[cAMP]_i$ dynamics from the onset of aggregation to slug formation by Flamindo2.**

(a) Fluorescent images of *Dictyostelium* cells expressing Flamindo2 in each developmental stage. Maximum intensity projections of Z-stack images are shown. Scale bars, 100 μm. (b) Time course plot of inverse Flamindo2 signals during development from the onset of aggregation to slug formation. Data were obtained 3.5–10.75 hours after starvation. The mean intensity of Flamindo2 in a 30 $\mu m^2$ region in the cell population shown in (a) was measured. (c) Autocorrelation of Flamindo2 signals at each development stage are shown by the gray bars in (b).

These data suggests the possibility that $[cAMP]_i$ signaling dynamics show the transition from the oscillation to no oscillation state during the multicellular body formation of *Dictyostelium*. Analyses of $[cAMP]_i$ signaling dynamics shown in **Fig. 13** are based on the measurements of averaged Flamindo2 signals in cell populations. However, this approach cannot demonstrate whether the apparent disappearance of the oscillations in multicellular bodies (**Fig. 13b and c (4)**) resulted from a desynchronization of oscillations between cells or a synchronous disappearance of the oscillations. To clarify the actual state of disappearance of the $[cAMP]_i$ oscillations, $[cAMP]_i$ dynamics during the damping of oscillations in an elongating mound was monitored at the single cell level by individual cell tracking based on the position defining from Histone2B-RFP signals (**Fig. 14a and b**). When the oscillation of Flamindo2 signals in the entire mound had almost disappeared (**Fig. 14c**, left: 25 min ~), oscillation in single cells vanished almost at the same time (**Fig. 14c**, middle and right). Thus, the disappearance of the $[cAMP]_i$ oscillations in the entire mound during multicellular formation was caused by a synchronous disappearance of oscillations in individual cells and thus one kind of phase transition phenomenon of cell-cell communication.

Next, using the system for monitoring the dynamics of individual cells (**Fig. 14b**), I investigated the relationships between $[cAMP]_i$ signal dynamics and cell movements. Simultaneous monitoring of Flamindo2 signals and cell velocity indicated that both parameters oscillated cooperatively during collective cell migration. The cell velocity oscillated with the same period as $[cAMP]_i$ (**Table 5**) and that the two oscillations had tight correlation with each other (**Fig. 15a–d**) at aggregation, stream, loose and tight mound stages. As shown in **Fig 13c,** the periods of oscillations at aggregation and tight mound stages showed the almost same value (5.62 ± 0.36 min, loose mound: 4.70 ± 0.56 min, tight mound) and were significantly longer than the value at loose mound stage (2.47 ± 0.28 min). Individual cell data and power spectrum analysis revealed that $[cAMP]_i$ oscillations in the cell populations had the same intervals and were synchronized at the single cell level, while the oscillations of the cell velocity showed some variation in the populations (**Fig. 16, 17**).

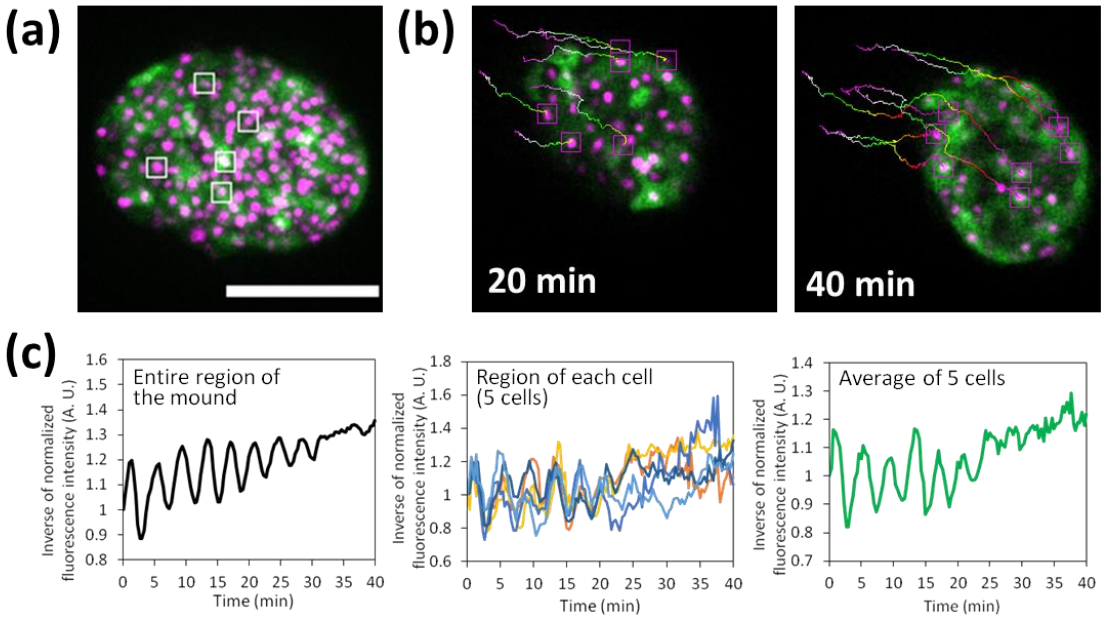


**Figure 14. Monitoring of $[cAMP]_i$ dynamics at single cell level in the mound during the disappearance of $[cAMP]_i$ oscillations.**

(a) A fluorescence image of Flamindo2 and Histone2B-RFP in an elongating mound. The maximum intensity projection of Z-stacks is shown. Scale bar, 50 μm. (b) Trajectories of tracked cells in elongating mounds. Cell positions at each time point was defined by the fluorescence signals of Histone 2B-RFP. (c) Time course plot of inverse Flamindo2 signals at the tissue (left) or individual cell level (middle and right) in the mound shown in (a). Left, average signals in the entire region of the mound. Middle, signals in 5 cells indicated by the white boxes in (d). In middle graph, individual cells were tracked as shown in (b), and Flamindo2 intensities within each cell were measured. Right, average of the signals in the middle graph.

| | Early aggregation | Loose mound | Tight mound | Slug |
|---|---|---|---|---|
| Periods of cell velocity (min) | 5.58 ± 0.47 | 2.48 ± 0.22 | 4.78 ± 0.31 | 5.32 ± 1.09 |
| Periods of $[cAMP]_i$ oscillation (min) | 5.62 ± 0.36 | 2.47 ± 0.28 | 4.70 ± 0.56 | ND |
| Phase difference between cell velocity and $[cAMP]_i$ oscillation (min) | 0.29 ± 0.29 | 1.26 ± 0.26 | 0.15 ± 0.12 | ND |

**Table 5. Periods of oscillation of $[cAMP]_i$ and cell velocity at three developmental stages.**

Mean values ± SD are shown. Sample numbers are as follows: 100 cells in 6 aggregation centers (early aggregation), 45 cells in 7 mounds (loose mound stage), 47 cells in 5 mounds (tight mound stage), and 20 cells in 11 slugs (slug stage). The periods of $[cAMP]_i$ oscillations and cell velocities in the loose mound stage are significantly shorter than those in the early aggregation and the tight mound stages ($P < 10^{-5}$: Student's *t*-test). ND, no detection of periodicity.

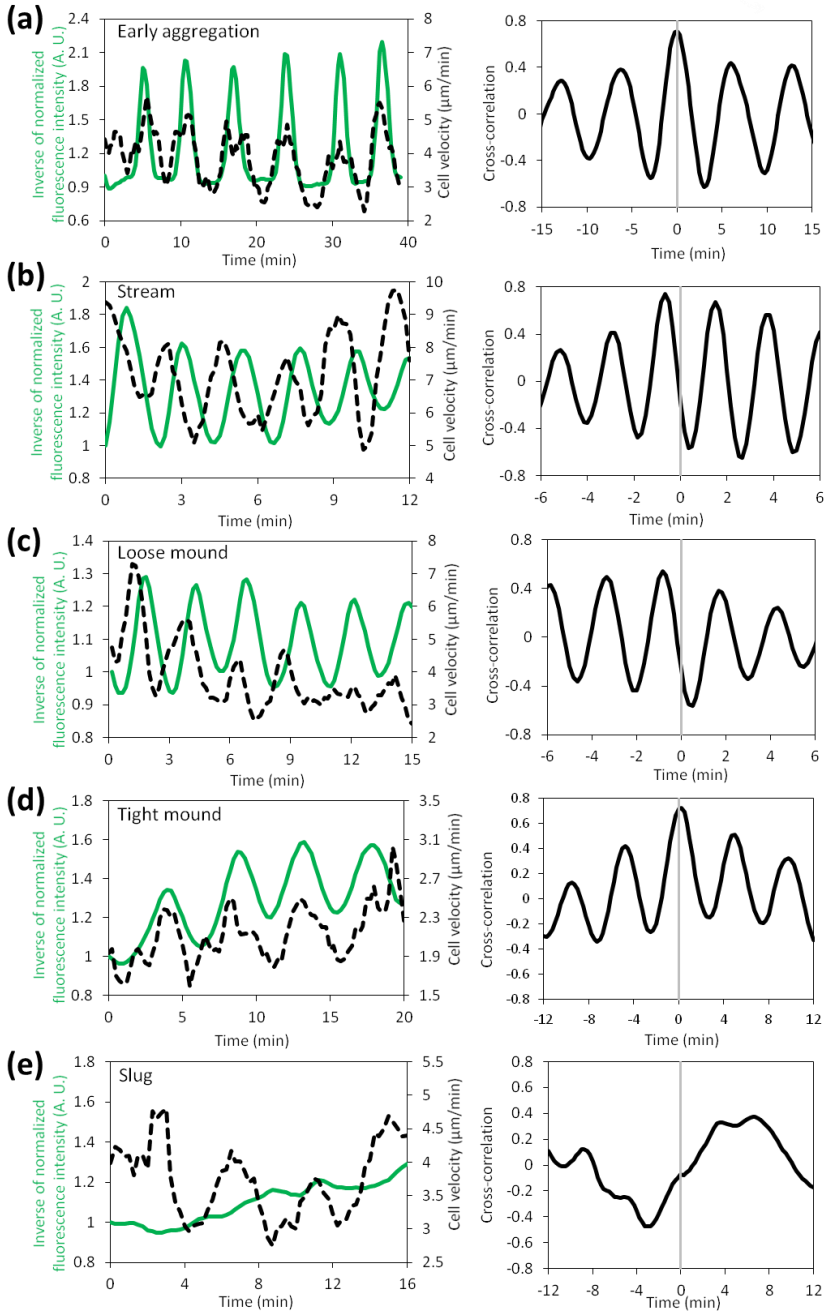


**Figure 15. Simultaneous monitoring of $[cAMP]_i$ and cell velocity in single cell levels at each developmental stage.**

Left graphs show time-course plots of $[cAMP]_i$ (green solid lines) and cell velocity (black dashed lines). Individual cells were tracked, and Flamindo2 intensities within each cell and cell velocities were measured. The signals of Flamindo2 and cell velocities were averaged across several representative cells, and the averages of representative cells are plotted against time. The curves of Flamindo2 signals and cell velocities were smoothed by a running average over four data points. Right graphs show the cross-correlation between $[cAMP]_i$ and cell velocity shown in the left graphs. (a) Early aggregation (n = 20 cells). (b) Aggregation stream (n = 14 cells). (c) Loose mound (n = 12 cells). (d) Tight mound (n = 10 cells). (e) Slug (n = 10 cells).

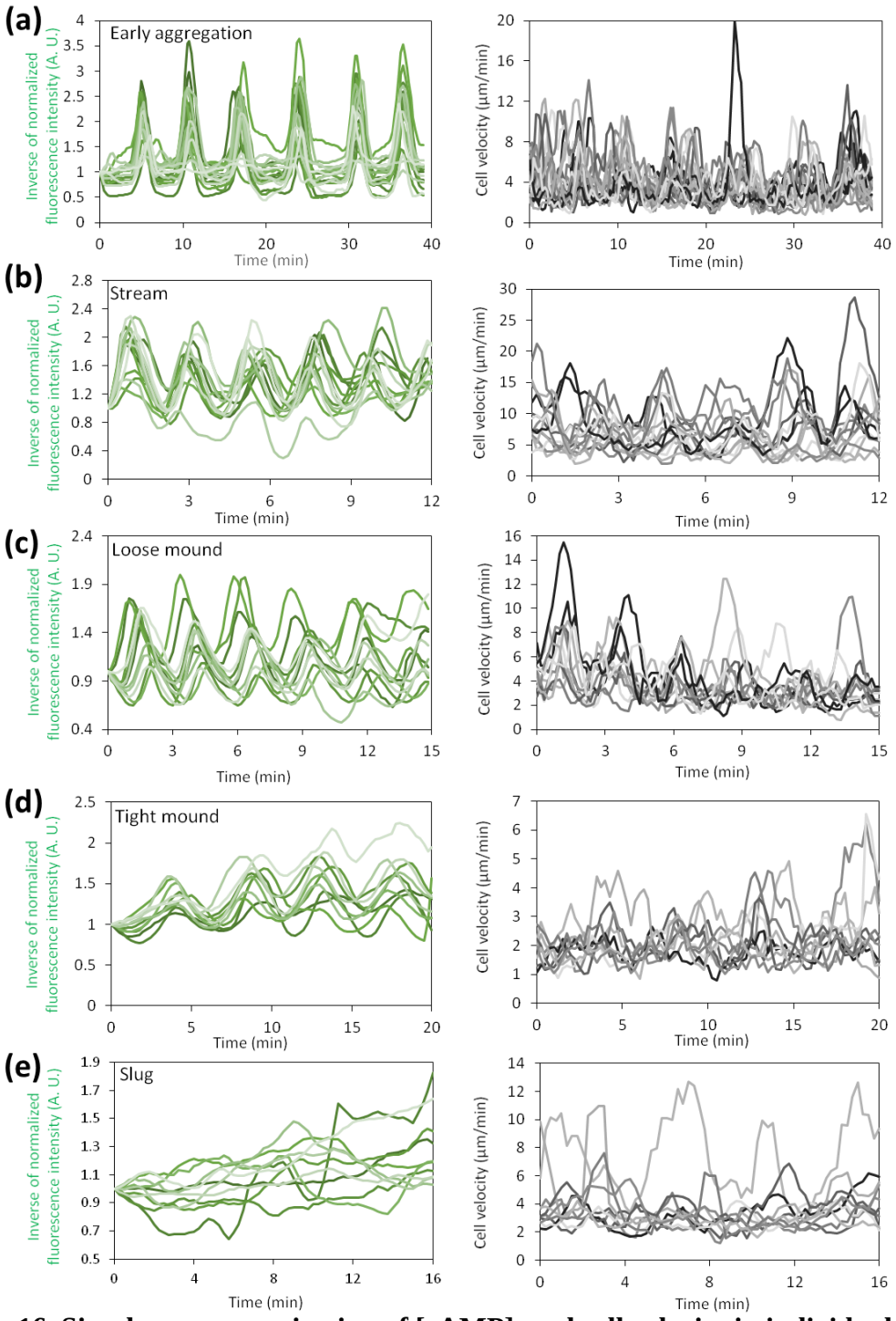


**Figure 16. Simultaneous monitoring of $[cAMP]_i$ and cell velocity in individual cells.** Data of individual cells as the basis of the average data shown in **Figure 15** are shown. Left graphs show Flamindo2 signals, and right graphs show cell velocities. The curves were smoothed by a running average over four data points. (a) Early aggregation (n = 20 cells). (b) Aggregation stream (n = 14 cells). (c) Loose mound (n = 12 cells). (d) Tight mound (n = 10 cells). (e) Slug (n = 10 cells).

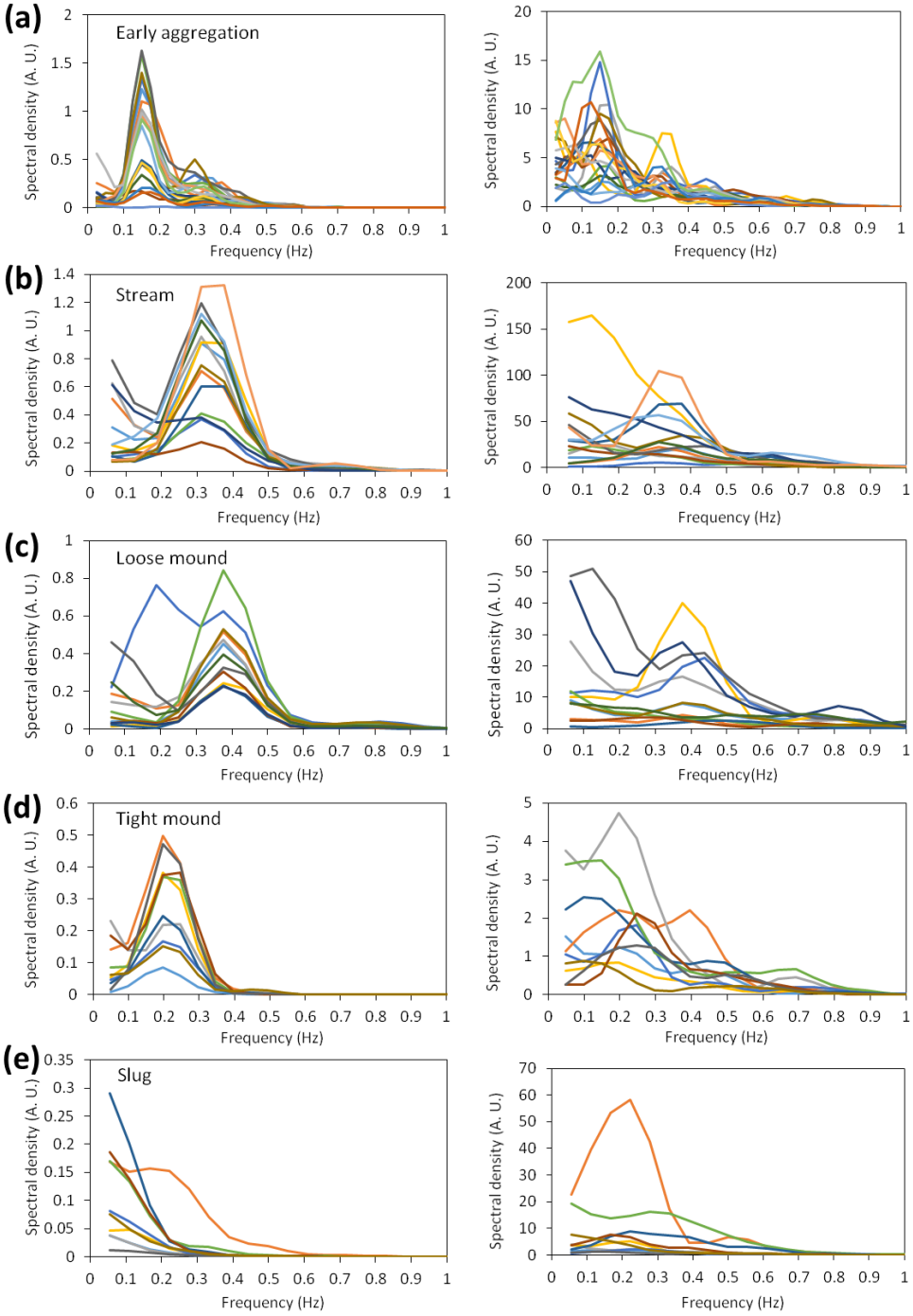


**Figure 17. Power spectrum of Flamindo2 signals and cell velocities of individual cells at each developmental stage.**

Power spectrum analysis was performed on the data of individual cells shown in **Figure 16**. Spectral densities plotted against the frequency are shown. Left graphs show Flamindo2 signals, and right graphs show cell velocities. (a) Early aggregation (n = 20 cells). (b) Aggregation stream (n = 14 cells). (c) Loose mound (n = 12 cells). (d) Tight mound (n = 10 cells). (e) Slug (n = 10 cells).

Furthermore, cross-correlation analysis indicated that there was a phase difference of a half period between the oscillation of $[cAMP]_i$ and cell velocity at the loose mound stage, but the two oscillations had the same phase at the aggregation and tight mound stages (**Fig. 15a–d, Table 5**). These findings indicate that cAMP relay organizes collective cell migration and cAMP signal dynamics are coupled with cell movements until the mound stages. Next, I also measured $[cAMP]_i$ and cell velocity of the two-type cells, prestalk and prespore cells in slugs. To trace slug cell efficiently, "mini slugs" were used for observation (see **Materials & methods**). Prestalk cells made up about 20% of slugs (anterior) and moved rotationally, while prespore cells made up about 80% of slugs (posterior) and moved straight (**Fig. 18a and b**). Cell movements in the anterior and posterior (respectively the prestalk and prespore regions) showed both oscillations with periods of 7.75 and 8.25 minutes, like normal slugs (**Fig. 15e, Fig. 18c and d**). However, no obvious oscillations in $[cAMP]_i$ associated with cell velocity were observed in spite of the cell type (**Fig. 15e, Fig. 18c and d**). These results suggest that the dynamics of cAMP relay changes after slug formation and that the collective cell migration in slugs was not organized dependently on periodic cAMP relay.

**4. Verification Flamindo2 functions as a cytosolic cAMP indicator in slugs.**

To see whether the absence of $[cAMP]_i$ oscillations was due to the loss of Flamindo2 function in slugs or not, cells dissociated from the slugs were stimulated with external cAMP and $[cAMP]_i$ response was monitored. The biochemical assay has been shown that slug cells show $[cAMP]_i$ elevation in response to external cAMP stimuli (Otte et al., 1986). In the investigation using Flamindo2, prestalk and prespore cells showed similar transient $[cAMP]_i$ responses to external cAMP stimulation (**Fig. 19a**, left), which is consistent with the results obtained from previous biochemical assays (Otte et al., 1986). The monitoring of $[cAMP]_i$ response also revealed that the return of the response in slug cells to the basal level was not perfect (**Fig. 19a**, left) compared with the response at the unicellular phase (**Fig. 9a**). The responses were inhibited when the cells were treated with caffeine (**Fig. 19a**, right). These results indicate that Flamindo2 function in slug cells was verified and the probe could detect the cAMP synthesis in cytosol of slug cells caused by adenylyl cyclases.

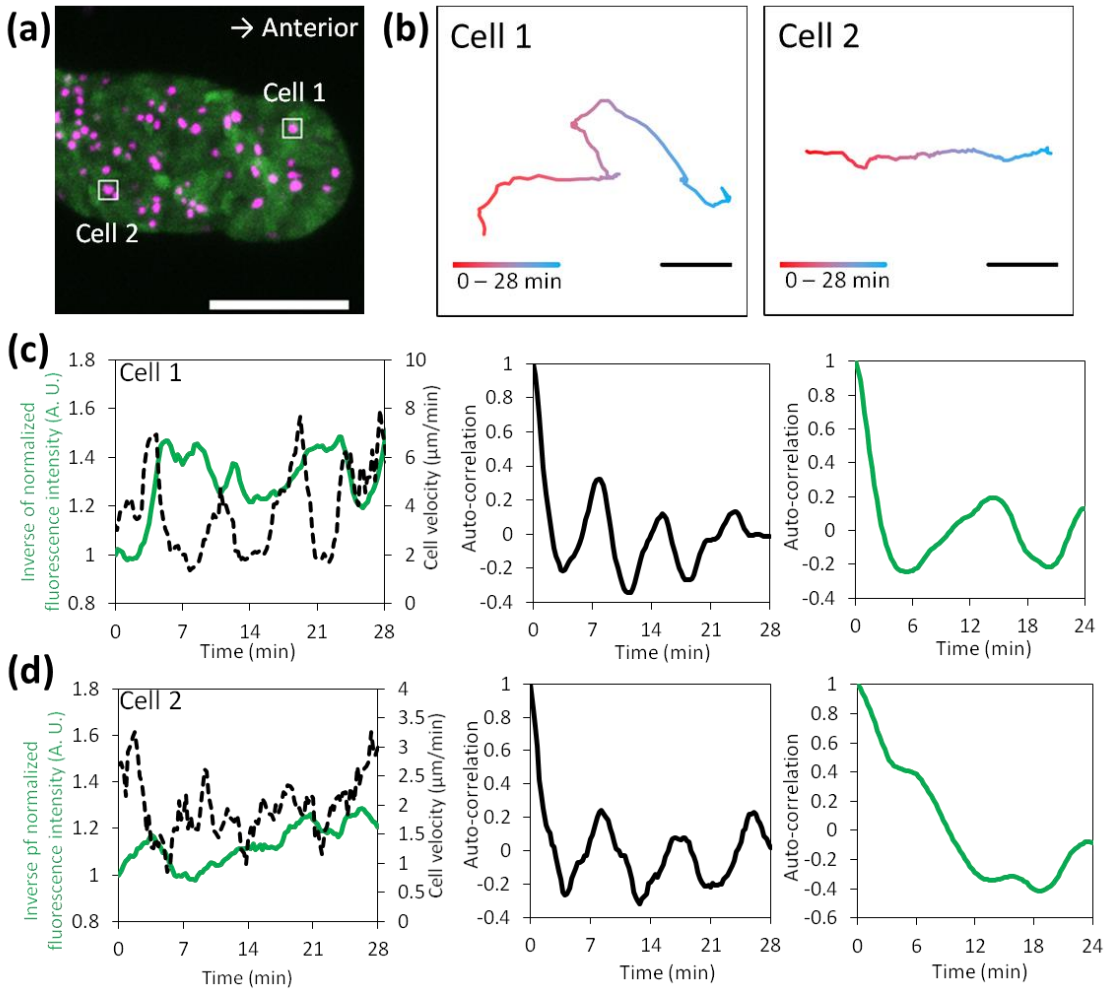


**Figure 18. $[cAMP]_i$ dynamics and cell movement of prestalk and prespore cells in migrating slugs.**

(a) Fluorescent images of a slug expressing Flamindo2 mixed with 2% Histone2B-RFP-labelled cells. 2D slugs (see **Material & methods**) were used for cell tracking. Scale bar, 50 μm. (b) Trajectories of prestalk (cell 1) and prespore (cell 2) cells for 28 minutes. Scale bars, 10 μm. (c), (d) Dynamics of Flamindo2 signals and velocity of cell 1 and cell 2. Left graphs show the time-course plots of Flamindo2 signals (green solid line) and cell velocities (black dashed line). Middle and right graphs show the auto-correlation of the cell velocity and Flamindo2 signal, respectively.

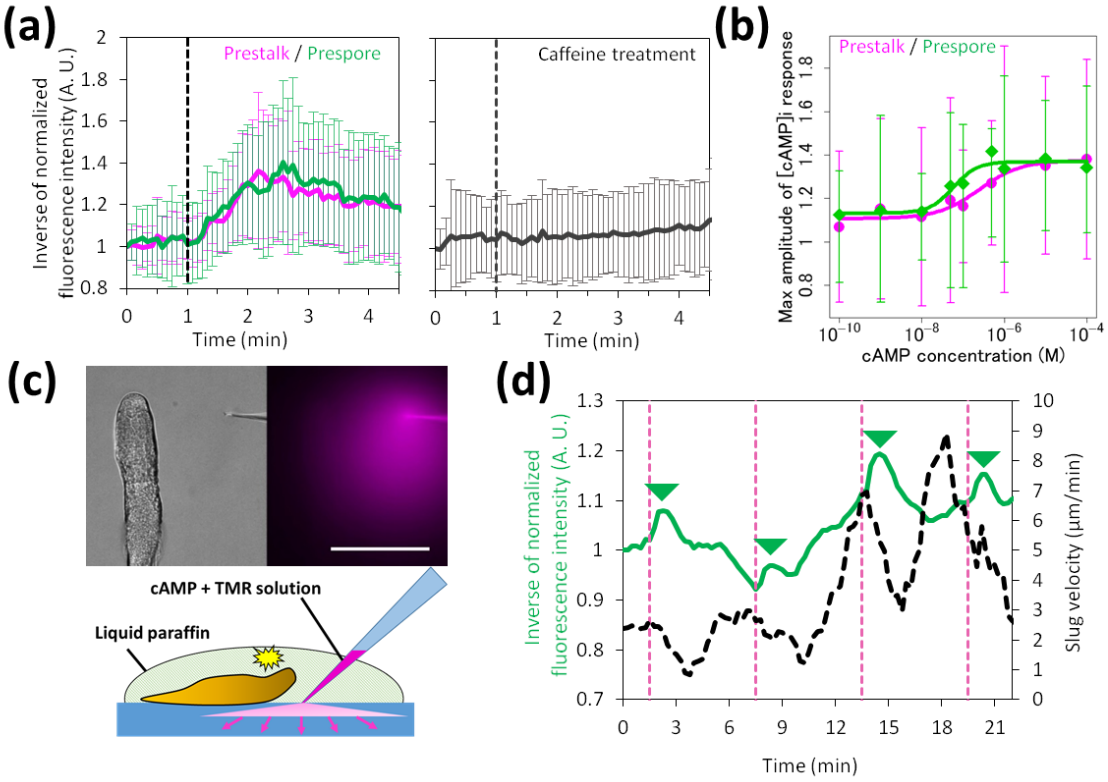


**Figure 19. $[cAMP]_i$ elevation of slug cells in response to external cAMP stimulation.**

(a) Time course plot of inverse Flamindo2 signals in slug-disaggregated cells after 10 μM cAMP stimulation (mean ± SD). Left, no-treatment cells (magenta, prestalk cells, n = 22 cells; green, prespore cells, n = 22 cells). Right, caffeine-treated cells (n = 45). (b) A dose-dependent curve of [cAMP]i response to various concentrations of cAMP stimuli (0.01–10 μM, mean ± SD). Magenta, prestalk cells (n = 20–24 cells at each data point). Green, prespore cells (n = 20–22 cells at each data point). (c) External cAMP stimulation to the slug by injection of cAMP into agar near the slug from a microcapillary. Left, DIC image. Right, fluorescent image of diffusing dye mixed with cAMP to visualize the injected solution. Scale bar, 100 μm. Bottom, a scheme of the cAMP microinjection experiment. cAMP solution mixed with the dye is diffused from the tip of a micropipette into agar to stimulate the entire slug. (d) Time-course plot of inverse Flamindo2 signals in whole slug (green solid line) and slug velocity (black dashed line). Dashed magenta lines indicate time of the cAMP injection. The mean intensity of Flamindo2 in a 43×186 $\mu m^2$ region in the slug shown in (c) was measured. The curves of slug velocity were smoothed by a running average over six data points. The peaks of Flamindo2 signals after cAMP stimulation are shown as green triangles.

Compared with the response at unicellular phase (**Fig. 9a**), the response in slug cells only showed one peak after cAMP stimulation (**Fig. 19a**), suggesting that the signal pathway downstream of cAMP reception altered and cGMP production in response to external cAMP stimulation was suppressed in slugs, which agrees well with the fact that slug cell does not show cAMP-induced increase in $[cGMP]_i$ (Mee, Tortolo, & Coukell, 1986). The dose-dependency of the response showed an $EC_{50}$ of 250 ± 136 nM and 58 ± 22 nM in the prestalk and prespore cells, respectively (**Fig. 19b**), values that are about 100-fold higher than in the unicellular phase (**Fig. 9c**). The difference of $EC_{50}$ between prestalk and prespore cells was not significant. I next examined the response of intact slugs by using a micropipette containing cAMP solution. In previous studies (Dormann & Weijer, 2001; Rietdorf et al., 1998), the response of slugs to cAMP stimulation has been investigated by the direct injection of cAMP solution into slugs from a micropipette, but I stimulated slugs by injecting cAMP from the micropipette into agar to diffuse it and avoid mechanical stimulation through sticking the micropipette to slugs (**Fig. 6a, Fig. 19c**). This application of cAMP stimulation to a slug caused transient changes in the Flamindo2 signals and slug velocity (**Fig. 19d**). Thus, extracellular cAMP signals could modify slug movements, as reported previously (Dormann & Weijer, 2001), and induce cAMP production, although endogenous $[cAMP]_i$ waves were not detected in slugs. Thus, these results proved the correct function of Flamindo2 as the cAMP indicator in slugs and that there is no obvious cAMP oscillations during the collective cell migration in slugs.

**5. Transient cAMP signal propagation in slugs of bacterially grown strain.**

The previous study has reported that propagation of optical density waves under dark filed observation, which is index of cAMP relay, was detected in migrating slugs and its frequency depended on the cell strain (Dormann & Weijer, 2001). Researchers of cellular slime molds usually use AX2 strain, which is one derivate from parental NC4 strain, and I also used AX2 strain through this study. However, XP55 strain, which is the other derivate from parental strain NC4, is the optimal strain for observation of optical density waves in slugs compared with AX2 strain (Dormann & Weijer, 2001). This suggest the possibility that the cAMP relay occurs in slugs of XP55 strain in certain condition. I confirmed that cAMP signaling dynamics in slugs of XP55 strains using Flamindo2 observation system.

To investigate the cAMP signal dynamics in XP55 strain using the genetically encoded fluorescence probe, the problems of transforming XP55 strain is needed to be resolved. Usually, when axenically growth cells of AX2 strain were transformed, drug resistant cassette is expressed under the control of *act6* promoter. However, this promoter does not work well in bacterially growth cells such as NC4 and XP55 strain (Wetterauer et al., 1996). It has been reported that such problem can be resolved by using other active promoter V18 (*rpl11* promoter) (Wetterauer et al., 1996), thus I constructed the new expression vector named pDMV18neo for transformation of bacterially growth cells by replacing the *act6* promoter in pDM304 plasmid with ribosome promoter V18. Using this vector, cells of NC4 and XP55 strain were transformed under the two-membered culture with bacteria and I succeeded in allowing these cells for expressing Flamindo2 (**Fig. 20a**). To assess whether Flamindo2 works properly in bacterially growth cells, fluorescence time-lapse images were taken during the aggregation stage in NC4 and XP55 strain. Both NC4 and XP55 cells show onset of $[cAMP]_i$ pulses and oscillations during aggregation, meaning that Flamindo2 shows correct function in bacterially growth cells (**Fig. 20b**). Next, slugs of NC4 and XP55 cells expressing Flamindo2 were observed to investigate the $[cAMP]_i$ dynamics in slugs of these strain. In NC4 strain, any slugs show no obvious changes in the probe signal during migration (**Fig. 20c, left**). On the other hand, a slug of XP55 strain showed transient changes in the probe signals (**Fig. 20c, right**) and its propagation at the anterior side of the slug (**Fig. 20d**), although such event was observed so rarely. These results suggest that in certain condition such as strain dependency cAMP relay surely propagates in migrating slugs and Flamindo2 can detect the relay if it occurs. Furthermore, no detection of cAMP signal propagation in AX2 slugs means that cAMP relay does not occurs actually during slug migration in AX2 strain.

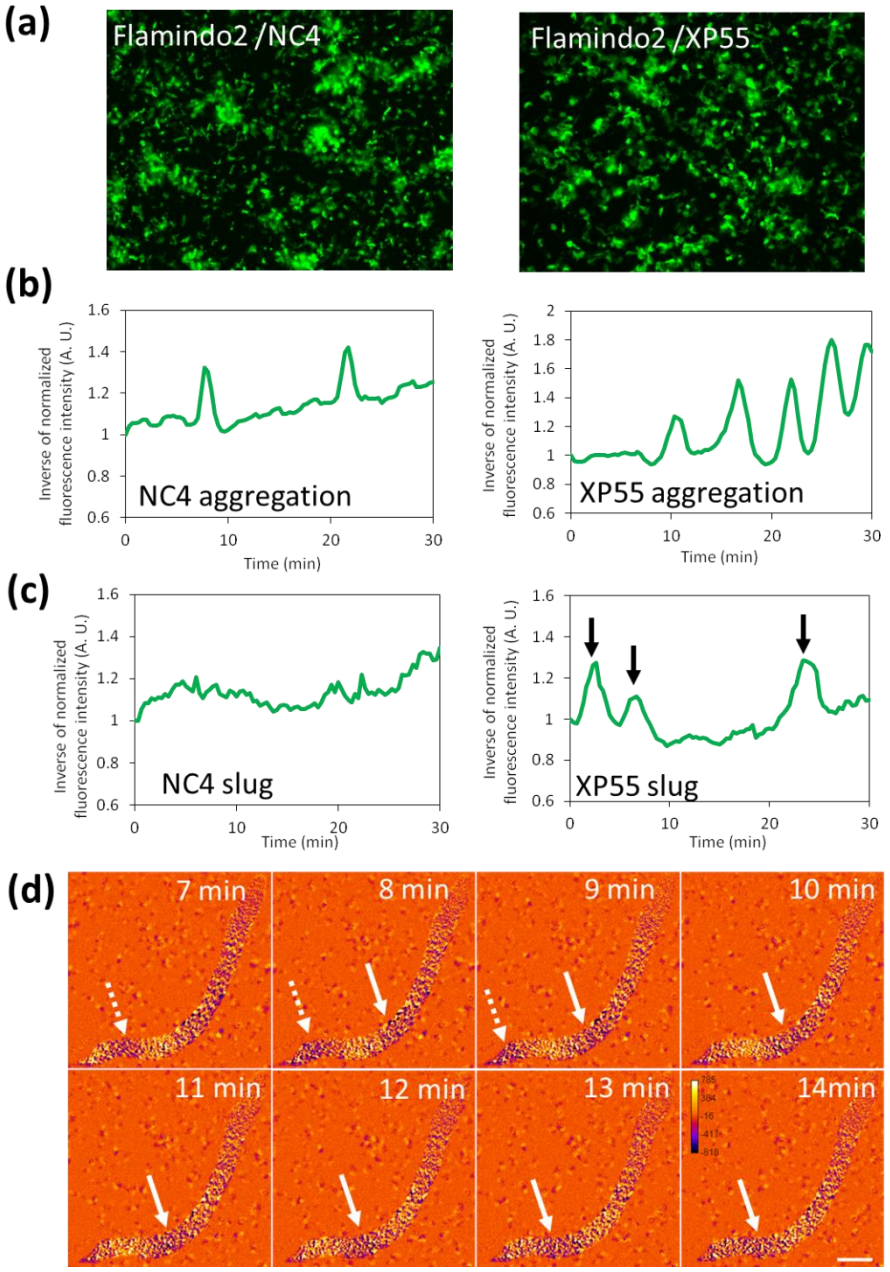


**Figure 20. Monitoring of [cAMP]i dynamics in bacterially growth strain using Flamindo2.**

(a) Fluorescence images of NC4 and XP55 cell expressing Flamindo2. (b) Time course plot of inverse Flamindo2 signals during aggregation of NC4 (left) and XP55 (right) strain. (c) Time course plot of inverse Flamindo2 signals during slug migration of NC4 (left) and XP55 (right) strain. The mean intensity of Flamindo2 in a 30 μm$^2$ region in the cell population was measured. Black arrows show the peak of transient changes in Flamindo2 signals. (d) Transient propagation of probe signals at the anterior part of the migrating slug. Fluorescence images were subtracted at 3 frame intervals to emphasize changes in fluorescence intensity. Anterior part of the slug faces the upper right side of the image. Solid and broken arrows show the positions of the first and second waves in each sequential image, respectively. Scale bars, 100 μm,

**6. Aggregation and multicellular movements of *acaA*-null cells without $[cAMP]_i$ oscillations.**

The results described above suggest the hypothesis that cAMP relay does not occur in multicellular slugs at normal condition and thus it is dispensable for the collective cell migration of slugs. This challenges the traditional model that assumes cAMP relay plays key roles in organizing collective cell migration in slugs. However, this hypothesis is supported by a previous report that *acaA*-null cells, which lacks ACA and the ability of cAMP-induced cAMP production, can aggregate and develop to form multicellular bodies when the expression of developmentally regulated genes is induced by exogenous and uniform cAMP pulses (Pitt et al., 1993) or downstream of cAMP signal pathway PKA was constitutively active in mutant cells (Wang & Kuspa, 1997). These imply the nonessentiality of cAMP relay for collective cell migration in slugs. However, the dynamics of the cAMP signals during development in the ACA-null mutant has not been examined directly and the absence of cAMP signals during the development has not been verified in previous studies. To confirm whether *acaA*-null cells could develop and migrate as multicellular organisms without $[cAMP]_i$ oscillations, we monitored Flamindo2 signals during their development. To induce the development of *acaA*-null cells, the mutant cells were starved under the exposure of exogenous uniform cAMP pulses. Under the microscopic observation with exogenous cAMP pulses (**Fig. 21a**), *acaA*-null cells gradually aggregated and form small clumps (**Fig. 21b**). After terminating the cAMP pulse treatment, the clumps were deposited on agar to induce further development. Several hours after settling down on agar, the clumps started to elongate and then formed slugs which migrate like the wild type slugs (**Fig. 21c**). The Flamindo2 signals from cell clumps formed by aggregation were unresponsive to external cAMP stimulation (**Fig. 21d**), indicating no ability of cAMP relay in the clumps of *acaA*-null cells. Monitoring of Flamindo2 signals during the development of *acaA*-null cells revealed that no obvious $[cAMP]_i$ oscillations were observed during the aggregation, slug formation and migration stages (**Fig. 21e and f**). Therefore, these observations using mutant cells give support to the proposition that cAMP relay is not essential for collective cell movements in migrating slugs.

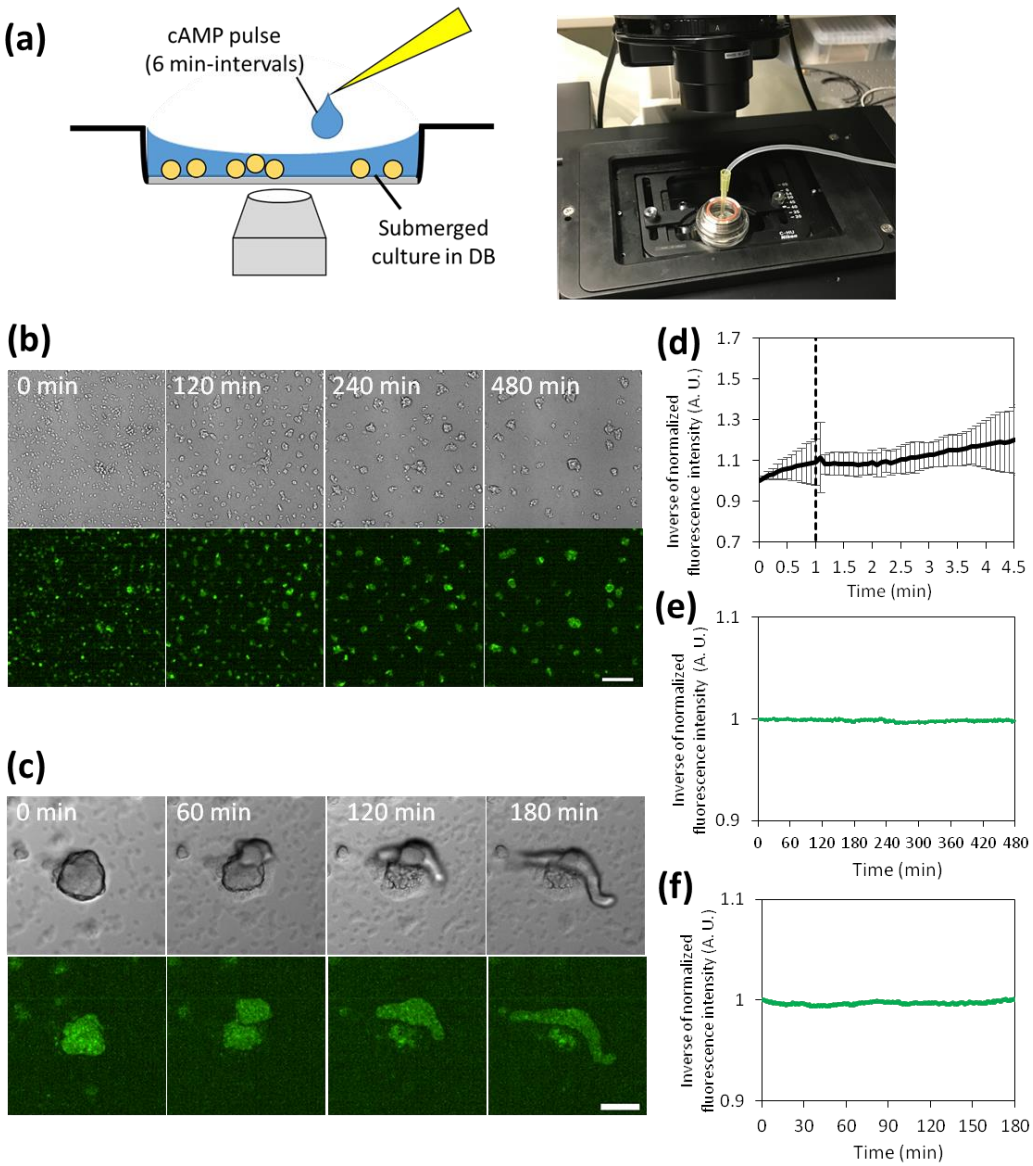


**Figure 21. Monitoring of $[cAMP]_i$ dynamics during development of *acaA*-null cells.** (a) Experimental scheme of exogenous cAMP pulse treatment to *acaA*-null cell in buffer under the microscopic observation. (b) Aggregation and cell clump formation of *acaA*-null cells expressing Flamindo2 in DB with exogenous cAMP pulses under microscopic observation. Top panels, DIC images. Lower panels, fluorescent images of Flamindo2. Scale bar, 100 μm. (b) Slug formation and migrating start of *acaA*-null cells expressing Flamindo2 on agar. Upper panels, DIC images. Lower panels, fluorescent images of Flamindo2. Inside the fluorescent images, maximum intensity projections of Z-stacks are shown. Scale bar, 100 μm. (c) Time-course plot of Flamindo2 signals in cell clumps after 100 μM cAMP stimulation. The mean intensity of Flamindo2 in a 25 $\mu m^2$ region in the cell mass was measured, and the inverse of the fluorescence intensity of Flamindo2 is plotted on the y-axis (mean ± SD, n = 13 clumps). (d) Time-course plot of Flamindo2 signals in *acaA*-null cells during aggregation. The mean intensity of Flamindo2 in a 100 $\mu m^2$ region on the aggregation field shown in (c) was measured, and the inverse of the fluorescence intensity was plotted against time. (e) Time-course plot of Flamindo2 signals in *acaA*-null cells during slug formation. The mean intensity of Flamindo2 in a 100 $\mu m^2$ region in the cell mass shown in (c) was measured, and the inverse of the fluorescence intensity was plotted against time.

**7. Non-oscillation cAMP signals was required for maintaining slug movements.**

Investigation using cells lacking ACA suggests that periodic cAMP-induced cAMP signal propagation namely cAMP relay is not required for collective cell migration in slugs. However, *D. discoiudeum* cell has the other type of adenylyl cyclases ACB and ACG, of which activities are stimulated by $Mg^{2+}$ ion and high osmolarity, respectively (Kim et al., 1998; van Es et al., 1996), and there is a possibility that non-oscillation cAMP signals rather than periodic signals work for organizing slug movement. To see whether the tonic cAMP signals are required for slug movement, the effect of treatment with adenylyl cyclases inhibitor caffeine on slug migration was investigated (**Fig. 22a**). Caffeine treatment caused significant inhibition of slug migration, although the morphology of slugs was maintained (**Fig. 22b and c**). These suggest that tonic cAMP signals (not oscillating signals) function as the signals for maintaining the collective cell migration of slugs.

**8. Transition of signaling dynamics at the upstream of cAMP production, PIP3 signaling with progression of *Dictyostelium* development.**

The results obtained by observation using Flamindo2 suggests that there is no cAMP relay in multicellular slugs. However, it is needed to be careful about the detection limit of the cAMP probe to interpret of cAMP signal dynamics in slugs. To overcome the limit of using only one kind of probe for detecting cAMP signal dynamics, I applied the method for monitoring the upstream of cAMP signal pathway, PIP3 signaling. When cells were stimulated by extracellular cAMP, PIP3 levels on the plasma membrane show transient increase which finally causes the activation of ACA and intracellular cAMP production (Swaney et al., 2010). Therefore, monitoring of PIP3 signal dynamics is another approach which enables us to investigate the dynamics of cAMP signaling. It has been reported that GFP fused with PH domain of CRAC ($PH_{CRAC}$-GFP), which binds to the PIP3 on the membrane and thus works as the probe of PIP signal dynamics, show the periodic translocation to the leading edge of cells in the mound, which indicates a transient increase of PIP3 levels on the plasma membrane in response to cAMP signals, and such periodicity is not shown in slugs (Dormann, et al., 2002).

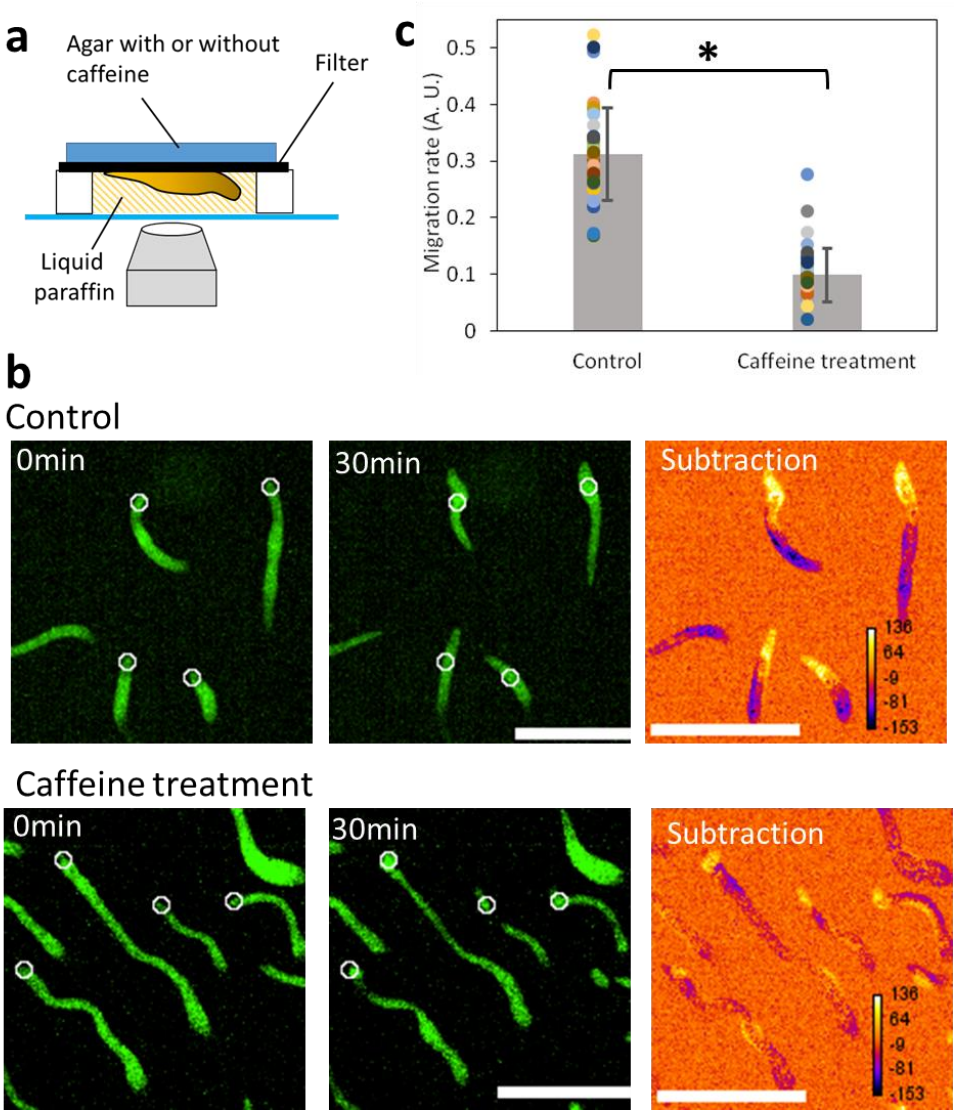


**Figure 22. Caffeine treatment inhibits the migration of slugs.**

(a) The scheme of experiments for monitoring the effect of caffeine treatment on slug migration. Slugs were formed on a filter. Agar containing 4 mM or 0 mM caffeine (control) was put on the filter during the observation. (b) Snap shots of migrating slugs under the condition treated with or without 4mM caffeine. Fluorescence images of slugs expressing Citrine at t = 0 (left) and 30 min (middle) and subtracted images between t = 30 and t = 0 images (right) are shown. In subtracted images, white zone around the tips of the slugs indicates the migration space for 30 min. White circles shown in t = 0 and 30 min images indicate the positions of the tips of the slugs at t = 0 min. Scale bar, 500μm. (c) Comparison of migration rates between no treatment (Control) and caffeine-treated slugs (Caffeine treatment). n = 36 slugs in both data point. Dots plotted on the graph are original data point. *: $P < 10^{-20}$, Student's t-test.

To confirm whether such a transition of dynamics is also observed with my observation system and whether the PIP3 signal dynamics such as oscillation periods corresponds to the $[cAMP]_i$ dynamics, the dynamics of PIP3 signaling at each developmental stages was investigated using GFP fused to the PH domain of Akt/PKB ($PH_{Akt/PKB}$-GFP). It has been reported that $PH_{Akt/PKB}$-GFP shows transient localization to the plasma membrane in response to external cAMP stimulation dependently on PI3-kinase activity (Funamoto, Milan, Meili, & Firtel, 2001; Meili et al., 1999), which regards $PH_{Akt/PKB}$-GFP as the probe of PIP3 dynamics. I confirmed that cells dissociated from loose mounds or slugs show a translocation of $PH_{Akt/PKB}$-GFP to the plasma membrane in response to external cAMP stimulation (**Fig. 23a–c**), although the previous study using $PH_{CRAC}$-GFP did not succeed in detecting the transient elevation of PIP3 levels on the plasma membrane of slug-dissociated cells in response to cAMP stimulation (Dormann et al., 2002). This may be resulted from the difference of experimental condition: in the previous study, the slight cAMP gradient stimulation was applied to the slug dissociated cells (Dormann et al., 2002), while the slug cells were exposed to the uniform "strong" cAMP stimulation in this study. External cAMP stimulation test also revealed that the adaptation of PIP3 transient translocation in slug-dissociated cells was imperfect compared with loose mound cells (**Fig. 23a–c**). In vivo imaging at each developmental stages revealed that loose and tight mounds exhibited periodic translocations of $PH_{Akt/PKB}$-GFP to the leading edge of individual cells and its propagation between cells (**Fig. 24a–d**). The periods of translocation in loose and tight mounds were 2.89 ± 0.95 minutes (25 cells, 4 mounds) and 5.17 ± 1.32 minutes (20 cells, 4 mounds), respectively, which agrees well with the periods of $[cAMP]_i$ oscillations (**Table 5**). On the other hand, in slugs, $PH_{Akt/PKB}$-GFP was continuously localized at the leading edge of the cells and did not show any periodic translocation to the membrane (44 cells, 15 slugs; **Fig. 24a–d**). These indicate that the cAMP signaling pathway upstream of cAMP production undergoes a transition in its dynamics from oscillations to steady state during slug formation similarly with $[cAMP]_i$ dynamics. Additionally, these results raises the possibility that the continuous localization of $PH_{Akt/PKB}$-GFP cells of intact slugs are caused by tonic cAMP signals and/or other signals in slugs.

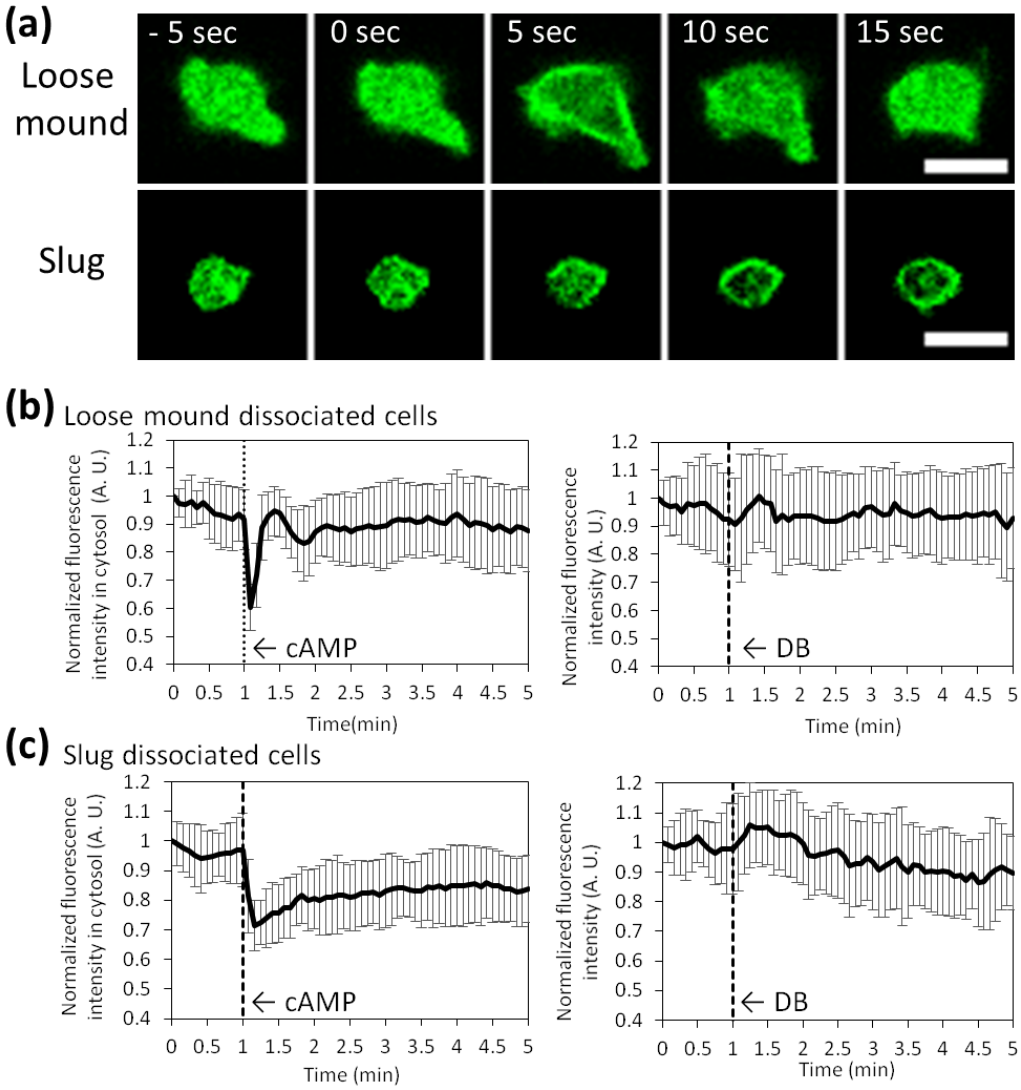


**Figure 23. Translocation of $PH_{AKT/PKB}$-GFP to the plasma membrane of cells dissociated from loose mound or slug in response to external cAMP stimulation.**

(a) Translocation of $PH_{AKT/PKB}$-GFP to the plasma membrane of cells dissociated from loose mounds (upper panels) or slugs (lower panels) in response to uniform cAMP stimulation. Scale bar, 5 μm. (b), (c) Time course plot of fluorescence intensity of $PH_{AKT/PKB}$-GFP in the cytosol of cells dissociated from loose mounds or slugs. Dashed lines indicate the time point of the stimulation with developmental buffer (DB) with or without 10 μM cAMP. Loose mound (n = 24 cells), slug (n = 30 cells).

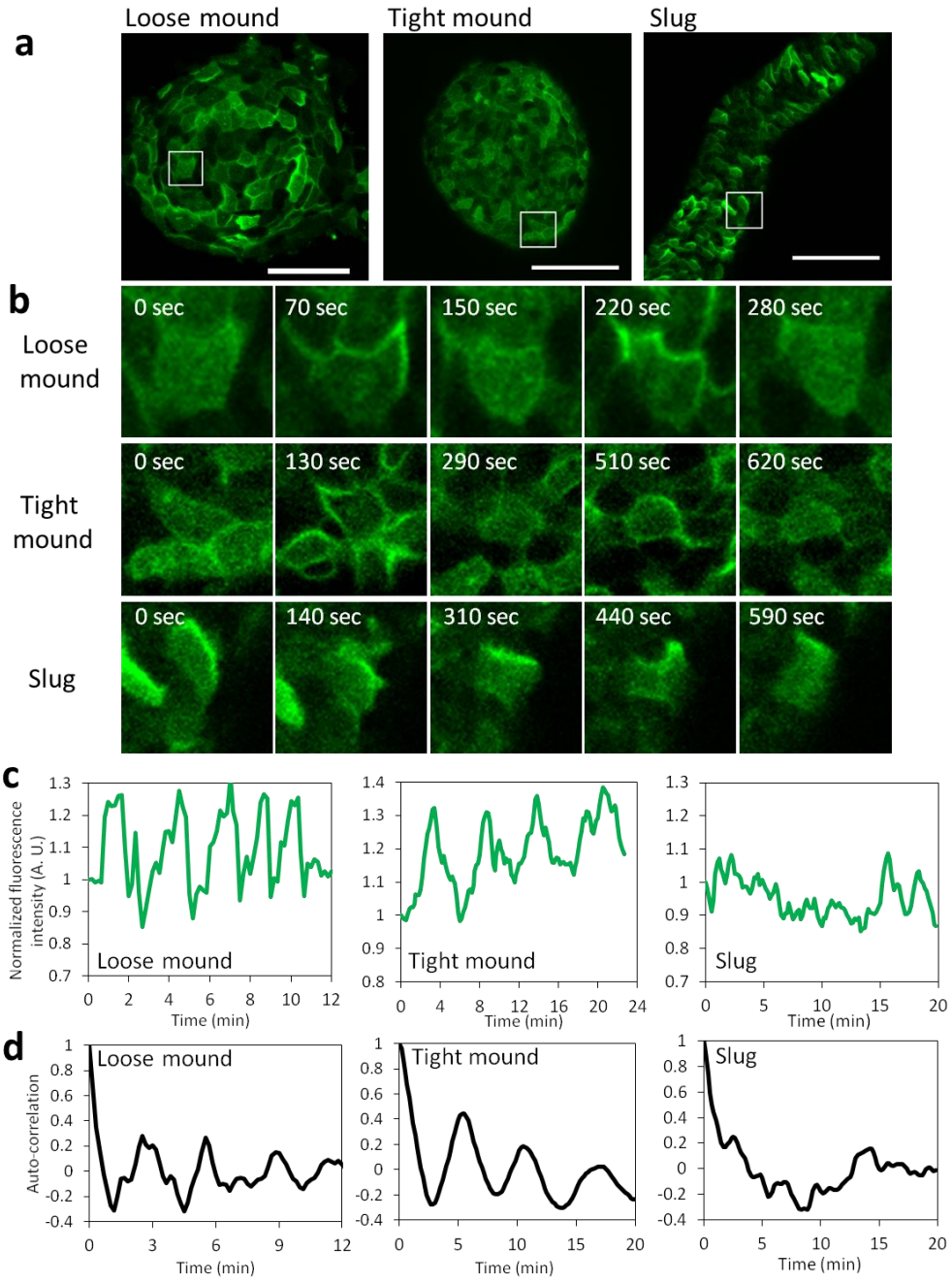


**Figure 24. Periodic translocation of $PH_{Akt/PKB}$-GFP to the leading edge of cells in the mound stages and continuous localization of $PH_{Akt/PKB}$-GFP in slug cells.**

(a) Fluorescent images of cells expressing $PH_{Akt/PKB}$-GFP in a loose mound, a tight mound and a slug. Scale bars, 50 μm. (b) $PH_{Akt/PKB}$-GFP localization to the leading edge of cells in the white boxes shown in (a). (c) Time-course plots of fluorescence intensity of $PH_{Akt/PKB}$-GFP in the cytosol. Mean intensity of the signals in a 3–5 $\mu m^2$ region positioned in the cytosol of a representative cell was measured. (d) Auto-correlation of the time course changes shown in (c).

To see whether continuous localization of $PH_{Akt/PKB}$-GFP in slug cells depended on cAMP signals or not, interference on the localization of $PH_{Akt/PKB}$-GFP in intact slugs by cAMP stimulation was investigated by the cAMP microinjection assay (**Fig. 6b**). External cAMP stimulation to the intact slug did not affect the localization of $PH_{Akt/PKB}$-GFP in cells of intact slugs (**Fig. 25a**). This finding is consistent with a previous results using $PH_{CRAC}$-GFP (Dormann et al., 2002). Furthermore, interference of cAMP signaling by caffeine treatment performed as **Fig. 22a** also did not affect the localization of $PH_{Akt/PKB}$-GFP in slug cells (**Fig. 25b**). These results suggest that the continuous localization of $PH_{Akt/PKB}$-GFP to the leading edge of cells in slugs depend on the signals other than tonic cAMP signals generating by slug cells.

**9. Transition of $[cAMP]_i$ dynamics occurs with the progression of *Dictyostelium* development.**

Monitoring of $[cAMP]_i$ dynamics throughout the development of *Dictyostelium* revealed that the mode of signal dynamics dramatically changes after multicellular slug formation. To reveal the temporal relationship between the such transition of cAMP signaling dynamics and developmental progression in detail, $[cAMP]_i$ dynamics and morphological changes of multicellular bodies (tip formation on the mound) were observed simultaneously using Flamindo2 and *ecmAO*::mRFPmars (**Fig. 26a**). Because the tip region of the mound is regarded as a cluster of prestalk cells characterized by the high expression of the *ecmAO* gene (Early, Gaskell, Traynor, & Williams, 1993), live imaging with *ecmAO*::mRFPmars (expression of mRFPmars under the control of the *ecmAO* promoter) can visualize the developmental process of cell differentiation into prestalk cells and their sorting to the tip of the mound. From the loose to tight mound stage, $[cAMP]_i$ showed clear oscillation and with no obvious fluorescence signals of *ecmAO*::mRFPmars (**Fig. 26b**, 0–120 min). When the tight mound begun to elongate and cells highly expressing *ecmAO*::mRFPmars were sorted on the top of the mound to form the tip (**Fig. 26c**), $[cAMP]_i$ oscillations became weaker and finally disappeared after the formation of the obvious tip on the mound (**Fig. 26b**, 120–210 min).

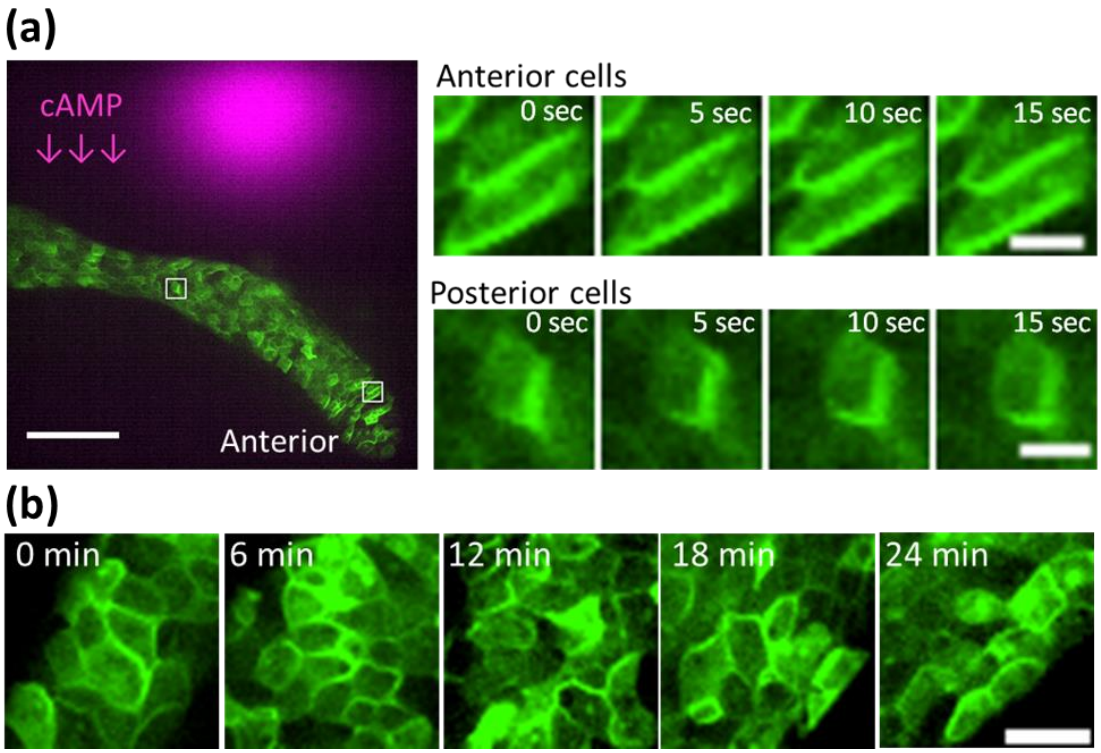


**Figure 25. Interference with cAMP signals in intact slugs did not affect the continuous localization of $PH_{Akt/PKB}$-GFP to the leading edge of cells.**

(a) External cAMP stimulation to an intact slug by cAMP injection into agar near the slug from a micropipette. Left, fluorescent image of $PH_{AKT/PKB}$-GFP in the slug and diffusing dye mixed with cAMP solution to visualize the injected solution during the stimulation. cAMP solution was diffused from the tip of the micropipette positioned on the top of the image and stimulated the slug. Fluorescence images of the focal plane near the bottom of the slug were taken by a confocal microscope. Anterior part of the slug faces the bottom side of the image. Scale bar, 50 μm. Right, fluorescence images of $PH_{AKT/PKB}$-GFP of anterior and posterior cells in the slug during the cAMP stimulation. The regions indicated by the white boxes in the left image were expanded and shown in the right images. Time after the cAMP stimulation (seconds) is shown in the upper right of the images. Scale bar, 5 μm. (b) Interference with cAMP signaling in an intact slug by 4 mM caffeine treatment. The caffeine treatment to slugs were performed as shown in **Fig. 22**. Fluorescence images of $PH_{AKT/PKB}$-GFP in the slug cells are shown. Anterior part of the slug faces the upper right side at each images. Time after the caffeine treatment to the slug (minutes) is shown in the upper left of the images. Scale bar, 10 μm.

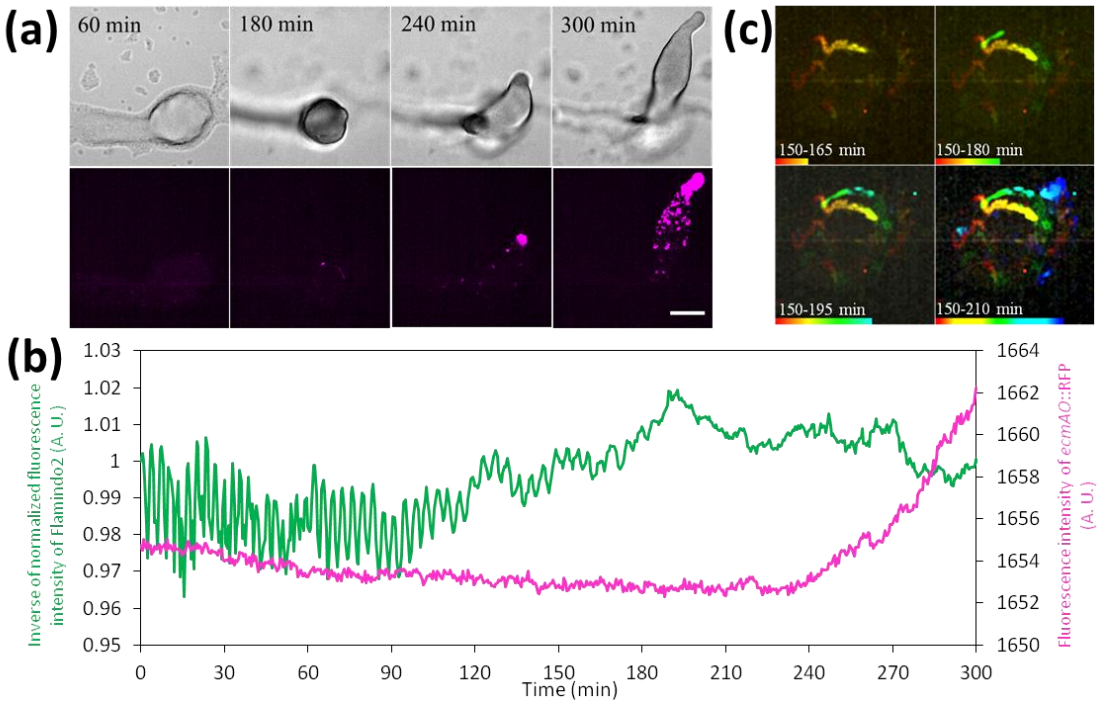


**Figure. 26 Association of transition of $[cAMP]_i$ dynamics with developmental progression marked with tip formation in the mound.**

(a) Expression of *ecmAO*::mRFPmars during mound elongation and slug formation. Upper panels, DIC images. Lower panels, fluorescent images of *ecmAO*::mRFPmars. Scale bar, 100 μm. (b) Time course plot of Flamindo2 (green) and *ecmAO*::mRFPmars (magenta) signals during mound development. Data were obtained 8–13 hours after starvation. The mean intensity of Flamindo2 in a 30 $\mu m^2$ region in the mound shown in (a) and the mean intensity of *ecmAO*::mRFPmars in the entire region of the mound were measured. (c) The sorting of cells expressing *ecmAO*::mRFPmars at the top of the tight mound. This figure shows trajectories of sorted prestalk cells marked by the expression of *ecmAO*::mRFPmars at the top of the mound (upper right side of images) during the mound elongation.

Considering the maturation time of mRFP has a time lag of about 90 minutes (Bevis & Glick, 2002), both the accumulation of prestalk cells to the tip and the loss of cAMP waves started to occur around the same time (**Fig. 26b and c,** ~150 min), suggesting that the transition of the $[cAMP]_i$ dynamics occurred simultaneously with the tip formation.

To confirm whether the transition of cAMP signaling is a developmentally regulated event, I examined the $[cAMP]_i$ dynamics of a mutant lacking *gbfA*, which encodes the transcription factor G-box binding factor (GBF). GBF regulates the expression of late-development gene, and the development of *gbfA*-null arrest at the loose mound stage without tip formation (**Fig. 27**) due to the lack of post-aggregative and cell-type specific genes (Schnitzler et al., 1994). Monitoring of Flamindo2 signals during the development of *gbfA*-null mutant shows that mutant cells had impaired transitions in $[cAMP]_i$ dynamics, in which $[cAMP]_i$ waves continued duration of 3–10 hours after starvation and their propagation persisted 24 hours after starvation with arrest in the loose mound stage (**Fig. 28a–c**). These results are consistent with a previous report that found mounds of a *gbfA*-null mutant showed optical density waves, although the pattern of the wave propagation was aberrant (Sukumaran, Brown, Firtel, & McNally, 1998). Thus, these results indicate that the cAMP dynamics transition from propagating waves to steady state was due to developmental regulation.

**10. Developmentally regulated expression pattern of genes involved in cAMP signaling pathway**

This study proposes that cAMP signal dynamics show the transition from oscillation to steady state during the multicellular development of *Dictyostelium* cells and open a new question how the transition of signal dynamics occurs during development. One possible mechanism for the transition is the changes of expression pattern of developmentally regulated genes. Analyses of transcription profile through the development of *Dictyostelium* cells has suggested that expression pattern of genes involved in cAMP signaling (e. g., cARs and ACA) dramatically changes after the multicellular formation (**Fig. 29a**) (Parent & Devreotes, 1996).

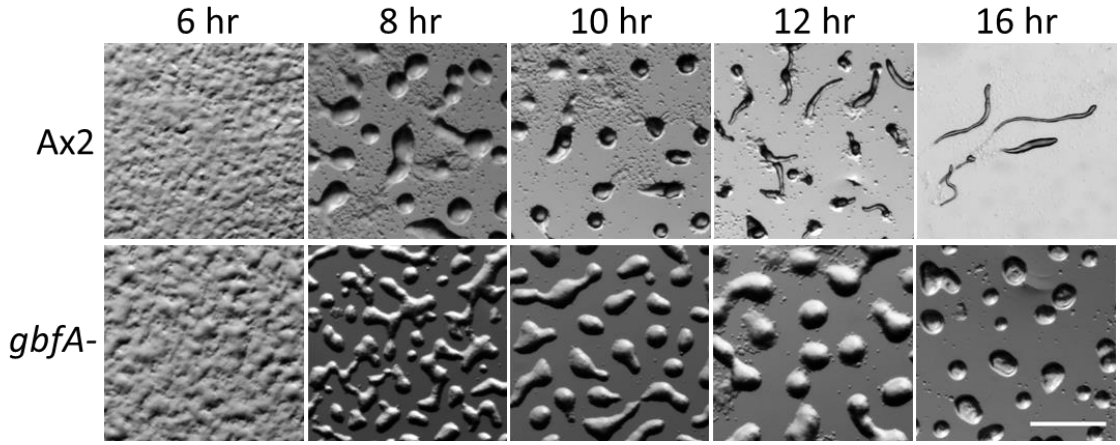


**Figure. 27 Developmental time course of wild-type and *gbfA*$^{-}$ mutant cells.**

Cells were deposited on agar and allowed to develop. (Upper panels) Wild-type Ax2 cells show several developmental stages which could be distinguished by morphology: early aggregation (6 hr), loose mounds (8 hr), tight mounds (10 hr), and slugs (12, 16 hr). (Lower panels) Development of *gbfA*$^{-}$ mutant cells arrested at the loose mound stage (8–16 hr). Scale bar, 1 mm.

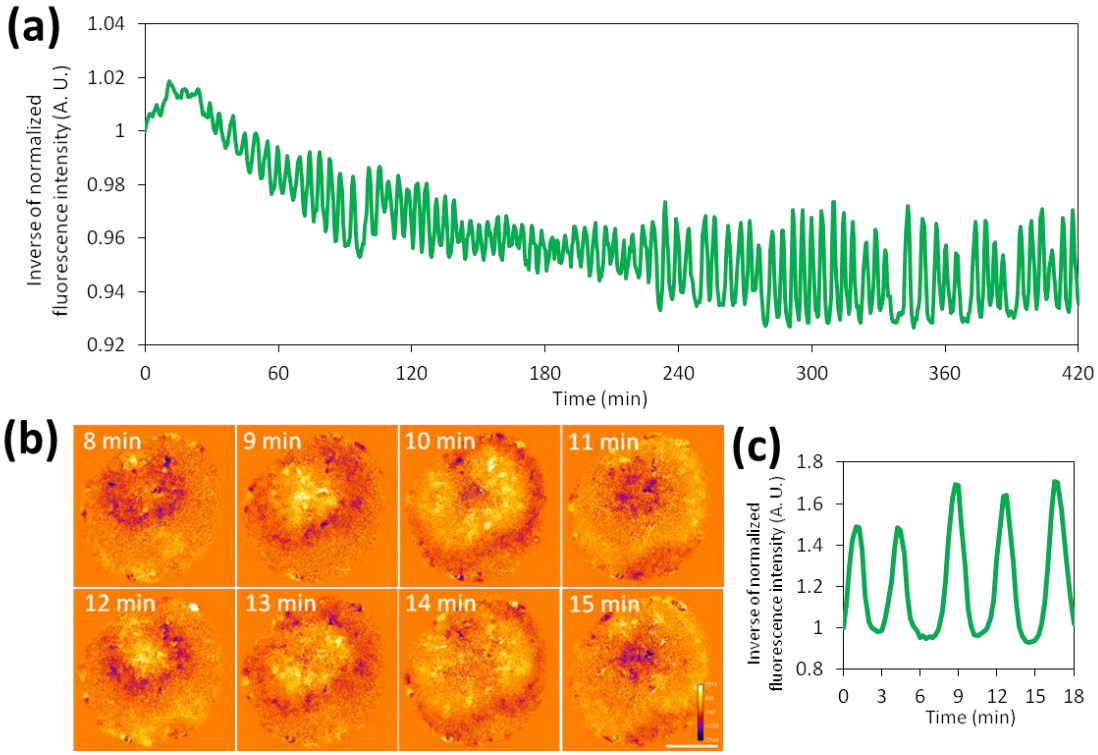


**Figure. 28 Persistence of $[cAMP]_i$ oscillation and wave propagation during the development of *gbfA*-null cells.**

(a) Time course plot of inverse Flamindo2 signals during the development of *gbfA*$^-$ cells. Data were obtained 3–10 hours after starvation. The mean intensity of Flamindo2 in a 50 μm$^2$ region of the cell population was measured. (b) Wave propagation of Flamindo2 signals in the loose mound of *gbfA*$^-$ cells after 24 hours starvation. Images were subtracted at 4 frame intervals to emphasize changes in the signals. (c) Time course plot of inverse Flamindo2 signals in the mound shown in (b). The mean intensity of Flamindo2 in a 20 μm$^2$ region in the mound shown in (b) was measured.

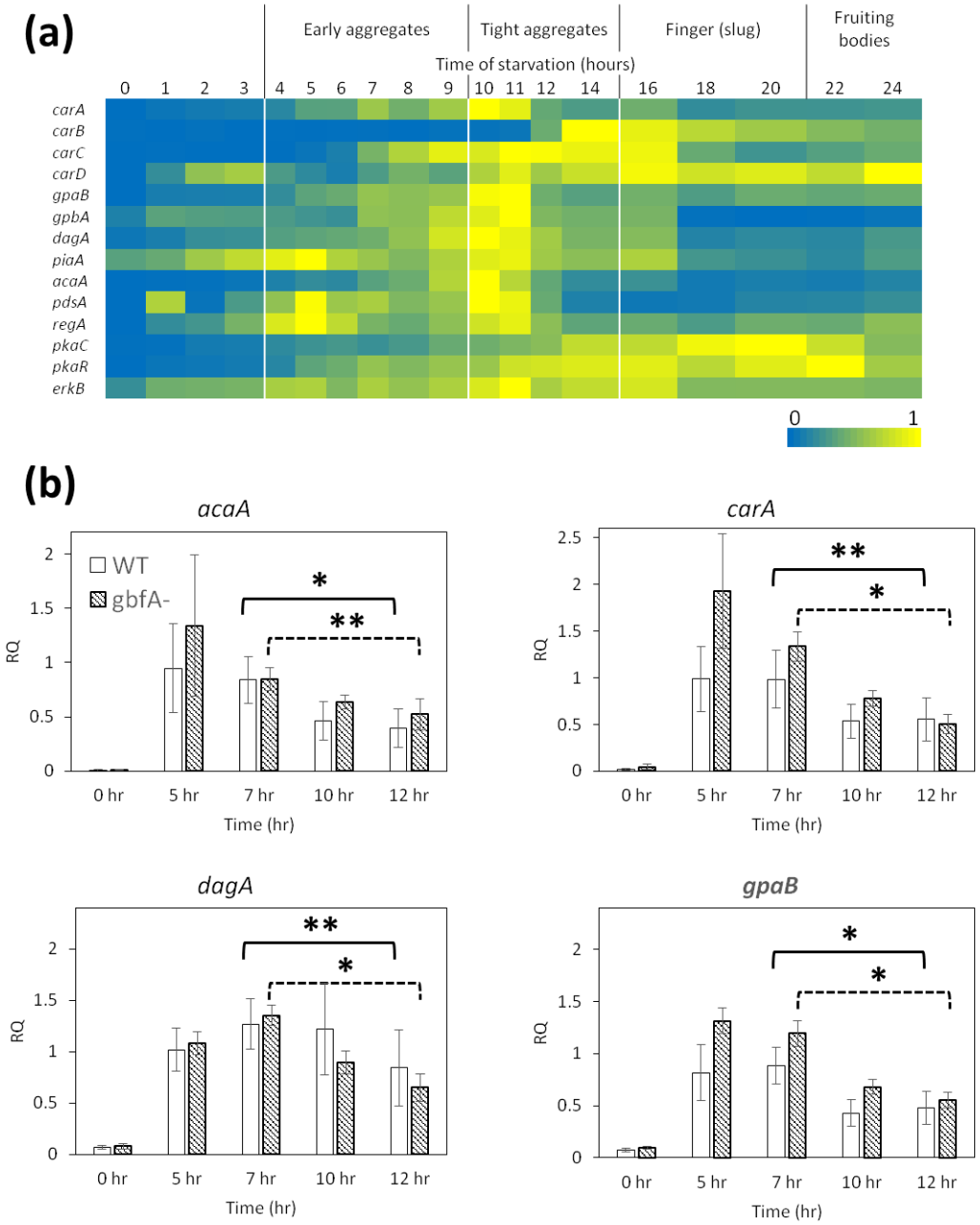


**Figure. 29 Expression profile of genes involved in cAMP signaling along the time course of development.**

(a) Gene expression profiles of cAMP receptors (*carA*, *carB*, *carC*, *carD*), G proteins (*gpaB*, *gpbA*), regulators (e. g., cytosolic regulator of adenylyl cyclase, *dagA*) and effectors (e. g., adenylyl cyclase, *acaA*) are shown. The profiles are based on RNA-seq data obtained from a web-based platform for the sequence data dictyExpress (Stajdohar et al., 2017). The indicated developmental time courses of the relative gene expression levels are based on the notation in Rosengarten et al. (2015). (b) qRT-PCR analysis targeting four genes involved in cAMP signaling. Relative quantities of gene expression (RQ) were shown. *: $P < 0.01$, **: $P < 0.05$, Student's *t*-test.

To confirm whether the expression pattern of components in cAMP signal pathway in cells using this study also changes with developmental progression, I performed the qRT-PCR experiment. For the analysis, four genes, *acaA, carA, dgcA, gpaB* which encode ACA, CAR1, CRAC, Gα2 subunit, respectively, were used as targets. In wild type cells, expression of four genes show the peak at 5hr (aggregation stage) or 7hr (loose mound stage) after starvation, and the expression of genes at 12hr (slug stage) were significantly lower than those at 7hr (**Fig. 29b**). This result is consistent with the previous studies (Parent & Devreotes, 1996; Rosengarten et al., 2015) and the fact that cAMP relay disappears at the slug stage. Furthermore, I also examined the developmental expression profile of the four genes in *gbfA*-mutant cells to see whether the changes of expression pattern occurs or not in the mutant which shows developmental arrest at the stage before multicellular formation. Unexpectedly, *gbfA*-null cells show the similar down-regulated expression pattern of genes along their developmental course with wild type cells (**Fig. 29b**), although this mutant persists the cAMP oscillations 12hr after starvation. This implies that the down-regulation of these four genes are not involved in the transition of cAMP signaling dynamics and that not only the changes in expression pattern of genes involved in cAMP signal pathway but also other factors are related with the transition of cAMP signaling dynamics.

**11. The cAMP receptor was internalized with the developmental progression.**

Other possible mechanism for transition of cAMP signal dynamics than changes of gene expression pattern is the changes in localization of cAMP receptors in cells with developmental progression. It has been reported that CAR1, which is the receptor of extracellular cAMP and mainly mediates cAMP relay during aggregation, is localized on the peripheral membrane, but internalized at the later developmental stage (Sergé et al., 2011). To investigate the localization pattern of CAR1 at each developmental stage, CAR1-RFP was expressed in RI9 strain which is the CAR1/CAR3 double knock out mutant and have no endogenous receptors mediating cAMP relay. RI9 cells usually cannot aggregate, but expression of CAR1-RFP rescue the development defect of the mutant.

At the loose mound stage, CAR1-RFP signals were observed at the peripheral membrane of the cells (**Fig. 30a, loose mound**). When the mound became the tight mound, CAR1-RFP was localized at the peripheral membrane but also seen in the cytosol as the granules (**Fig. 30a, tight mound**). This suggest that the CAR1 internalization from peripheral membrane to the cytosol occurs at the tight mound stage. Furthermore, CAR1 localization in slugs was also investigated. In anterior prestalk region, CAR1 accumulated in cytosol and did not localize at the peripheral membrane at all (**Fig. 30a, slug anterior**). On the other hand, in posterior prespore region, cAR1 mainly accumulated in cytosol but could be seen at peripheral membrane a little compared with the prestalk region (**Fig. 30a, slug posterior**). These results is consistent with the immunostaining observation of cAR1 in wild-type cells along the developmental time course (Wang et al., 1988). Therefore, the monitoring of CAR1 localization at each developmental stages suggest that CAR1 internalization occurs during the slug formation in which cAMP oscillations disappeared simultaneously. To confirm whether the CAR1 internalization is developmentally regulated event, CAR1-RFP localization in *gbfA*-null mutant was investigated during their development. In this mutant, CAR1-RFP was observed at the peripheral membrane as wild-type cells (**Fig. 30b, 9 hr**). Such localization pattern was maintained even in the mound of *gbfA*-mutant cells 24 hours after starvation and the internalization of CAR1-RFP did not occurs compared with the wild-type slugs which were formed 18 hours after starvation (**Fig. 30b, 24 hr**). These indicated that CAR1 internalization occurs with developmental progression from loose mound to slug stages. Furthermore, the fact that *gbfA*-null mutant remained $[cAMP]_i$ oscillations and CAR1 localization at the peripheral membrane suggests the possibility that changes in localization of cAR1 is involved in the transition of cAMP signal dynamics.

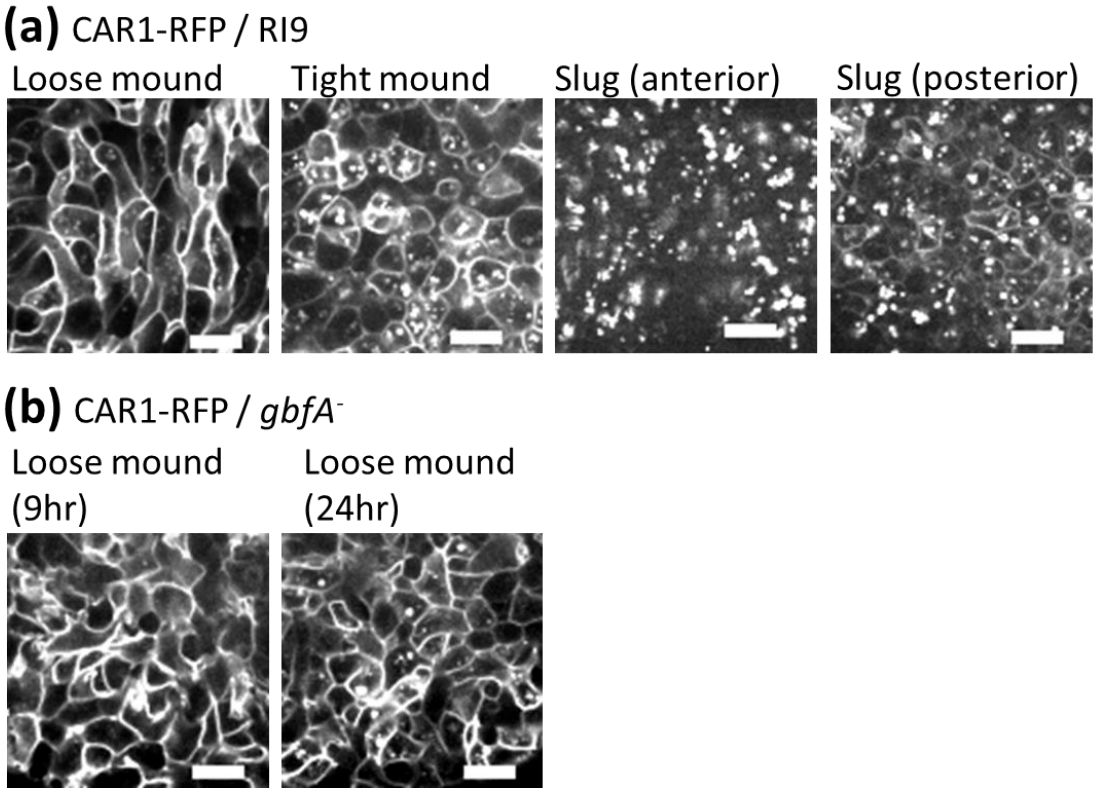


**Figure. 30 Localization pattern of CAR1 at each developmental stages.**

(a) Fluorescence images of CAR1-RFP expressed in RI9 (*carA*$^{-}$ / *carC*$^{-}$) cells. Scale bar, 10 μm.
(b) Fluorescence images of CAR1-RFP expressed in *gbfA*$^{-}$ cells. Scale bar, 10 μm.

## Discussion

In multicellular organisms, collective cell migration can be organized by chemical guidance. For example, cell population in embryo move cooperatively toward gradients of the chemoattractant such as SDF-1 (Donà et al., 2013; Theveneau et al., 2013). Other type of chemical guidance for collective cell migration is signal propagation between cells. It has been reported that EGF and ERK signal propagation between cells drive collective cell migration (Aoki et al., 2017, 2013). In *Dictyostelium* cells, it has been thought that propagating signal waves of chemoattractant cAMP (cAMP relay) organize collective cell migration through the development (Friedl & Gilmour, 2009; Weijer, 2009). However, the characteristics of cAMP signal dynamics have been examined only at the unicellular aggregation stage in past studies (Gregor et al., 2010; Sgro et al., 2015). In contrast, this study investigated the dynamics of cAMP signaling throughout the development of *Dictyostelium* cells including the multicellular stage by using the fluorescence cAMP indicator Flamindo2. Flamindo2 has already been used to monitor cAMP relay during aggregation by Ohta et al (2018). However, the cAMP signal dynamics at later developmental stages, such as mounds and slugs, has not been investigated using Flamindo2. Thus, I confirmed whether this probe can be used as the indicator of cAMP signaling dynamics throughout the development of *Dictyostelium* cells. The $EC_{50}$ (3.2 μM) and Hill coefficient (0.95) of Flamindo2 (Odaka et al., 2014) are optimal to monitor the cytosolic cAMP levels in unstimulated and cAMP-stimulated *Dictyostelium* cells at all development stages which can be estimated to be about 0.3–12 μM (**Table 4**). The probe is expressed stably at both unicellular and multicellular phase (**Fig. 8**), and could detect the $[cAMP]_i$ changes of *Dictyostelium* cells in response to external cAMP stimuli at both unicellular and multicellular stages (**Fig. 9 and 19**). These estimates and investigation indicate that Flamindo2 is an appropriate tool for monitoring the cAMP signaling dynamics in *Dictyostelium* cells throughout their development. Monitoring of $[cAMP]_i$ through the development of *Dictyostelium* cells by Flamindo2 revealed the dramatic transition of cAMP signaling dynamics during the development.

**1. Changes in periods of $[cAMP]_i$ oscillations and geometry of $[cAMP]_i$ wave propagation during the development.**

In the aggregation and mound stages, observation system using Flamindo2 visualized $[cAMP]_i$ oscillations and wave propagations in the cell populations (**Fig. 11 and 12**). The pattern of $[cAMP]_i$ wave propagation in the aggregation and mound stages agreed well with synchronous changes in the optical density of cell populations and its propagation between cells previously reported (Siegert & Weijer, 1989). Investigation of $[cAMP]_i$ dynamics and cell movements revealed that the cAMP wave oscillations were coupled with the cell movement (**Fig. 15–17**). Live imaging also showed that the geometry of wave propagation changed from the rotation in loose mounds to the top-bottom pattern in tight mounds coupled with mound elongation (**Fig. 12**). Overall, these findings show collective cell migration was coordinated with cAMP relay from the aggregation to tight mound stages, which is consistent with the mechanism of collective cell migration in *Dictyostelium* cells (Friedl & Gilmour, 2009; Weijer, 2009).

Simultaneous monitoring of $[cAMP]_i$ and cell velocity shows that these two parameters both oscillated with a same periods and these oscillations correlated with each other at aggregation and mound stages (**Fig. 15**). Cross-correlation analysis revealed that the phase relationship between the $[cAMP]_i$ oscillation and cell velocity was dependent on the wave periods and not on the developmental stage (**Table 5**), suggesting that the kinetic relationship between cAMP synthesis and chemotactic movement caused by directed pseudopod formation in response to the cAMP signal until the tight mound stage depends on the period of external stimulation, not on the developmental stages. The periods of $[cAMP]_i$ oscillation in the aggregation and mound stages (**Table 5**) agreed well with those of synchronous changes in the optical density of cell populations previously reported (Rietdorf et al., 1996). The oscillation period decreased in loose mounds, but again increased in tight mounds to the same period as that in the aggregation stage (**Table 5**). These changes would be explained by two reasons; previous reports suggest that the decrease of the oscillation period can be caused by an increase in the cell density and extracellular cAMP (Gregor et al., 2010; Noorbakhsh, et al., 2015; Sgro et al., 2015).

Other, the increase of oscillation period would be involved in expression of different CARs which have different affinity to cAMP each other. *D. discoideum* genome encodes 4 CARs: high affinity receptor CAR1 and CAR3, low affinity receptor CAR2 and CAR4 (Dormann, et al., 2001; Ginsburg et al., 1995; Johnson et al., 1992). These receptors are expressed at the different time course along the developmental progression (Parent & Devreotes, 1996). It has been reported that the oscillation period is increased by the expression of low-affinity cAMP receptors during the mound stage instead of high-affinity receptors expressed in the aggregation stage (Dormann et al., 2001). It has also been suggested that the expression of low-affinity cAMP receptors causes changes in the cAMP wave geometry (Dormann et al., 2001), which is agreement with the hypothesis that the expression of low-affinity cAMP receptor at the mound stage plays a key role in changing the $[cAMP]_i$ wave propagation pattern at the loose mounds transform into tight mounds (**Fig. 12b and c**).

The physiological role of changes in geometry of cAMP wave propagation is clear: changes in the direction of chemotactic waves from horizontal rotation to top-bottom propagation (**Fig. 12b and c**) causes the synchronous upward movements of multiple cells in the mound resulting in the morphological changes of the entire mound (mound elongation). This also agrees with the traditional model, which assumes that cells differentiated into prestalk cells are sorted on the top of the tight mound to form the tip by chemotaxis toward cAMP signals (Weijer, 2009). On the other hand, the physiological roles of changes in the period of cAMP oscillations are not obvious. One candidate is the effect on periodic nucleocytoplasmic shuttling of a transcription factor GtaC which is related with the expression of developmentally-regulated genes (Cai et al., 2014). In *Dictyostelium* cells, GtaC shows nucleocytoplasmic shuttling in a cAMP-dependent manner and the shuttling oscillates in cells with a same period about 6 min as cAMP relay during aggregation. Furthermore, the periodic nucleocytoplasmic shuttling of GtaC is induced by external cAMP pulses with a period of 6 min but the rate of GtaC in nucleus decreases when the period of cAMP pulses decreases to 3 min. When the cells aggregate to form mound-like structures, little GtaC was found in the nucleus in the cells (Cai et al., 2014).

Considering the result of this study that the period of cAMP relay decreases from about 6 min to 3 min during the transition from aggregation to the loose mound stage (**Table 5**), the lack of GtaG shuttling during the mound formation can be explained by such changes in the period of cAMP relay. Because the periodic translocation of GtacC induces proper expression of developmentally-regulated genes such as *csaA* (Cai et al., 2014), arresting the GtatC shuttling resulted from the changes in period of cAMP relay would affect the transcriptional state during the mound formation. Furthermore, considering the result that the period of cAMP relay again increases from 3 to 6 min at the tight mound stage (**Table 5**), there is a possibility that GtaC shuttling occurs again and regulate expression of developmentally-regulated genes at the later development stage, tight mounds. In fact, GtaC is involved in cell differentiation into subtype of prestalk cells, pstB cells (Keller & Thompson, 2008), implying the role of GtaC at the later developmental stage. To confirm the hypothesis, spontaneous monitoring of cAMP signal dynamics and GtaC shuttling during the transition from loose mound to tight mound stages will be required.

**2. Transition of $[cAMP]_i$ signal dynamics from oscillations to steady state after slug formation.**

Live imaging throughout the multicellular formation revealed that $[cAMP]_i$ oscillations and wave propagations gradually weakened with slug formation and eventually disappeared at both tissue and single cell levels (**Fig. 13, 14**). The disappearance of $[cAMP]_i$ oscillations is consistent with the previous report using the other cAMP probe Epac-camp (McQuade, et al., 2013). Cells in streams which flowed into the posterior side of the slug did not mature completely as the cells at the multicellular phase and thus maintained the cAMP oscillations and signal propagation although the anterior part of the slug did not show any cAMP relay (**Fig. 12d**). Because a transient elevation of $[cAMP]_i$ in slug cells in response to external cAMP stimuli was detected by the changes in Flamindo2 signals (**Fig. 19**), the vanishing of the $[cAMP]_i$ oscillation was not due to impaired Flamindo2 function.

Furthermore, signal propagation was observed in migrating slugs using Flamindo2 in certain condition (**Fig. 20**), indicating that cAMP relay in slugs can be detected by Flamindo2 if it occurs and thus no detection of oscillations and propagation of Flamindo2 signals in slugs under normal observation condition means no cAMP relay in migrating slugs. Therefore, the results obtained by observation system using Flamindo2 show that a transition of cAMP signaling dynamics occurs after slug formation and that any endogenous $[cAMP]_i$ changes in slugs was below the detection limit of Flamindo2. Although no obvious cAMP oscillations were detected in slugs, cell velocity show oscillations in slugs similarly with those in aggregation and mound stages (**Fig. 15 and 18**). It has been reported that MDCK cells show coordinated cell movements and oscillating waves of motion spontaneously resulted from physical interaction between cells under the physical confined condition (Notbohm et al., 2016). Because the inside of the slug can be regarded as the physical confined environment consisting of extracellular matrix, periodic cell movements in slugs can be explained by the physical constrained condition of multiple cells, not by periodic chemical guidance.

In addition, to support the results by Flamindo2, we monitored the upstream of cAMP signal pathway, PIP3 signaling which activates ACA and in turn cAMP production. This is another approach which enables us to investigate the dynamics of cAMP signaling. Monitoring PIP3 levels on the plasma membrane using $PH_{Akt/PKB}$-GFP found periodic changes and its propagation at the mound stages. Additionally, the periods of $PH_{Akt/PKB}$-GFP translocation was similar with those of $[cAMP]_i$ at mound stages (**Results Section 8, Table 5**). On the other hand, $PH_{Akt/PKB}$-GFP in cells show continuous localization, not periodic translocation at the slug stage (**Fig. 24**). This contrast of signal dynamics between mound and slug stages is consistent with a previous report that tracked the PH domain of CRAC by GFP labelling in mounds and slugs (Dormann et al., 2002). Although the cells dissociated from slugs showed a transient translocation of $PH_{AKT/PKB}$-GFP in response to cAMP stimulation, the continuous localization of $PH_{AKT/PKB}$-GFP to the leading edge of cells in intact slugs was not inhibited by external cAMP stimuli and pharmacological inhibition of adenylyl cyclase (**Fig. 25**).

These observations suggest that the continuous polarity of PIP3 levels on the plasma membrane of slug cells at the cell boundary depends on tonic cAMP signals and/or other signals such as cell-cell contacts, as indicated in a previous study (Dormann et al., 2002). Thus, our findings demonstrate transitions from oscillations to steady state upstream of the cAMP signaling pathway during slug formation.

From these results and interpretation, this study raise the possibility that collective cell migration at the slug stage does not depend on cAMP relay for cell-cell communication, which challenges existing models (Dormann & Weijer, 2001; Friedl & Gilmour, 2009; Weijer, 1999; Weijer, 2009). However, this hypothesis is supported by the fact that *acaA*-null mutant cells lacking the ability of cAMP relay and development can aggregate and form multicellular bodies when prestimulated with exogenous cAMP pulses (Pitt et al., 1993) or when PKA, which is downstream of the cAMP signaling pathway, is constitutively activated (Wang & Kuspa, 1997). Monitoring $[cAMP]_i$ in *acaA*$^-$ mutant using Flamindo2 showed that the mutant cells could aggregate and form migrating slugs without $[cAMP]_i$ oscillations after the cAMP pulse treatment (**Fig. 21**). Previous reports (Pitt et al., 1993; Wang & Kuspa, 1997) and investigation in this study using the *acaA*-mutant imply a development capacity without periodic cAMP signals between cells. However, my approach using wild-type cells and live imaging technique reveals for the first time that the disappearance of periodic cAMP signals occurs even with normal developmental progression. Therefore, this study concluded that cAMP relay is not necessary for collective cell migration at the slug stage. On the other hand, this conclusion does not exclude the possibility that cAMP signals affect slug movement. We found that $[cAMP]_i$ and slug movement are sensitive to external cAMP stimuli (**Fig. 19**), indicating that collective cell migration could depend on any endogenous cAMP relay that occurs in slugs. The existence of optical density waves, which reflects cooperative changes in cell shape, namely collective cell migration and act as an index of cAMP relay in slugs, is controversial (Dormann & Weijer, 2001; Rietdorf et al., 1996). Therefore, it is possible that other experimental conditions would allow us to detect $[cAMP]_i$ wave propagation relevant to slug movement by using Flamindo2.

Actually, transient propagation of $[cAMP]_i$ waves was observed in slugs of bacterially growth XP55 strain (**Fig. 20d**). The reason why the wave propagation was observed only in the posterior tail region of the slug may be that anterior-like (prestalk-like) cells which exist in the tail region of slugs (Sternfeld & David, 1982) could emit the cAMP signals in response to the signals other than cAMP relay propagated from the anterior region of the slug. However, the frequency of $[cAMP]_i$ wave propagation is so rare even in the XP55 strain which can be regarded as the most suitable strain for observing the wave propagation in migrating slugs as previously described (Dormann & Weijer, 2001). Thus, further investigation about factors inducing cAMP relay in slugs and the relationship between cell movements and $[cAMP]_i$ waves is required for understanding the cAMP signal dynamics and its effect on collective cell migration in slugs.

**3. How does the transition of cAMP signaling occur during the development of *Dictyostelium* cells?**

The simultaneous monitoring of $[cAMP]_i$ and the marker of cell differentiation and sorting in *Dictyostelium* cells (**Fig. 26**) suggested that the transition of cAMP signaling dynamics was a developmentally regulated event. This proposition was confirmed in *gbfA*- mutants that were developmentally arrested at the loose mound stage and showed no transition in $[cAMP]_i$ dynamics during development (**Fig. 28**). In *Dictyostelium* cells, the expression pattern of genes essential for cAMP signaling is dramatically changed after slug formation (Parent & Devreotes, 1996). For example, the expression of high-affinity cAMP receptor CAR1 is high and seen in all cells during the aggregation stage, but becomes low after the mound stages (Johnson et al., 1993; Klein et al., 1987). In contrast, after slug formation, the expression of the high-affinity receptor CAR3 is seen in prespore cells, but the low-affinity receptors CAR2 and CAR4 are expressed in prestalk cells (Louis et al., 1994; Yu & Saxe III, 1996). These changes in expression pattern along the developmental time course are consistent with the sensitivity of the $[cAMP]_i$ response to external cAMP stimulation at the multicellular phase being lower than at the unicellular phase (**Fig. 9 and 19**) and that the responsiveness of chemotaxis to cAMP gradients becomes weaker with mound formation (Hirose, et al, 2015). The different sensitivities suggest changes in the cAMP signaling systems during multicellular formation.

Furthermore, it has been reported that signals of GFP fused with full-length CRAC is no detectable in slugs although it is expressed under the control of a constitutively active promoter *act15* and its fluorescence signals can be detected until the mound stage, suggesting that expression of fully functional CRAC is forcibly downregulated (Dormann et al., 2002). Additionally, imperfect adaptation to external cAMP stimulation observed in slug cells (Fig. 23) suggests the possibility that the systems for the response to cAMP signals which consist of various signal molecules such as PIP3 and Ras proteins (e. g., RasG: Swaney, et al., 2010) are altered in slugs and that such changes in the systems are also involved in the transition of cAMP signaling dynamics. Therefore, results in this study and previous reports suggest the active downregulation of molecules that mediate cAMP signaling and the developmental regulation of gene expression patterns during slug formation are involved in the transition of cAMP signaling dynamics.

On the other hand, there is a possibility that the transition of cAMP signaling dynamics is caused by the mechanisms other than the changes in expression pattern of genes involved in cAMP signal pathway, because the *gbfA*-mutant which shows development arrest at the loose mound stage and maintains $[cAMP]_i$ oscillations shows similar down-regulated expression pattern of genes involved in cAMP relay with the wild type (**Fig. 29**). The other possible mechanisms for the transition of cAMP signaling dynamics are the changes in protein localization and thus protein function. It has been reported that CAR1 is intrinsically internalized at the later development stage (Sergé et al., 2011). In the previous study, CAR1 localization has investigated under the submerged culture condition which is not the optimal development condition because submerged environment inhibit the mound formation after aggregation. In this study, CAR1 localization was monitored during the development on agar which allowed cells to normal developmental progression such as mound and slug formation. During the mound development and slug formation, CAR1 was gradually internalized and localization of CAR1 on the plasma membrane dramatically decreased in slugs, while the *gbfA*-mutant cells maintained CAR1 on the plasma membrane throughout their development (**Fig. 30**).

Therefore, these suggest that the CAR1 internalization occurs simultaneously with disappearance of $[cAMP]_i$ oscillations during the multicellular development and that CAR1 internalization is related with the transition of cAMP signaling dynamics. It has been widely known that internalization of G protein-coupled receptors is mediated by its phosphorylation and arrestin binding (Marchese, Paing, Temple, & Trejo, 2008). In *D. discoideum,* CAR1 is internalized when the cells are exposed to high-concentration cAMP (Cao et al., 2014) or persistent cAMP stimulation (Wang et al., 1988), and the internalization is regulated by phosphorylation of cAR1 and arrestin-dependent manner (Cao et al., 2014; Sergé et al., 2011). Mutant cells lacking arrestins (*adcB*$^-$*C*$^-$) which has no ability to cAR1 internalization show aberrant development and alteration of cAMP oscillations during aggregation (Cao et al., 2014), implying that the arrestin-dependent signal pathway is involved in the transition of cAMP signaling dynamics via CAR1 internalization. Investigation of cAMP dynamics using observation system developed in this study during the development of mutant cells such as *adcB*$^-$*C*$^-$ will give a new insight into the mechanism for transition of cAMP signaling dynamics.

**4. Possible mechanisms for organizing collective cell migration in slugs alternative to cAMP relay.**

This study revealed the disappearance of cAMP relay after multicellular slug formation and thus suggests the presence of mechanisms other than cAMP relay for the organization of collective cell migration in slugs. One possible mechanism is that extracellular cAMP signals such as a steady gradient in slugs work as the guidance cue of the direction of cell movements, like gradients of chemoattractant involved in collective cell migration in other multicellular organisms (Mayor & Etienne-Manneville, 2016). Blocking the cAMP signal pathway by caffeine treatment results in inhibition of the slug migration, although the morphology of the slug is maintained under caffeine treatment by cell-cell adhesions and the extracellular matrix (**Fig. 22**). Similarly, it has been reported that pharmacological inhibition of cAMP signaling caused the disorganization of collective cell migration of slugs including the cooperative changes in direction of cell movements such as phototactic movement of slugs (Darcy & Fisher, 1990; Rietdorf et al., 1998; Wang & Schaap, 1985).

Furthermore, although the developmental arrest phenotype of *acaA*$^{-}$ cells can be rescued by the expression of constitutively active PKA (Wang & Kuspa, 1997), mutant cells lacking *acaA* and *acrA*, which encode ACA and ACB, respectively, cannot form normal multicellular bodies even if constitutively active PKA is expressed (Anjard, Söderbom, & Loomis, 2001). These findings indicate that cAMP is still required for the collective migration of slugs although the detectable cAMP oscillations are absent in migrating slugs. In order to clarify the role of cAMP in slugs, molecular genetics approaches and more sensitive cAMP measurements are required.

In addition, it is possible that gradients of other chemoattractants in slugs are also involved in the organization of collective cell migration in slugs. One candidate of chemoattractants other than cAMP is pterin, which is derivate of folic acid. *D. discoideum* cells show chemotaxis toward pterin during the development (Tillinghast & Newell, 1987) and the signal pathway is mediated by receptors coupled to the Gα protein subunit Gα4 (J A Hadwiger, Lee, & Firtel, 1994). The Gα4 protein are expressed at high levels at the early mound stage and its expression levels are maintained through the subsequent development (Hadwiger, Wilkie, Strathmann, & Firtel, 1991). Mutant lacking Gα4 show aberrant formation of multicellular bodies, indicating the pterin-Gα4 signal pathway is required for morphogenesis of multicellular bodies(J A Hadwiger & Firtel, 1992; J A Hadwiger et al., 1994). The other candidate of chemical guidance is $Ca^{2+}$ signaling. *Dictyostelium* cells show chemotactic movement toward $Ca^{2+}$ gradients (Scherer et al., 2010). In slugs, $Ca^{2+}$ concentration of anterior prestalk cells is higher than posterior prespore cells (Saran et al., 1994; Yumura, Furuya, & Takeuchi, 1996). Furthermore, transient burst of $[Ca^{2+}]_i$ was observed in the anterior part of migrating slugs (Cubitt et al., 1995). These suggest the possibility that self-organized $Ca^{2+}$ gradients in slugs plays key roles in organizing collective cell migration of slugs.

In addition to chemical guidance, it is widely known that collective migration is regulated by physical guidance cues through cell-cell contacts and cell-substrate adhesion in higher organisms during various events such as epithelial wound healing and cancer invasion (Haeger et al., 2015; Ladoux & Mège, 2017).

Numerical simulations have shown that physical interactions between cells such as collision can organize collective cell migration in the absence of any chemical interaction (Li & Sun, 2014; Rappel et al., 1999). These studies raise the possibility that the collective cell migration in *Dictyostelium* multicellular bodies is organized by physical guidance cues. One possible physical interaction is "contact following", which is the property that cells follow other cells with which they have direct physical cell-cell contact (Shaffer, 1964). Cells in slugs adhere each other and show organized movements to the same direction, but the cells dissociated from slugs are also aligned each other through contact following and move cooperatively as a single group (**Fig. 31**). *D. discoideum* has several proteins mediating cell-cell adhesion (e. g., DdCAD-1, CsA, TgrB1) and their expression pattern are developmentally regulated (Benabentos et al., 2009; Siu, Harris, Wang, & Wong, 2004; Wong & Siu, 1986; Yang, Brar, Desbarats, & Siu, 1997). In particular, the adhesion proteins TgrC1 which are expressed at the later mound stage (Wang et al., 2000) play key roles in morphogenesis of multicellular bodies. The mutant lacking TgrC1 show development arrest at the loose mound stage like the *gbfA* mutant (Dynes et al., 1994). Blocking of TgrC1 by binding of antibodies causes defect in cell sorting and slug formation (Siu, Des Roches, & Lam, 1983). Furthermore, cell-cell contact via TgrB1/TgrC1 proteins leads to cell polarization including PIP3 localization on cell membrane and coordinated cell migration at the mound stage (Hirose et al., 2015). Additionally, mutant cells which lack chemotaxis toward any known chemoattractants show an organized collective migration that is mediated by cell-cell adhesions (Kuwayama & Ishida, 2013). Therefore, these suggest that cell-cell contacts play important roles on collective cell migration at the multicellular stage of *Dictyostelium* cells.

Additionally, it has been know that extracellular matrix are involved in organization of collective cell migration in higher organisms (Ilina, Friedl, Li, Meinkoth, & Herlyn, 2009). Therefore, there is a possibility that extracellular matrix in *Dictyostelium* called slime sheath also play important roles on maintaining collective cell migration in slugs. Slime sheath are mainly secreted by prestalk cells and consists of various proteins, cellulose and polysaccharide (Morrison et al., 1994; Wilkins & Williams, 1995).

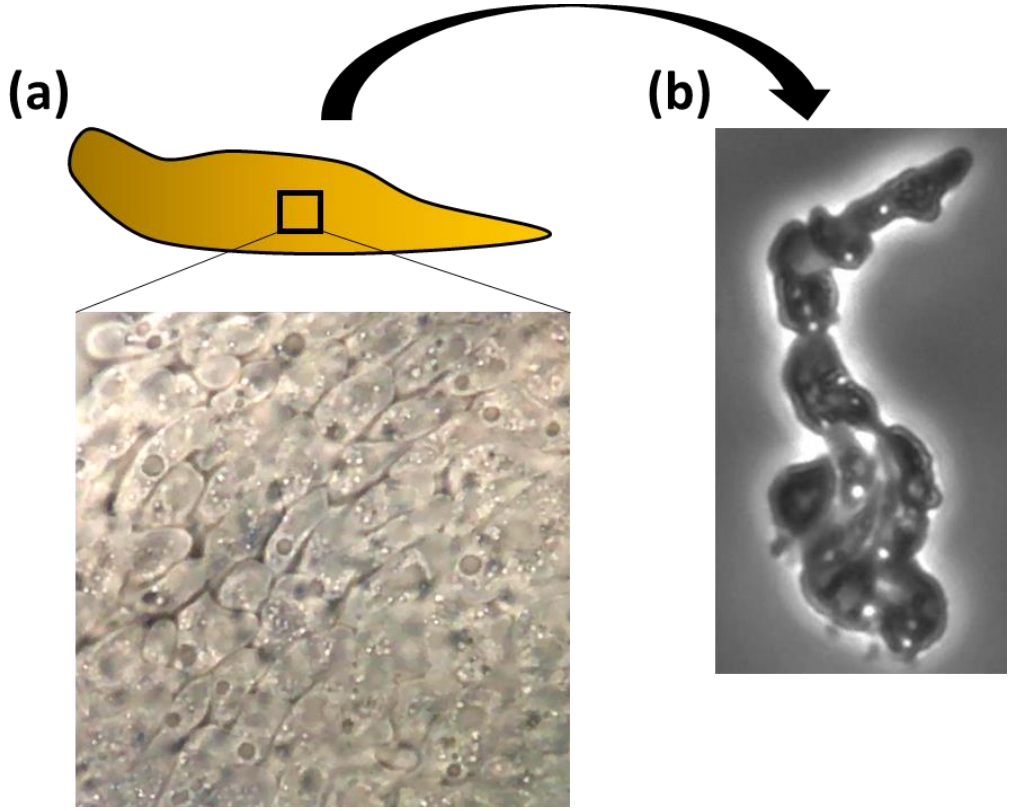


**Figure. 31 Contact following of slug cells.**

(a) Cell alignment via cell-cell contact in the intact slug. The DIC image of surface of slugs attached to the glass is shown. (b) Contact following of cells dissociated from the slug. The phase contrast image of slug dissociated cells enclosed between glass and agar is shown. Cells adhere via the head-to-tail contact and move as a single cell group.

The compounds of protein in slime sheath includes EGFL repeat-containing protein which are involved in regulating cell motility, suggesting slime sheath works as the substrate modulating cell motility (Huber & O'Day, 2017). Because the slime sheath surround the slug like a "stocking", the physical constrain by slime sheath would help to maintain the direction of multiple cell movements which is aligned during the mound elongation. In fact, it has been recently reported that epithelial cells show apical-basal polarity and organized cell movements when the cell sheets are confined in tubular structures, suggesting environmental constrain contributes the organization of polarity and coordinated movements of cell populations (Xi et al., 2017). Furthermore, the observation using the electron microscope has found that the thickness of slime sheath increases towards the posterior side of the slug (Farnsworth & Loomis, 1975). Such gradient of surrounding physical restriction also may arise the supracellular polarity of cell populations during the slug migration.

## Conclusion

It has been assumed that the cell-cell communication via chemical signals, namely cAMP relay plays important roles on organization of collective cell migration through the development of *Dictyostelium* cells, but the dynamics and roles of cAMP relay at the multicellular phase is still unclear. In this study, monitoring cAMP signals in cell populations through the development based on live cell imaging technique directly demonstrated that the cAMP relay organizes the collective cell migration until the intermediate stage of multicellular development (mound) but is gradually weakened and finally disappeared at the multicellular stage (slug). These observation and investigation of mutant cells concluded that collective cell migration in the multicellular slugs is independent of cAMP relay (**Fig. 32**). Thus, this work calls for reconsideration of the role that cAMP relay has in collective cell migration in *Dictyostelium* and proposes a possibility that alternative mechanisms such as physical and/or other chemical factors to cAMP relay contribute to the organization of collective cell migration at the multicellular phase. In future, investigation using more sensitive cAMP probe or probes targeting other chemical signals and numerical simulation focusing on physical interaction without any chemical guidance will give a further understanding of the mechanism for organizing collective cell migration of *Dictyostelium* cells without cAMP relay.

Researchers have investigated various organisms and biological events as a model for the study of mechanisms for collective cell migration. However, many of those focuses on only a limited scene of biological activities, although various collective behavior actually occurs even in one organism through their life cycle. Such approaches can only reveal the mechanisms for collective cell migration in particular cases and thus how the diverse collective cell movements in one organism are organized has not been considered. This study using *Dictyostelium* demonstrated that the role of a mechanism in collective cell migration dramatically changes during the transition of cooperative behavior. Thus, this open a new window on the strategies that organisms customize according to collective behavior of each biological scenes through their life style.

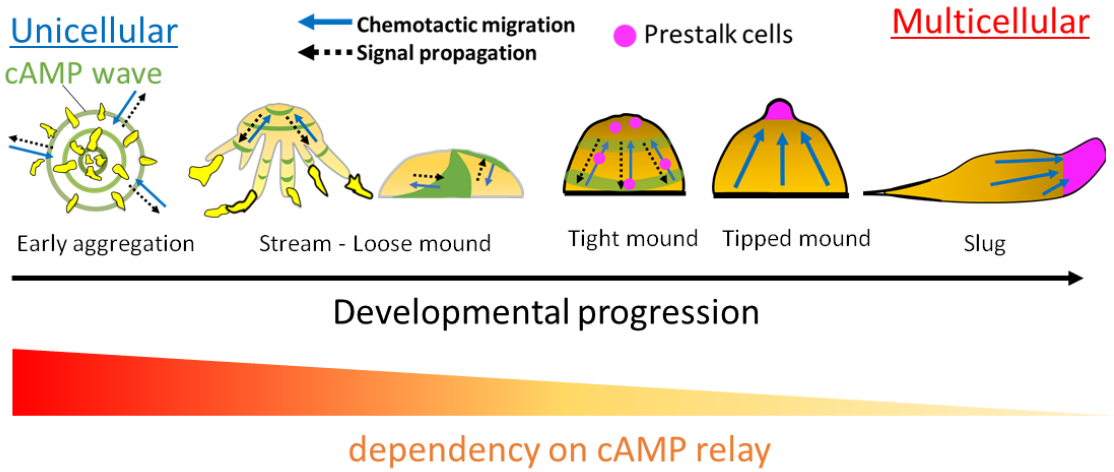


**Figure 32. Model of transition of cAMP signal dynamics throughout the development of *D. discoideum* cells.**

At the unicellular phase, cAMP signals are propagated between starved cells to chemotactic aggregation. cAMP waves are also propagated in streams and loose mounds in a spiral manner, which causes rotational cell movements in mounds. Then the geometry of wave propagation changes from rotational to top-bottom pattern in tight mounds, resulting in prestalk cell sorting and mound elongation. During the mound elongation, cAMP signal oscillation and propagation gradually becomes weaker, and finally disappear after the obvious tips were formed on the top of the mound. At the slug stage, cell populations show cooperative migration without cAMP relay. This model supersedes the traditional assumption of the relationship between cAMP signals and collective cell migration (see **Fig. 3**).

## References


Alvarez-Curto, E., Weening, K. E., & Schaap, P. (2007). Pharmacological profiling of the *Dictyostelium* adenylate cyclases ACA, ACB and ACG. *The Biochemical Journal*, *401*(1), 309–316.

Anjard, C., Söderbom, F., & Loomis, W. F. (2001). Requirements for the adenylyl cyclases in the development of *Dictyostelium*. *Development (Cambridge, England)*, *128*(18), 3649–3654.

Aoki, K., Kondo, Y., Naoki, H., Hiratsuka, T., Itoh, R. E., & Matsuda, M. (2017). Propagating Wave of ERK Activation Orients Collective Cell Migration. *Developmental Cell*, *43*(3), 305–317.e5.

Aoki, K., Kumagai, Y., Sakurai, A., Komatsu, N., Fujita, Y., Shionyu, C., & Matsuda, M. (2013). Stochastic ERK Activation Induced by Noise and Cell-to-Cell Propagation Regulates Cell Density-Dependent Proliferation. *Molecular Cell*, *52*(4), 529–540.

Asano, Y., Nagasaki, A., & Uyeda, T. Q. P. (2008). Correlated waves of actin filaments and PIP $_3$ in *Dictyostelium* cells. *Cell Motility and the Cytoskeleton*, *65*(12), 923–934.

Aubry, L., & Klein, G. (2006). Purification Techniques of Subcellular Compartments for Analytical and Preparative Purposes. In *Dictyostelium discoideum Protocols* (Vol. 346, pp. 171–186). New Jersey: Humana Press.

Bailly, M., Ichetovkin, I., Grant, W., Zebda, N., Machesky, L. M., Segall, J. E., & Condeelis, J. (2001). The F-actin side binding activity of the Arp2/3 complex is essential for actin nucleation and lamellipod extension. *Current Biology*, *11*(8), 620–625.

Bajec, I. L., & Heppner, F. H. (2009). Organized flight in birds. *Animal Behaviour*, *78*(4), 777–789.

Benabentos, R., Hirose, S., Sucgang, R., Curk, T., Katoh, M., Ostrowski, E. A., … Kuspa, A. (2009). Polymorphic Members of the lag Gene Family Mediate Kin Discrimination in *Dictyostelium*. *Current Biology*, *19*(7), 567–572.

Bevis, B. J., & Glick, B. S. (2002). Rapidly maturing variants of the Discosoma red fluorescent protein (DsRed). *Nature Biotechnology*, *20*(1), 83–87.

Bonner, J. T. (1952). The Pattern of Differentiation in Amoeboid Slime Molds. *The American Naturalist*, *86*(827), 79–89.

Bonner, J. T. (1998). A way of following individual cells in the migrating slugs of *Dictyostelium discoideum*. *Proceedings of the National Academy of Sciences of the*

*United States of America*, *95*(16), 9355–9359.

Bonner, J. T., Barkley, D. S., Hall, E. M., Konijn, T. M., Mason, J. W., O'Keefe, G., & Wolfe, P. B. (1969). Acrasin, acrasinase, and the sensitivity to acrasin in *Dictyostelium discoideum*. *Developmental Biology*, *20*(1), 72–87.

Brenner, M. (1978). Cyclic AMP levels and turnover during development of the cellular slime mold *Dictyostelium discoideum*. *Developmental Biology*, *64*(2), 210–223.

Butt, T., Mufti, T., Humayun, A., Rosenthal, P. B., Khan, S., Khan, S., & Molloy, J. E. (2010). Myosin motors drive long range alignment of actin filaments. *The Journal of Biological Chemistry*, *285*(7), 4964–4974.

Cai, D., Chen, S.-C., Prasad, M., He, L., Wang, X., Choesmel-Cadamuro, V., … Montell, D. J. (2014). Mechanical Feedback through E-Cadherin Promotes Direction Sensing during Collective Cell Migration. *Cell*, *157*(5), 1146–1159.

Cai, H., Katoh-Kurasawa, M., Muramoto, T., Santhanam, B., Long, Y., Li, L., … Devreotes, P. N. (2014). Nucleocytoplasmic shuttling of a GATA transcription factor functions as a development timer. *Science (New York, N.Y.)*, *343*(6177), 1249531.

Cao, X., Yan, J., Shu, S., Brzostowski, J. A., & Jin, T. (2014). Arrestins function in cAR1 GPCR-mediated signaling and cAR1 internalization in the development of *Dictyostelium discoideum*. *Molecular Biology of the Cell*, *25*(20), 3210–3221.

Chen, Z.-H., Singh, R., Cole, C., Lawal, H. M., Schilde, C., Febrer, M., … Schaap, P. (2017). Adenylate cyclase A acting on PKA mediates induction of stalk formation by cyclic diguanylate at the *Dictyostelium* organizer. *Proceedings of the National Academy of Sciences of the United States of America*, *114*(3), 516–521.

Comer, F. I., & Parent, C. A. (2002). PI3-Kinases and PTEN: How Opposites Chemoattract. *Cell*, *109*(5), 541–544.

Cubitt, A. B., Firtel, R. A., Fischer, G., Jaffe, L. F., & Miller, A. L. (1995). Patterns of free calcium in multicellular stages of *Dictyostelium* expressing jellyfish apoaequorin. *Development*, *121*(8).

Darcy, P. K., & Fisher, P. R. (1990). Pharmacological evidence for a role for cyclic AMP signalling in *Dictyostelium discoideum* slug behaviour. *Journal of Cell Science*, *96*(4).

Devreotes, P. N., Derstine, P. L., & Steck, T. L. (1979). Cyclic 3',5' AMP relay in *Dictyostelium discoideum*. I. A technique to monitor responses to controlled stimuli. *The Journal of Cell Biology*, *80*(2), 291–299.

Dinauer, M. C., MacKay, S. A., & Devreotes, P. N. (1980). Cyclic 3',5'-AMP relay in *Dictyostelium discoideum* III. The relationship of cAMP synthesis and secretion

during the cAMP signaling response. *The Journal of Cell Biology*, *86*(2), 537–544.

Dingle, H., & Drake, V. A. (2007). What Is Migration? *BioScience*, *57*(2), 113–121.

Doitsidou, M., Reichman-Fried, M., Stebler, J., Köprunner, M., Dörries, J., Meyer, D., … Raz, E. (2002). Guidance of Primordial Germ Cell Migration by the Chemokine SDF-1. *Cell*, *111*(5), 647–659.

Donà, E., Barry, J. D., Valentin, G., Quirin, C., Khmelinskii, A., Kunze, A., … Gilmour, D. (2013). Directional tissue migration through a self-generated chemokine gradient. *Nature*, *503*(7475), 285–289.

Dormann, D., Kim, J. Y., Devreotes, P. N., & Weijer, C. J. (2001). cAMP receptor affinity controls wave dynamics, geometry and morphogenesis in *Dictyostelium*. *Journal of Cell Science*, *114*(Pt 13), 2513–2523.

Dormann, D., & Weijer, C. J. (2001). Propagating chemoattractant waves coordinate periodic cell movement in *Dictyostelium* slugs. *Development*, *128*(22).

Dormann, D., & Weijer, C. J. (2006). Visualizing Signaling and Cell Movement During the Multicellular Stages of *Dictyostelium* Development. In *Dictyostelium discoideum Protocols* (pp. 297–310). New Jersey: Humana Press.

Dormann, D., Weijer, G., Parent, C. A., Devreotes, P. N., & Weijer, C. J. (2002). Visualizing PI3 Kinase-Mediated Cell-Cell Signaling during *Dictyostelium* Development. *Current Biology*, *12*(14), 1178–1188.

Duchek, P., & Rørth, P. (2001). Guidance of cell migration by EGF receptor signaling during *Drosophila* oogenesis. *Science*, *291*(5501), 131–133.

Duchek, P., Somogyi, K., Jékely, G., Beccari, S., & Rørth, P. (2001). Guidance of Cell Migration by the *Drosophila* PDGF/VEGF Receptor. *Cell*, *107*(1), 17–26.

Dumortier, J. G., Martin, S., Meyer, D., Rosa, F. M., & David, N. B. (2012). Collective mesendoderm migration relies on an intrinsic directionality signal transmitted through cell contacts. *Proceedings of the National Academy of Sciences of the United States of America*, *109*(42), 16945–16950.

Dynes, J. L., Clark, A. M., Shaulsky, G., Kuspa, A., Loomis, W. F., & Firtel, R. A. (1994). LagC is required for cell-cell interactions that are essential for cell-type differentiation in *Dictyostelium*. *Genes & Development*, *8*(8), 948–958.

Early, A., Abe, T., & Williams, J. (1995). Evidence for positional differentiation of prestalk cells and for a morphogenetic gradient in dictyostelium. *Cell*, *83*(1), 91–99.

Early, A. E., Gaskell, M. J., Traynor, D., & Williams, J. G. (1993). Two distinct populations of prestalk cells within the tip of the migratory *Dictyostelium* slug with differing fates at culmination. *Development*, *118*(2).

Farnsworth, P. A., & Loomis, W. F. (1975). A gradient in the thickness of the surface sheath in pseudoplasmodia of *Dictyostelium discoideum*. *Developmental Biology*, *46*(2), 349–357.

Firtel, R. A. (1995). Integration of signaling information in controlling cell-fate decisions in *Dictyostelium*. *Genes & Development*, *9*(12), 1427–1444.

Friedl, P., & Gilmour, D. (2009). Collective cell migration in morphogenesis, regeneration and cancer. *Nature Reviews Molecular Cell Biology*, *10*(7), 445–457.

Friedl, P., Hegerfeldt, Y., & Tusch, M. (2004). Collective cell migration in morphogenesis and cancer. *The International Journal of Developmental Biology*, *48*(5–6), 441–449.

Funamoto, S., Milan, K., Meili, R., & Firtel, R. A. (2001). Role of phosphatidylinositol 3' kinase and a downstream pleckstrin homology domain-containing protein in controlling chemotaxis in dictyostelium. *The Journal of Cell Biology*, *153*(4), 795–810.

Gaggioli, C., Hooper, S., Hidalgo-Carcedo, C., Grosse, R., Marshall, J. F., Harrington, K., & Sahai, E. (2007). Fibroblast-led collective invasion of carcinoma cells with differing roles for RhoGTPases in leading and following cells. *Nature Cell Biology*, *9*(12), 1392–1400.

Gerisch, G., Maeda, Y., Malchow, D., Roos, W., Wick, U., & Wurster, B. (1977). CYCLIC AMP SIGNALS AND THE CONTROL OF CELL AGGREGATION IN DICTYOSTELIUM DISCOIDEUM. *Development and Differentiation in the Cellular Slime Moulds*, 105–124.

Ginsburg, G. T., Gollop, R., Yu, Y., Louis, J. M., Saxe, C. L., & Kimmel, A. R. (1995). The Regulation of *Dictyostelium* Development by Transmembrane Signalling. *The Journal of Eukaryotic Microbiology*, *42*(3), 200–205.

Gregor, T., Fujimoto, K., Masaki, N., & Sawai, S. (2010). The onset of collective behavior in social amoebae. *Science*, *328*(5981), 1021–1025.

Gruler, H., & Bültmann, B. D. (1984). Analysis of cell movement. *Blood Cells*, *10*(1), 61–77.

Hadwiger, J. A. (2007). Developmental morphology and chemotactic responses are dependent on Gα subunit specificity in *Dictyostelium*. *Developmental Biology*, *312*(1), 1–12.

Hadwiger, J. A., & Firtel, R. A. (1992). Analysis of G alpha 4, a G-protein subunit required for multicellular development in *Dictyostelium*. *Genes & Development*, *6*(1), 38–49.

Hadwiger, J. A., Lee, S., & Firtel, R. A. (1994). The G alpha subunit G alpha 4 couples

to pterin receptors and identifies a signaling pathway that is essential for multicellular development in *Dictyostelium*. *Proceedings of the National Academy of Sciences of the United States of America*, *91*(22), 10566–10570.

Hadwiger, J. A., Wilkie, T. M., Strathmann, M., & Firtel, R. A. (1991). Identification of *Dictyostelium* G alpha genes expressed during multicellular development. *Proceedings of the National Academy of Sciences of the United States of America*, *88*(18), 8213–8217.

Haeger, A., Wolf, K., Zegers, M. M., & Friedl, P. (2015). Collective cell migration: guidance principles and hierarchies. *Trends in Cell Biology*, *25*(9), 556–566.

Harwood, A. J., Hopper, N. A., Simon, M.-N., Bouzid, S., Veron, M., & Williams, J. G. (1992). Multiple roles for cAMP-dependent protein kinase during *Dictyostelium* development. *Developmental Biology*, *149*(1), 90–99.

Hirose, S., Santhanam, B., Katoh-Kurosawa, M., Shaulsky, G., & Kuspa, A. (2015). Allorecognition, via TgrB1 and TgrC1, mediates the transition from unicellularity to multicellularity in the social amoeba *Dictyostelium discoideum*. *Development*, *142*(20), 3561–3570.

Huber, R. J., & O'Day, D. H. (2017). Extracellular matrix dynamics and functions in the social amoeba *Dictyostelium*: A critical review. *Biochimica et Biophysica Acta (BBA) - General Subjects*, *1861*(1), 2971–2980.

Ilina, O., Friedl, P., Li, G., Meinkoth, J. L., & Herlyn, M. (2009). Mechanisms of collective cell migration at a glance. *Journal of Cell Science*, *122*(Pt 18), 3203–3208.

Inouye, K., & Gross, J. (1993). In vitro stalk cell differentiation in wild-type and 'slugger' mutants of *Dictyostelium discoideum*. *Development*, *118*(2).

Inouye, K., & Takeuchi, I. (1979). Analytical studies on migrating movement of the pseudo-plasmodium of *Dictyostelium discoideum*. *Protoplasma*, *99*(4), 289–304.

Insall, R., Kuspa, A., Lilly, P. J., Shaulsky, G., Levin, L. R., Loomis, W. F., & Devreotes, P. (1994). CRAC, a cytosolic protein containing a pleckstrin homology domain, is required for receptor and G protein-mediated activation of adenylyl cyclase in *Dictyostelium*. *The Journal of Cell Biology*, *126*(6), 1537–1545.

Iranfar, N., Fuller, D., & Loomis, W. F. (2003). Genome-wide expression analyses of gene regulation during early development of *Dictyostelium discoideum*. *Eukaryotic Cell*, *2*(4), 664–670.

Johnson, R. L., Saxe, C. L., Gollop, R., Kimmel, A. R., & Devreotes, P. N. (1993). Identification and targeted gene disruption of cAR3, a cAMP receptor subtype expressed during multicellular stages of *Dictyostelium* development. *Genes &*

*Development*, *7*(2), 273–282.

Johnson, R. L., Van Haastert, P. J., Kimmel, A. R., Saxe, C. L., Jastorff, B., & Devreotes, P. N. (1992). The cyclic nucleotide specificity of three cAMP receptors in *Dictyostelium*. *The Journal of Biological Chemistry*, *267*(7), 4600–4607.

Kareiva, P. M., & Shigesada, N. (1983). Analyzing insect movement as a correlated random walk. *Oecologia*, *56*(2–3), 234–238.

Kay, R. R. (1989). Evidence that elevated intracellular cyclic AMP maturation in Dictyostelium. *Development*, *105*(4).

Keller, T., & Thompson, C. R. L. (2008). Cell type specificity of a diffusible inducer is determined by a GATA family transcription factor. *Development (Cambridge, England)*, *135*(9), 1635–1645.

Kim, H. J., Chang, W. T., Meima, M., Gross, J. D., & Schaap, P. (1998). A novel adenylyl cyclase detected in rapidly developing mutants of *Dictyostelium*. *The Journal of Biological Chemistry*, *273*(47), 30859–30862.

Kim, J. Y., Soede, R. D., Schaap, P., Valkema, R., Borleis, J. A., Van Haastert, P. J., … Hereld, D. (1997). Phosphorylation of chemoattractant receptors is not essential for chemotaxis or termination of G-protein-mediated responses. *The Journal of Biological Chemistry*, *272*(43), 27313–27318.

Klein, P., Vaughan, R., Borleis, J., & Devreotes, P. (1987). The surface cyclic AMP receptor in *Dictyostelium*. Levels of ligand-induced phosphorylation, solubilization, identification of primary transcript, and developmental regulation of expression. *The Journal of Biological Chemistry*, *262*(1), 358–364.

Konijn, T. M., Chang, Y.-Y., & Bonner, J. T. (1969). Synthesis of Cyclic AMP in *Dictyostelium discoideum* and *Polysphondylium pallidum*. *Nature*, *224*(5225), 1211–1212.

Konijn, T. M., van de Meene, J. G., Chang, Y. Y., Barkley, D. S., & Bonner, J. T. (1969). Identification of adenosine-3',5'-monophosphate as the bacterial attractant for myxamoebae of *Dictyostelium discoideum*. *Journal of Bacteriology*, *99*(2), 510–512.

Kumagai, A., Hadwiger, J. A., Pupillo, M., & Firtel, R. A. (1991). Molecular genetic analysis of two G alpha protein subunits in *Dictyostelium*. *The Journal of Biological Chemistry*, *266*(2), 1220–1228.

Kunwar, P. S., Siekhaus, D. E., & Lehmann, R. (2006). In Vivo Migration: A Germ Cell Perspective. *Annual Review of Cell and Developmental Biology*, *22*(1), 237–265.

Kuwayama, H., & Ishida, S. (2013). Biological soliton in multicellular movement.

*Scientific Reports*, *3*(1), 2272.

Kuwayama, H., Yanagida, T., & Ueda, M. (2008). DNA oligonucleotide-assisted genetic manipulation increases transformation and homologous recombination efficiencies: Evidence from gene targeting of *Dictyostelium discoideum*. *Journal of Biotechnology*, *133*(4), 418–423.

Kwong, L., Sobolewski, A., & Weeks, G. (1988). The effect of cAMP on differentiation inducing factor (DIF)-mediated formation of stalk cells in low-cell-density monolayers of *Dictyostelium discoideum*. *Differentiation*, *37*(1), 1–6.

Ladoux, B., & Mège, R.-M. (2017). Mechanobiology of collective cell behaviours. *Nature Reviews Molecular Cell Biology*, *18*(12), 743–757.

Li, B., & Sun, S. X. (2014). Coherent Motions in Confluent Cell Monolayer Sheets. *Biophysical Journal*, *107*(7), 1532–1541.

Lilly, P., Wu, L., Welker, D. L., & Devreotes, P. N. (1993). A G-protein beta-subunit is essential for *Dictyostelium* development. *Genes & Development*, *7*(6), 986–995.

Loomis, W. F. (1971). Sensitivity of *Dictyostelium discoideum* to nucleic acid analogues. *Experimental Cell Research*, *64*(2), 484–486.

Loomis, W. F. (2014). Cell signaling during development of *Dictyostelium*. *Developmental Biology*, *391*(1), 1–16.

Louis, J. M., Ginsburg, G. T., & Kimmel, A. R. (1994). The cAMP receptor CAR4 regulates axial patterning and cellular differentiation during late development of *Dictyostelium*. *Genes & Development*, *8*(17), 2086–2096.

Magurran, A. E. (1990). The adaptive significance of schooling as an anti-predator defence in fish. *Annales Zoologici Fennici*. **27**, 51–66.

Mann, S. K. O., & Firtel, R. A. (1991). A developmentally regulated, putative serine/threonine protein kinase is essential for development in *Dictyostelium*. *Mechanisms of Development*, *35*(2), 89–101.

Mann, S. K., Yonemoto, W. M., Taylor, S. S., & Firtel, R. A. (1992). DdPK3, which plays essential roles during *Dictyostelium* development, encodes the catalytic subunit of cAMP-dependent protein kinase. *Proceedings of the National Academy of Sciences of the United States of America*, *89*(22), 10701–10705.

Marchese, A., Paing, M. M., Temple, B. R. S., & Trejo, J. (2008). G Protein–Coupled Receptor Sorting to Endosomes and Lysosomes. *Annual Review of Pharmacology and Toxicology*, *48*(1), 601–629.

Matsubayashi, Y., Razzell, W., & Martin, P. (2011). "White wave" analysis of epithelial scratch wound healing reveals how cells mobilise back from the leading edge in a myosin-II-dependent fashion. *Journal of Cell Science*, *124*(Pt 7), 1017–1021.

Matsuoka, S., Iijima, M., Watanabe, T. M., Kuwayama, H., Yanagida, T., Devreotes, P. N., & Ueda, M. (2006). Single-molecule analysis of chemoattractant-stimulated membrane recruitment of a PH-domain-containing protein. *Journal of Cell Science*, *119*(Pt 6), 1071–1079.

Mayor, R., & Etienne-Manneville, S. (2016). The front and rear of collective cell migration. *Nature Reviews Molecular Cell Biology*, *17*(2), 97–109.

McMahon, A., Supatto, W., Fraser, S. E., & Stathopoulos, A. (2008). Dynamic analyses of *Drosophila* gastrulation provide insights into collective cell migration. *Science*, *322*(5907), 1546–1550.

McQuade, K. J., Nakajima, A., Ilacqua, A. N., Shimada, N., & Sawai, S. (2013). The green tea catechin epigallocatechin gallate (EGCG) blocks cell motility, chemotaxis and development in *Dictyostelium discoideum*. *PloS one*, *8*(3), e59275.

Mee, J. D., Tortolo, D. M., & Coukell, M. B. (1986). Chemotaxis-associated properties of separated prestalk and prespore cells of *Dictyostelium discoideum*. *Biochemistry and Cell Biology*, *64*(8), 722–732.

Meili, R., Ellsworth, C., Lee, S., Reddy, T. B., Ma, H., Firtel, R. A., & Hemmings, B. A. (1999). Chemoattractant-mediated transient activation and membrane localization of Akt/PKB is required for efficient chemotaxis to cAMP in *Dictyostelium*. *The EMBO Journal*, *18*(8), 2092–2105.

Meima, M. E., & Schaap, P. (1999). Fingerprinting of Adenylyl Cyclase Activities during *Dictyostelium* Development Indicates a Dominant Role for Adenylyl Cyclase B in Terminal Differentiation. *Developmental biology*, *212*(1), 182-190.

Migeotte, I., Omelchenko, T., Hall, A., & Anderson, K. V. (2010). Rac1-Dependent Collective Cell Migration Is Required for Specification of the Anterior-Posterior Body Axis of the Mouse. *PLoS Biology*, *8*(8), e1000442.

Morio, T., Yasukawa, H., Urushihara, H., Saito, T., Ochiai, H., Takeuchi, I., … Tanaka, Y. (2001). FebA: a gene for eukaryotic translation initiation factor 4E-binding protein (4E-BP) in *Dictyostelium discoideum*. *Biochimica et Biophysica Acta (BBA) - Gene Structure and Expression*, *1519*(1–2), 65–69.

Morrison, A., Blanton, R. L., Grimson, M., Fuchs, M., Williams, K., & Williams, J. (1994). Disruption of the Gene Encoding the EcmA, Extracellular Matrix Protein of *Dictyostelium* Alters Slug Morphology. *Developmental Biology*, *163*(2), 457–466.

Nobes, C. D., & Hall, A. (1999). Rho GTPases control polarity, protrusion, and adhesion during cell movement. *The Journal of Cell Biology*, *144*(6), 1235–1244.

Noorbakhsh, J., Schwab, D. J., Sgro, A. E., Gregor, T., & Mehta, P. (2015). Modeling

oscillations and spiral waves in *Dictyostelium* populations. *Physical Review E*, *91*(6), 062711.

Notbohm, J., Banerjee, S., Utuje, K. J. C., Gweon, B., Jang, H., Park, Y., … Marchetti, M. C. (2016). Cellular Contraction and Polarization Drive Collective Cellular Motion. *Biophysical Journal*, *110*(12), 2729–2738.

Odaka, H., Arai, S., Inoue, T., & Kitaguchi, T. (2014). Genetically-Encoded Yellow Fluorescent cAMP Indicator with an Expanded Dynamic Range for Dual-Color Imaging. *PLoS ONE*, *9*(6), e100252.

Ohta, Y., Furuta, T., Nagai, T., & Horikawa, K. (2018). Red fluorescent cAMP indicator with increased affinity and expanded dynamic range. *Scientific Reports*, *8*(1), 1866.

Ohta, Y., Kamagata, T., Mukai, A., Takada, S., Nagai, T., & Horikawa, K. (2016). Nontrivial Effect of the Color-Exchange of a Donor/Acceptor Pair in the Engineering of Förster Resonance Energy Transfer (FRET)-Based Indicators. *ACS Chemical Biology*, *11*(7), 1816–1822.

Otte, A. P., Plomp, M. J. E., Arents, J. C., Janssens, P. M. W., & van Driel, R. (1986). Production and turnover of cAMP signals by prestalk and prespore cells in *Dictyostelium discoideum* cell aggregates. *Differentiation*, *32*(3), 185–191.

Pan, P., Hall, E. M., & Bonner, J. T. (1972). Folic Acid as Second Chemotactic Substance in the Cellular Slime Moulds. *Nature New Biology*, *237*(75), 181–182.

Parent, C. A., Blacklock, B. J., Froehlich, W. M., Murphy, D. B., & Devreotes, P. N. (1998). G Protein Signaling Events Are Activated at the Leading Edge of Chemotactic Cells. *Cell*, *95*(1), 81–91.

Parent, C. A., & Devreotes, P. N. (1996). Molecular Genetics of Signal Transduction in *Dictyostelium*. *Annual Review of Biochemistry*, *65*(1), 411–440.

Parikh, A., Miranda, E. R., Katoh-Kurasawa, M., Fuller, D., Rot, G., Zagar, L., … Shaulsky, G. (2010). Conserved developmental transcriptomes in evolutionarily divergent species. *Genome Biology*, *11*(3), R35.

Parrish, J. K., & Hamner, W. M. (1997). Animal Groups in Three Dimensions : How Species Aggregate. Cambridge University Press.

Parrish, J. K., Viscido, S. V, & Grünbaum, D. (2002). Self-organized fish schools: an examination of emergent properties. *The Biological Bulletin*, *202*(3), 296–305.

Partridge, B. L., & Pitcher, T. J. (1979). Evidence against a hydrodynamic function for fish schools. *Nature*, *279*(5712), 418–419.

Pitt, G. S., Brandt, R., Lin, K. C., Devreotes, P. N., & Schaap, P. (1993). Extracellular cAMP is sufficient to restore developmental gene expression and morphogenesis in

*Dictyostelium* cells lacking the aggregation adenylyl cyclase (ACA). *Genes & Development*, *7*(11), 2172–2180.

Pitt, G. S., Milona, N., Borleis, J., Lin, K. C., Reed, R. R., & Devreotes, P. N. (1992). Structurally distinct and stage-specific adenylyl cyclase genes play different roles in dictyostelium development. *Cell*, *69*(2), 305–315.

Pollard, T. D. (2007). Regulation of Actin Filament Assembly by Arp2/3 Complex and Formins. *Annual Review of Biophysics and Biomolecular Structure*, *36*(1), 451–477.

Raper, B, K. (1935). *Dictyostelium discoideum*, a new species of slime mold from decaying forest leaves. *J. Agricul. Res.*, *50*, 135–147.

Rappel, W.-J., Nicol, A., Sarkissian, A., Levine, H., & Loomis, W. F. (1999). Self-organized Vortex State in Two-Dimensional *Dictyostelium* Dynamics. *Physical Review Letters*, *83*(6), 1247–1250.

Ratner, D. I., & Newell, P. C. (1978). Linkage Analysis in *Dictyostelium discoideum* using Multiply Marked Tester Strains: Establishment of Linkage Group VII and the Reassessment of Earlier Linkage Data. *Journal of General Microbiology*, *109*(2), 225–236. 5

Redd, M. J., Kelly, G., Dunn, G., Way, M., & Martin, P. (2006). Imaging macrophage chemotaxis in vivo: Studies of microtubule function in zebrafish wound inflammation. *Cell Motility and the Cytoskeleton*, *63*(7), 415–422.

Rietdorf, J., Siegert, F., & Weijer, C. J. (1996). Analysis of Optical Density Wave Propagation and Cell Movement during Mound Formation in *Dictyostelium discoideum*. *Developmental Biology*, *177*(2), 427–438.

Rietdorf, J., Siegert, F., & Weijer, C. J. (1998). Induction of Optical Density Waves and Chemotactic Cell Movement in *Dictyostelium discoideum*by Microinjection of cAMP Pulses. *Developmental Biology*, *204*(2), 525–536.

Rieu, J.-P., Barentin, C., Sawai, S., Maeda, Y., & Sawada, Y. (2004). Cell Movements and Mechanical Force Distribution During the Migration of *Dictyostelium* Slugs. *Journal of Biological Physics*, *30*(4), 345–364.

Rørth, P. (2009). Collective Cell Migration. *Annual Review of Cell and Developmental Biology*, *25*(1), 407–429.

Rosengarten, R. D., Santhanam, B., Fuller, D., Katoh-Kurasawa, M., Loomis, W. F., Zupan, B., & Shaulsky, G. (2015). Leaps and lulls in the developmental transcriptome of *Dictyostelium discoideum*. *BMC Genomics*, *16*(1), 294.

Sahai, E. (2005). Mechanisms of cancer cell invasion. *Current Opinion in Genetics & Development*, *15*(1), 87–96.

Saran, S., Nakao, H., Tasaka, M., Iida, H., Tsuji, F. I., Nanjundiah, V., & Takeuchi, I. (1994). Intracellular free calcium level and its response to cAMP stimulation in developing *Dictyostelium* cells transformed with jellyfish apoaequorin cDNA. *FEBS Letters*, *337*(1), 43–47.

Sato, M. J., Kuwayama, H., van Egmond, W. N., Takayama, A. L. K., Takagi, H., van Haastert, P. J. M., … Ueda, M. (2009). Switching direction in electric-signal-induced cell migration by cyclic guanosine monophosphate and phosphatidylinositol signaling. *Proceedings of the National Academy of Sciences of the United States of America*, *106*(16), 6667–6672.

Scarpa, E., & Mayor, R. (2016). Collective cell migration in development. *The Journal of Cell Biology*, *212*(2), 143–155.

Schaap, P., Van Lookeren Campagne, M. M., Van Driel, R., Spek, W., Van Haastert, P. J. M., & Pinas, J. (1986). Postaggregative differentiation induction by cyclic AMP in *Dictyostelium*: Intracellular transduction pathway and requirement for additional stimuli. *Developmental Biology*, *118*(1), 52–63.

Scherer, A., Kuhl, S., Wessels, D., Lusche, D. F., Raisley, B., & Soll, D. R. (2010). Ca2+ chemotaxis in *Dictyostelium discoideum*. *Journal of Cell Science*, *123*(Pt 21), 3756–3767.

Schnitzler, G. R., Fischer, W. H., & Firtel, R. A. (1994). Cloning and characterization of the G-box binding factor, an essential component of the developmental switch between early and late development in *Dictyostelium*. *Genes & Development*, *8*(4), 502–514.

Sergé, A., de Keijzer, S., Van Hemert, F., Hickman, M. R., Hereld, D., Spaink, H. P., … Snaar-Jagalska, B. E. (2011). Quantification of GPCR internalization by single-molecule microscopy in living cells. *Integrative Biology*, *3*(6), 675.

Sgro, A. E., Schwab, D. J., Noorbakhsh, J., Mestler, T., Mehta, P., & Gregor, T. (2015). From intracellular signaling to population oscillations: bridging size- and time-scales in collective behavior. *Molecular Systems Biology*, *11*(1), 779.

Shaffer, B. M. (1964). Intracellular movement and locomotion of cellular slime-mold amoebae. *Primitive motile systems in cell biology*, 387-405.

Siegert, F., & Weijer, C. (1989). Digital image processing of optical density wave propagation in *Dictyostelium discoideum* and analysis of the effects of caffeine and ammonia. *Journal of Cell Science*, *93*(2).

Siu, C. H., Harris, T. J. C., Wang, J., & Wong, E. (2004). Regulation of cell–cell adhesion during *Dictyostelium* development. *Seminars in Cell & Developmental Biology*, *15*(6), 633–641.

Siu, C. H., Des Roches, B., & Lam, T. Y. (1983). Involvement of a cell-surface glycoprotein in the cell-sorting process of *Dictyostelium discoideum*. *Proceedings of the National Academy of Sciences of the United States of America*, *80*(21), 6596–6600.

Soede, R. D., Insall, R. H., Devreotes, P. N., & Schaap, P. (1994). Extracellular cAMP can restore development in *Dictyostelium* cells lacking one, but not two subtypes of early cAMP receptors (cARs). Evidence for involvement of cAR1 in aggregative gene expression. *Development*, *120*(7).

Stajdohar, M., Rosengarten, R. D., Kokosar, J., Jeran, L., Blenkus, D., Shaulsky, G., & Zupan, B. (2017). dictyExpress: a web-based platform for sequence data management and analytics in *Dictyostelium* and beyond. *BMC Bioinformatics*, *18*(1), 291.

Sternfeld, J., & David, C. N. (1982). Fate and regulation of anterior-like cells in *Dictyostelium* slugs. *Developmental Biology*, *93*(1), 111–118.

Sternfeld, J., & David, C. N. (1981). Cell Sorting daring Pattern Formation in *Dictyostelium*. *Differentiation*, *20*(1–3), 10–21.

Sukumaran, S., Brown, J. M., Firtel, R. A., & McNally, J. G. (1998). lagC-Null and gbf-Null Cells Define Key Steps in the Morphogenesis of *Dictyostelium*Mounds. *Developmental Biology*, *200*(1), 16–26.

Sumino, Y., Nagai, K. H., Shitaka, Y., Tanaka, D., Yoshikawa, K., Chaté, H., & Oiwa, K. (2012). Large-scale vortex lattice emerging from collectively moving microtubules. *Nature*, *483*(7390), 448–452.

Sun, T. J., Van Haastert, P. J., & Devreotes, P. N. (1990). Surface cAMP receptors mediate multiple responses during development in *Dictyostelium*: evidenced by antisense mutagenesis. *The Journal of Cell Biology*, *110*(5), 1549–1554.

Swaney, K. F., Huang, C.-H., & Devreotes, P. N. (2010). Eukaryotic Chemotaxis: A Network of Signaling Pathways Controls Motility, Directional Sensing, and Polarity. *Annual Review of Biophysics*, *39*(1), 265–289.

Takagi, H., Sato, M. J., Yanagida, T., & Ueda, M. (2008). Functional Analysis of Spontaneous Cell Movement under Different Physiological Conditions. *PLoS ONE*, *3*(7), e2648.

Theveneau, E., Marchant, L., Kuriyama, S., Gull, M., Moepps, B., Parsons, M., & Mayor, R. (2010). Collective Chemotaxis Requires Contact-Dependent Cell Polarity. *Developmental Cell*, *19*(1), 39–53.

Theveneau, E., Steventon, B., Scarpa, E., Garcia, S., Trepat, X., Streit, A., & Mayor, R. (2013). Chase-and-run between adjacent cell populations promotes directional

collective migration. *Nature Cell Biology*, *15*(7), 763–772.

Tillinghast, H. S., & Newell, P. C. (1987). Chemotaxis towards pteridines during development of *Dictyostelium*. *Journal of Cell Science*, *87*(1).

Tomchik, K. J., & Devreotes, P. N. (1981). Adenosine 3',5'-monophosphate waves in *Dictyostelium discoideum*: a demonstration by isotope dilution--fluorography. *Science*, *212*(4493), 443–446.

Traynor, D., Kessin, R. H., & Williams, J. G. (1992). Chemotactic sorting to cAMP in the multicellular stages of *Dictyostelium* development. *Proceedings of the National Academy of Sciences of the United States of America*, *89*(17), 8303–8307.

van Es, S., Virdy, K. J., Pitt, G. S., Meima, M., Sands, T. W., Devreotes, P. N., … Schaap, P. (1996). Adenylyl cyclase G, an osmosensor controlling germination of Dictyostelium spores. *The Journal of Biological Chemistry*, *271*(39), 23623–23625.

van Es, S., Wessels, D., Soll, D. R., Borleis, J., & Devreotes, P. N. (2001). Tortoise, a novel mitochondrial protein, is required for directional responses of *Dictyostelium* in chemotactic gradients. *The Journal of Cell Biology*, *152*(3), 621–632.

Veltman, D. M., Akar, G., Bosgraaf, L., & Van Haastert, P. J. M. (2009). A new set of small, extrachromosomal expression vectors for *Dictyostelium discoideum*. *Plasmid*, *61*(2), 110–118.

Veltman, D. M., & van Haastert, P. J. M. (2008). The role of cGMP and the rear of the cell in *Dictyostelium* chemotaxis and cell streaming. *Journal of Cell Science*, *121*(Pt 1), 120–127.

Venhuizen, J.-H., & Zegers, M. M. (2018). Making Heads or Tails of It: Cell-Cell Adhesion in Cellular and Supracellular Polarity in Collective Migration, *16*.

Vicsek, T., & Zafeiris, A. (2012). Collective motion. *Physics Reports*, *517*(3–4), 71–140.

Waddell, D. R. (1988). Cell size in *Dictyostelium*. *Developmental Genetics*, *9*(4–5), 673–681.

Wang, B., & Kuspa, A. (1997). *Dictyostelium* Development in the Absence of cAMP. *Science*, *277*(5323).

Wang, J., Hou, L., Awrey, D., Loomis, W. F., Firtel, R. A., & Siu, C.-H. (2000). The Membrane Glycoprotein gp150 Is Encoded by the lagC Gene and Mediates Cell–Cell Adhesion by Heterophilic Binding during *Dictyostelium* Development. *Developmental Biology*, *227*(2), 734–745.

Wang, M., & Schaap, P. (1985). Correlations between tip dominance, prestalk/prespore pattern, and CAMP-relay efficiency in slugs of *Dictyostelium discoideum*.

*Differentiation*, *30*(1), 7–14.

Wang, M., Van Haastert, P. J. M., Devreotes, P. N., & Schaap, P. (1988). Localization of chemoattractant receptors on *Dictyostelium discoideum* cells during aggregation and down-regulation. *Developmental Biology*, *128*(1), 72–77.

Watts, D. J., & Ashworth, J. M. (1970). Growth of myxameobae of the cellular slime mould *Dictyostelium discoideum* in axenic culture. *The Biochemical Journal*, *119*(2), 171–174.

Weijer, C. J. (1999). Morphogenetic cell movement in *Dictyostelium*. *Seminars in Cell & Developmental Biology*, *10*(6), 609–619.

Weijer, C. J. (2009). Collective cell migration in development. *Journal of Cell Science*, *122*(Pt 18), 3215–3223.

Wetterauer, B., Morandini, P., Hribar, I., Murgia-Morandini, I., Hamker, U., Singleton, C., & Macwilliams, H. K. (1996). Wild-Type Strains of *Dictyostelium discoideum*Can Be Transformed Using a Novel Selection Cassette Driven by the Promoter of the Ribosomal V18 Gene. *Plasmid*, *36*(3), 169–181.

Wilkins, M. R., & Williams, K. L. (1995). The extracellular matrix of the *Dictyostelium discoideum* slug. *Experientia*, *51*(12), 1189–1196.

Wong, L. M., & Siu, C. H. (1986). Cloning of cDNA for the contact site A glycoprotein of *Dictyostelium discoideum*. *Proceedings of the National Academy of Sciences of the United States of America*, *83*(12), 4248–4252.

Xi, W., Sonam, S., Beng Saw, T., Ladoux, B., & Teck Lim, C. (2017). Emergent patterns of collective cell migration under tubular confinement. *Nature Communications*, *8*(1), 1517.

Yang, C., Brar, S. K., Desbarats, L., & Siu, C.-H. (1997). Synthesis of the Ca2+-dependent cell adhesion molecule DdCAD-1 is regulated by multiple factors during *Dictyostelium* development. *Differentiation*, *61*(5), 275–284.

Yasui, M., Matsuoka, S., & Ueda, M. (2014). PTEN Hopping on the Cell Membrane Is Regulated via a Positively-Charged C2 Domain. *PLoS Computational Biology*, *10*(9), e1003817.

Yu, Y., & Saxe III, C. L. (1996). Differential Distribution of cAMP Receptors cAR2 and cAR3 during *Dictyostelium* Development. *Developmental Biology*, *173*(1), 353–356.

Yumura, S., Furuya, K., & Takeuchi, I. (1996). Intracellular free calcium responses during chemotaxis of *Dictyostelium* cells. *Journal of Cell Science*, *109*(11).

Zhang, N., Long, Y., & Devreotes, P. N. (2001). Gγ in *Dictyostelium* : Its Role in Localization of Gβγ to the Membrane Is Required for Chemotaxis in Shallow

Gradients. *Molecular Biology of the Cell*, *12*(10), 3204–3213.

**Publication list**

1. Collective cell migration of *Dictyostelium* without cAMP oscillations at multicellular stages.

H. Hashimura, Y. V. Morimoto, M. Yasui, M. Ueda.

*Communications Biology* **2**, Article number: 34, published on 24th, January.

https://www.nature.com/articles/s42003-018-0273-6 DOI: 10.1038/s42003-018-0273-6.

**List of conference presentation**

- Theme involved in this thesis

1. ○橋村秀典, 安井真人, 井上敬, 上田昌宏. “3D analysis of collective cell migration in Dictyostelium”、第53回日本生物物理学会年会、金沢大学、2015年9月13日。（ポスター）
2. ◦Hashimura, H., Yasui, M., Ueda, M., Inouye, K. “All-cell 3D tracking in “mini” slugs”, Annual International Dictyostelium Conference, Arizona Tucson, U. S.A., 2016年8月3日。（ポスター）
3. ○橋村秀典, 森本雄祐、安井真人, 上田昌宏. 「発生に伴うcAMPシグナル波の伝達様式の変遷」、第6回日本細胞性粘菌学会例会、上智大学、2016年10月15日。（口頭発表）
4. ◦橋村秀典, 森本雄祐、安井真人, 上田昌宏. ”Transition of the dynamics of cell-cell communication controlling collective cell migration during morphogenesis of *Dictyostelium* cells”、第55回日本生物物理学会年会、熊本大学、2017年9月19日。（ポスター）
5. ◦橋村秀典, 森本雄祐、安井真人, 上田昌宏. ”Collective cell migration of *Dictyostelium* without cAMP oscillations at multicellular stages”、第8回日本細胞性粘菌学会例会、山口大学、2018年10月20日（ベストプレゼンテーション賞受賞）。（口頭発表）
6. 橋村秀典, ◦森本雄祐、安井真人, 上田昌宏. ”細胞性粘菌の単細胞期から多細胞期へのシグナル伝達様式の変遷”、日本生体エネルギー研究会第44回討論会、千葉大学、2018年12月7日。（口頭発表）
7. ” 細胞性粘菌における単細胞から多細胞へのシグナル伝達様式の変遷”、第60回日本顕微鏡学会九州支部集会・学術講演会、熊本大学、2018年12月8日。（口頭発表）

- Presentation about the other theme

1. Hashimura, H., ◦Inouye, K. “Effects of temperature on growth and development of dictyostelids - their diversity and ecological implications –”, Annual International Dictyostelium Conference, Royal Holloway, U. K., 2015年8月9日。（ポスター）
2. ◦橋村秀典, 上田昌宏, 井上敬. 「活動温度域および最適増殖温度に見られる種間多様性」、第5回日本細胞性粘菌学会例会、弘前大学、2015年10月10日。（口頭発表）
3. ○橋村秀典、井上敬. 「細胞性粘菌における温度適応の系統進化および分布形成」 第19回進化生物学会、京都大学、2017年8月24日。（ポスター）

**Acknowledgement**

I would like to great appreciate to my supervisor, Professor Masahiro Ueda, PhD., Graduate School of Science, Osaka University. His constructive suggestion helps for progression of my study. I also express my deep and sincere gratitude to my supervisor, Assistant professor Yusuke V. Morimoto, PhD., Department of Bioscience and Bioinformatics, Faculty of Computer Science and Systems Engineering, Kyushu Institute of Technology. His meaningful advices for planning my study and help for performing experiments make a great contribution to my study. I wish to thank Masato Yasui, PhD., RIKEN BDR, for developing the software for 3D cell tracking. I also wish to deeply thank Seiya Fukushima, Takuma Degawa, Yuki Tanabe and other members of Ueda lab for technical support and useful discussion. I express sincere thanks to Lecturer Kei Inouye, PhD., Kyoto University for exciting discussion of my study and his warm encouragement. I also thank Satomi Matsuoka, PhD., (RIKEN BDR), Lecturer Tetsuya Muramoto, PhD., (Toho University), Yoichiro Kamimura., PhD., (RIKEN BDR) and Assistant Professor Yukihiro Miyanaga, PhD., (Osaka University) for the kind gift of plasmids and mutant cell lines. Several plasmids are provided from NBRP-Nenkin and Dicty Stock Center. I also thank Peter Karagiannis for correcting my manuscript. This work was supported in part by JSPS KAKENHI Grant Numbers JP15K14498 and JP15H05593 and MEXT KAKENHI Grant Numbers JP26115720 and JP15H0133. This work was supported partly by AMED-CREST (JP17gm0910001) from Japan Agency for Medical Research and Development, AMED. The author was supported by the RIKEN JRA program. Finally, through my PhD. course, my parents always supported and encouraged me. I would like to express my so deep and sincere gratitude for my parents.